REPUBLIC OF TURKEY
YILDIZ TECHNICAL UNIVERSITY
GRADUATE SCHOOL OF NATURAL AND APPLIED SCIENCES

MAXIMUM POWER POINT TRACKING CONTROLLED BOOST
CONVERTER DESIGN FOR BATTERY CHARGER

BASSAM AL-HANAHI

MSc. THESIS
DEPARTMENT OF ELECTRICAL ENGINEERING
PROGRAM OF ELECTRICAL MACHINE AND POWER
ELECTRONICS

ADVISER
ASSIST.PROF. DR. BURAK AKIN

ISTANBUL, 2018

REPUBLIC OF TURKEY
YILDIZ TECHNICAL UNIVERSITY
GRADUATE SCHOOL OF NATURAL AND APPLIED SCIENCES

MAXIMUM POWER POINT TRACKING CONTROLLED BOOST CONVERTER DESIGN FOR BATTERY CHARGER

A thesis submitted by Bassam AL-HANAHI in partial fulfillment of the requirements for the degree of **MASTER OF SCIENCE** is approved by the committee on 13.06.2018 in Department of Electrical Engineering, Electrical Machine and Power Electronics Program.

Thesis Adviser

Assist.Prof. Dr. Burak AKIN

Yildiz Technical University

Approved By the Examining Committee

Assist.Prof. Dr. Burak AKIN

Yildiz Technical University   _____

Assoc. Prof. Dr. Ozan ERDİNÇ

Yildiz Technical University   _____

Assoc. Prof. Dr. Emre ARSLAN

Marmara University   _____

ACKNOWLEDGEMENTS

June, 2018

Bassam AL-HANAHI

TABLE OF CONTENTS

LIST OF SYMBOLS

A	Current
AM	Air mass
C^o	Centimeter
K	Kelvin
KW/m^2	Kilowatt/ meter square
m	Milli
T	Temperature
V	Voltage
W	Power
Ώ	Ohms
μ	Micro
μH	Micro Henry
μF	Micro Farad
-	

LIST OF ABBREVIATIONS

C	Capacitor
CCM	Continuous Current Mode
CC-CV	Constant current –Constant voltage charging algorithm
D	Duty Cycle
Di	Diode
E_{BAT}	Energy of battery
I_{MPP}	Maximum power point current
I_{SC}	Short Circuit Current
I-V	Current-Voltage characteristic curves
InC	Incremental Conductance MPPT algorithm
I_{PV} (n)	PV current at instant (n)
I_{BAT}	Minimum charging current of Lead Acid battery
I_{ZE} (n)	Zener current at instant (n)
L	Inductor
MPP	Maximum Power Point
MPPT	Maximum Power Point Tracking
P_{MAX}	Maximum available power
P_{ZE}	Zener Power
P_{ZEH}	First high threshold value of Zener power
P_{ZEL}	First low threshold of Zener power
P_{ZEHH}	Second High threshold value Zener Power
P_{ZELL}	Second low threshold value Zener Power
P_{PVmin}	Minimum value of PV power indicates end of charge
P_{BAT}	Battery power
P&O	Perturb and observe MPPT algorithm
PPV	PV panel power
PV	Photovoltaic
P-V	Power-Voltage characteristic curves
STC	Standard Test Condition
SOC	State of Charge of Battery
T	Power Switch,
V_{PV} (n)	PV voltage at instant (n),
V_{BAT} (n)	Battery voltage at instant (n)
V_{ZE} (n)	Zener voltage at instant (n)
V_{MPP}	Maximum power point voltage
V_{OC}	Open Circuit Voltage
V_{low_limit}	Low pre-determined limit
V_{high_limit}	High pre-determined limit
Vg	Source Voltage

LIST OF FIGURES

xii

LIST OF TABLE

<div align="right">**ABSTRACT**</div>

MAXIMUM POWER POINT TRACKING CONTROLLED BOOST CONVERTER DESIGN FOR BATTERY CHARGER

<div align="center">

Bassam AL-HANAHI

Department of Electrical Engineering

MSc. Thesis

Adviser: Asst. Prof. Dr. Burak AKIN

</div>

MPPT controlled DC-DC converters are crucial in power systems which are supplied by PV panels. They extract maximum available power of PV panel irrespective of variable environmental conditions; thus increase the conversion efficiency of PV panels. In addition, especially in stand-alone PV system, they can control charging process of rechargable batteries in a way that reduces charging time and increases cycle life of battery.

In this reseach, the design of MPPT controlled DC-DC boost converter and its application as solar battery charger are presented. In this design, in order to meet the requirments of MPPT tracker and battery charger systems, an expanded MPPT algorithm is developed. The developed algorithm comprises Incremental conductance MPPT algorithm which is expanded to incorporate CC-CV charging algorithm. This developed algorithm adjusts directly the duty cycle of boost converter, which operates in 25 KHz,in order to control the operating point of PV panel. Depending on developed algorithm, the designed MPPT boost converter charges battery through three stages. These stages are pre-charging, in MPPT-CC charging and CV charging stages. Designed system operates as MPPT controller in MPPT-CC charging stages; whereas operates as charger controller in pre-charging and CV charging stages. The implementation of CV charging stage is performed by using voltage regulating device which is Zener diode. In addition, the designed system provides end of charge detection method which depends on measuring PV power instead of battery charging current.

The functionality and performance of designed, MPPT controlled DC-DC boost converter are simulated and validated by SIMULINK-MATLAB program.The simulation process is performed under two different cases of environmental conditions which are standard test condition (STC) and variable environmental condition.The

simulation results show the proper operation of designed system in the three stages of charging process. They show that the designed system has an averaged tracking efficiency of 99.444% over the simulated variable levels of irradiance for MPPT-CC charging, and an averaged conversion efficiency of 96,66%, 99,28%, and 98,3% over the simulated variable levels of irradiance for pre-charging, MPPT-CC charging and CV charging stages respectively. In addition, the designed system ensures input current ripples and output voltage ripples of 10mA and 100μV repectively, which are within the allowable limits of this designed. These simulation results prove the proper functionality and high performance of designed, MPPT controlled DC-DC boost converter as MPPT controller and charge controller.

Key words: Boost Converter, Incremental Conductance algorithm, CC-CV algorithm, Zener diode.

ÖZET

BATARYA ŞARJI İÇİN MAKSİMUM GÜÇ NOKTASI TAKİP KONTROLLÜ YÜKSELTİCİ DÖNÜŞTÜRÜCÜ

Bassam AL-HANAHI

Elektrik Mühendisliği Anabilim Dalı

Yüksek Lisans Tezi

Tez Danışmanı: Dr. Öğretim Üyesi Burak AKIN

PV panelleri tarafından sağlanan güç, MPPT kontrollü DC-DC dönüştürücüleri için önemlidir. Değişken çevre koşullarına bakılmaksızın PV panelin maksimum kullanılabilir gücünü ortaya çıkarırlar; Böylece PV panellerin dönüşüm verimliliği artar. Ek olarak, özellikle PV sisteminde, şarj edilebilir bataryaların şarj süresini azaltacak ve batarya ömrünü uzatacak şekilde kontrol edebilirler.

Bu çalışmada, MPPT kontrollü DC-DC boost dönüştürücünün tasarımı ve solar akü şarj cihazı olarak kullanımı sunulmaktadır. Bu tasarımda, MPPT takip sistemi ve akü şarj cihazı sistemlerinin gereksinimlerini karşılamak için genişletilmiş bir MPPT algoritması geliştirilmiştir. Geliştirilen algoritma, CC-CV şarj algoritmasını içerecek şekilde genişletilen Artımlı İletkenlik MPPT algoritmasını içermektedir. Bu geliştirilmiş algoritma, PV panelinin çalışma noktasını kontrol etmek için 25 KHz'de çalışan boost dönüştürücünün çalışma döngüsünü doğrudan ayarlar. Bu geliştirilen algoritmaya bağlı olarak, tasarlanan MPPT boost dönüştürücü bataryayi üç aşamada şarj eder. Bu aşamalar ön şarj, MPPT-CC şarj ve CV şarj aşamalarıdır. Tasarlanan sistem MPPT-CC şarj aşamalarında MPPT kontrollü sistem olarak çalışır; ön şarj ve CV şarj aşamalarında ise şarj kontrolörü olarak çalışır. CV şarj aşamasının uygulanmasında Zener diyot, voltaj regülasyon elemanı olarak kullanılır. Ayrıca tasarlanan sistem, akü şarj akımı yerine PV gücünün ölçülmesine bağlı olarak batarya şarj sonu algılama yöntemini sağlar.

Tasarlanan MPPT kontrollü DC-DC boost dönüştürücünün işlevselliği ve performansı simule edilmiş ve SIMULINK-MATLAB programı ile doğrulanmıştır. Simülasyon süreci, standart test koşulu (STC) ve değişken çevresel durum olan iki farklı çevresel koşulda gerçekleştirilir. simülasyon sonuçları, tasarlanan sistemin şarj işleminin üç aşamasında düzgün çalışmasını göstermektedir. Tasarlanan sistemin MPPT-CC şarj aşaması sırasında simüle edilen değişken ışınım seviyeleri üzerinde ortalama%

99.444'lük bir izleme etkinliğine sahip olduğunu göstermektedir. Buna ek olarak, tasarlanan sistemin, sırasıyla ön şarj, MPPT -CC şarj ve CV şarj aşamaları için simule edilen değişken ışınım seviyeleri üzerinden ortalama 96,66%, 99,28%, and 98,3% dönüşüm verimliliğine sahip olduğunu göstermektedir. Buna ek olarak, tasarlanan sistem izin verilen sınırlar dahilinde, 10mA ve 100µV'luk giriş akımı ve çıkış gerilimi dalgalanması sağlar. Bu simülasyon sonuçları, MPPT kontrol sistemi ve şarj regülatörü olarak tasarlanan MPPT kontrollü DC-DC boost dönüştürücünün uygun işlevselliğini ve yüksek performansını kanıtlamaktadır.

Anahtar Kelimeler: Yükseltici Dönüştürücü, Artımlı İletkenlik MPPT algoritmasını, CC-CV algoritması, Zener diyot.

INTRODUCTION

1.1 Literature Review

Solar photovoltaic (PV) panel is one of the most important application of solar energy. It can be used as source of power in stand-alone and grid connected systems. In grid connected system, PV panels supplies power directly into grid system. In contrast, PV panels are used to supply certain amount of power to specific load in stand-alone systems [1].

In general, PV panel has low conversion efficiency, which ranges between 10 to 20% depending on materials that are used in their manufacturing. Depending on this efficiency, maximum available power (P_{MAX}) that can be extracted from PV panel is determined under standard test condition (STC) of environment. But, P_{MAX} is not constant always and is affected by other parameters. The main parameters that affect P_{MAX} are illustrated in the following points [2], [3].

- P_{MAX} is affected by the nonlinearity of P-V and I-V characteristic curves that represent the performance of PV panel. Because of this nonlinearity, the maximum power of PV panel can be extracted just at certain operating point of these curves. This operating point is called maximum power point (MPP) and characterized by maximum power point voltage (V_{MPP}) and maximum power point current (I_{MPP}) in specification datasheet of PV panel. So, in order to extract the maximum power of PV panels, it is required to operate these panels at this operating point [3].

- P_{MAX} is affected by the variation of environmental conditions which affect P-V and I-V curves. This variation of environmental conditions results in changing of MPP of PV curves; thus reduce the maximum power that can be extracted. So, in order to extract the maximum power of PV panels at different environmental conditions, it is

crucial to ensure the operation of these panels at MPP that corresponds to certain environmental condition [3].

- In addition, P_{MAX} is affected by the mismatch between operating point of load and MPP of PV panel. This mismatch results because of dependence of energy produced by the PV panel on the energy required by the load; thus the operating point of PV panel is determined by operating point of load. In case of direct connection of the PV panel and load, the operating point of load and MPP of PV panel should be identical; otherwise the extracted power is reduced according to what explained previously. Unfortunately, this identicalness cannot be held mostly, because of change of load and change of environment conditions [4].

Therefore, in order to extract the maximum power of PV panels; thus increase the overall efficiency of PV system, it is necessary to continuously ensure the operation of these panels at MPP irrespective of environmental and load conditions. This function can be done by inserting MPPT controlled DC-DC converter unit between PV system and load. This unit matches the operating point of load with MPP of PV panel and tracks MPP of PV panel continuously. The operation of this unit depends mainly on MPPT algorithms which monitors voltage and current of PV panel and adjusts duty cycle of DC-DC converter to ensure the operation of PV panel at MPP [4], [5].

In stand-alone PV system, MPPT controlled DC-DC converter is used as interface unit between PV panel and rechargeable batteries which are used to supply load in case of dark or low insolation. Therefore, MPPT controlled DC-DC converter is operated as solar charger that provides battery with maximum available power of PV panel. However, rechargeable batteries are required to be charged according to charging algorithms which ensure the charging of battery fully and safely. As a consequence, two stages system has been proposed in literature to charge battery in stand-alone PV system as in [5] and [6]. In [5], boost converter and buck-boost converter have been used to implement the P&O MPPT and CC-CV charging algorithms respectively. The implementation of CC-CV charging algorithm is performed by current and voltage sliding mode regulator respectively. In [6], design of MPPT and charger controllers has been presented. In the MPPT controller, Buck-Boost converter has been proposed to track the MPP through P&O MPPT algorithm. In order to control the charging process of battery through CC-CV charging algorithm, normal MOSFET device has been used in the charger controller.

Although two stages charger system ensures the high performance of operation of MPPT and proper charging functions, its implementation is costly and less efficiently because of the two converters. Therefore, in order to improving the efficiency and decreasing cost of battery charger system, design trend have been directed toward single stage MPPT controlled DC-DC converter which has the ability of operating PV panel at MPP and controlling the charging process of battery. In literature, many designs of MPPT controlled DC-DC converter for charger system have been proposed as in [7], [8], [9], and [10].

In [7], buck-boost converter has been used as MPPT interface unit between PV panel and battery bank. Incremental conductance MPPT algorithm has been proposed to track the MPP of PV panel under different conditions. The charging process proposed in this research depends on the operation of buck-boost converter as MPPT system in order to supply the available maximum power of PV panel to battery bank. In this design, the end of charging is detected by the maximum allowance voltage of battery which leaves battery with SOC of 80% in better case. Therefore, the charging process of battery is not performed properly. As a result, the performance of battery may be degraded badly.

In [8], the designed system charges battery by buck converter which is controlled by P&O MPPT and CC-CV charging algorithm separately. These algorithms are activated by normal contact according to predetermined limit of battery voltage. When battery voltage is below predetermined value, buck converter operates as MPPT controller. Through this stage, the designed system is considered as CC controller. When the voltage of battery reaches the predetermined value, the buck converter operates as CV controller. In this design, voltage regulator is used in the CV stage of charging process which is operated separately from MPPT tracker.

In [9], boost converter is used as DC-DC converter which its duty cycle is controlled based on new developed MPPT algorithm, genetic algorithm, and CC-CV charging algorithm. The new developed algorithm based on binary search technique of MPP of PV panel. In addition, GA is used as optimization algorithm in order to search the optimum values of MPP parameters when changing of irradiance or temperature PV and battery is detected. In this design, this CC-CV charging algorithm has been implemented by using current and voltage regulator circuit respectively. The implementation of developed system requires more sensors, especially for temperature and irradiance.

In [10], MPPT and battery charging functions have been accomplished together by using SEPIC converter. In this design, charging process is performed through two modes which are pulsating current mode and constant voltage mode. These modes are activated by switch according to pre-determined value of battery voltage. Through the pulsating current mode, the designed system tracks MPP by Incremental conductance MPPT algorithm and supply the battery with pulsating current. When output voltage reaches predetermined value the constant voltage mode takes place. In the design, predictive controller has been proposed to ensure operation of system optimally.

A comparison of different designs of solar charger system that have been discussed previously are shown in Table 1.1. As can be shown in this table, solar charger systems that have single stage of converters incorporates MPPT and charging algorithms in order to control duty cycle of single DC-DC converter.

Table 1.1 Comparison of Previous Designs of Solar Charger System

Ref. No.	Power Rating	No. of stages	MPPT Controller		Charger Controller		Cost
			Topology	Algorithm	Topology	Algorithm	
[5]	250 W	2	Boost	P&O	Buck-Boost	CC-CV	High costly
[6]	100 W	2	Buck-Boost	P&O	MOSFET Device	CC-CV	Low costly
[7]	100 W	1	Buck-Boost	InC	____	CC	costly
[8]	300 W	1	Buck	P&O	____	CC-CV	Low costly
[9]	80 W	1	Boost	Developed Algorithm	____	CC-CV	High costly
[10]	230 W	1	SEPIC	InC	____	PC-CV	costly

The previous designs of single stage MPPT controlled DC-DC converter has accomplished the main functions of MPPT and battery charger system. However, these designs have not addressed all parameters that may affect performance of battery and PV system. These parameters are summarized in following points.

- The implementation and control of designed MPPT controlled DC-DC converter should be easy; otherwise the cost of overall system will increase, especially in case of low power charging systems.

- The charging process during low voltage condition of battery should be considered in designed system. This condition is resulted from deep discharge of battery and determined by low predetermined limit of battery voltage. During this condition, the battery should be charges with minimum current in order to ensure the high performance of battery.

- The variation of environment during CV stage of charging process should be considered in developed system. Since variations of environment impact the PV characteristics curves and thus power that can be supplied to battery is affected. In consequence, CV stage of charging process and end of charge detection may be affected.

Depending on discussion that has been presented, the design of MPPT controlled DC-DC converter that has the ability of operating PV panel at MPP and controlling the charging process of battery properly according to the parameters that are mentioned above is the interest of this research.

1.2   Objective of the Thesis

The final target of this research is to design a low cost, easily implemented, and MPPT controlled DC-DC converter system which can be used to charge batteries, effectively, in different application of stand-alone system. The designed system consists of high efficient DC-DC Boost converter, which is controlled by changing its duty cycle directly according to a new developed algorithm. This new developed algorithm incorporates Incremental Conductance (InC) MPPT and CC-CV battery charging algorithms in a way that extracts the maximum power of PV panel and ensures the proper charging of battery. Although new developed algorithm has been applied to low

power application, it can be applied for higher power application, after some adjustment. The selection of topology of DC-DC converter and algorithms of MPPT system and battery charger depends on discussing that will be presented in the following chapters.

1.3   Hypothesis

MPPT controlled DC-DC converter is applied to extract the maximum available power of PV panel under variable environment. In stand-alone system, MPPT controlled DC-DC converter can be applied to charge batteries by providing maximum power. However, proper and effective charging of battery is required to be performed according to charging algorithm which ensures charging of battery according to its requirements. Therefore, MPPT controlled DC-DC converter should have abilities of extracting maximum power of PV panel and charging battery properly. In addition, design of this converter should be implemented easily and less costly to be applicable in low power application. These requirements are accomplished by designing boost DC-DC converter that is controlled by Incremental Conductance MPPT algorithm to charge battery with maximum available power of PV panel. In addition, the designed system ensures the proper charging of battery by taking into consideration the charging of battery during low voltage and high voltage conditions of battery by including CC-CV charging algorithm into MPPT algorithm. The designed system is implemented easily by voltage sensor, current sensor, and low cost Zener diode which is used as voltage regulator during CV charging of battery.

GENERAL OVERVIEW OF MAIN COMPONENTS OF PV CHARGER SYSTEM

The main target of this research is to design MPPT controlled DC-DC converter that can be used to charge rechargeable battery. Before going into the design process of proposed system, general overview of the main components that can be used in stand-alone PV charger system should be presented. The main components are PV panels, MPPT controller, DC-DC converters, and Battery. Depending on this overview, the proper MPPT algorithm, battery charging algorithm, and DC-DC converter topology of the proposed system are selected. In addition, charging requirements of battery are determined. In the following sections, an overview of these components are presented.

2.1 PV Solar Panel

2.1.1 PV Panel Model

PV panels comprise of many solar cells, which are connected part by part in integrated series and parallel, as building blocks. A solar cell converts solar energy into electricity by means of the photoelectric action that occurs in specified types of semiconductor materials such as silicon i.e. generates electric voltage and current on exposure to light. The ideal PV cell is modelled as single diode circuit as shown in Figure 2.1 [11].
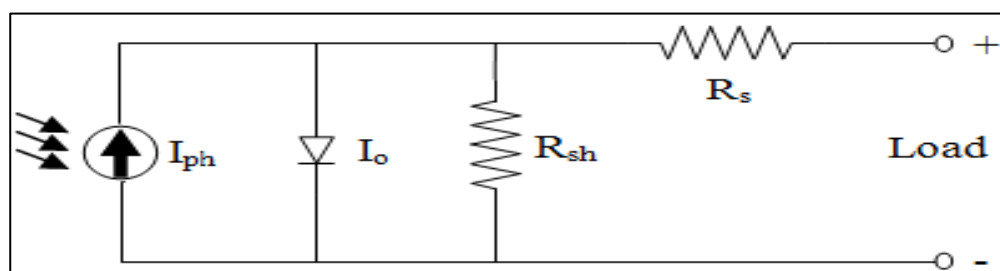
Figure 2.1 Single Diode Circuit Modelling of Ideal PV Cell

7

This circuit contains of a current source, a diode in parallel with source, series resistors R_S, and parallel R_{SH} to represent dissipation of PV cell [11].

The mathematical relation between voltage and current of PV cell can be described, as in (2.1) [12].

$$I = I_{PV} - I_o[\exp((V + Rs\ I)/kT) - 1] - (V + Rs\ I)/Rp \qquad (2.1)$$

Where, I is the PV cell current (A). I_{PV} is the PV cell photocurrent (A). Io is the diode saturation current. T is the cell temperature (K). R_S and R_P are the series and shunt resistance of PV cell (Ω) and V is the output voltage of PV cell (V) [12].

Equation (2.1) of the ideal PV cell does not define the I-V characteristic of a practical PV panel. Practical panels are manufactured by using several connected PV cells and the determination of the characteristics is done at the terminals of the PV array. If the panel is composed of Np parallel connections of cells the terminal characteristics of PV and diode saturation currents may be expressed as in (2.2) and (2.3). In this case, R_S represents the equivalent series resistance of the panel and R_P represents the equivalent parallel resistance of the panel [12].

$$I_{PV} = I_{PV,cell} * N\_P \qquad (2.2)$$
$$I_O = I_{O,cell} * N\_P \qquad (2.3)$$

2.1.2 PV Panel Curves

Terminal characteristics of PV panel are represented as P-V and I-V curves which are generally supplied by manufacturer. Figures 2.2 and 2.3 show I-V and P-V curves of 100W PV panel at Standard Test Conditions (STC) respectively. STC condition can be described by 1 KW/m2, 25 C°, and 1.5 AM [12].

These curves have highly nonlinear characteristics and can be divided into three regions as shown in Figures 2.2 and 2.3. In region 1, the PV panel works as current source because PV current is mostly constant with change of PV voltage. Power, in region 1, increases with increasing of voltage and verse vice. In contrary, in region 3, the relation between PV current and voltage can be described as in constant voltage source. Through this region, PV voltage is nearly constant as compared to change of PV current. Power, in region 3, decreases with increasing of voltage and verse vice. In region 2, which is located between region 1 and 3, the change of PV voltage is accompanied by corresponding change in PV current. In this region, when voltage increases from region

8

1, PV power increases correspondingly until reaches maximum point. This point is called maximum power point (MPP) of PV panel and characterized by V_{MPP} and I_{MPP} in nameplate of PV panel. With increase of PV voltage more than V_{MPP}, PV power starts to decrease from this maximum power point until reaches region 3.
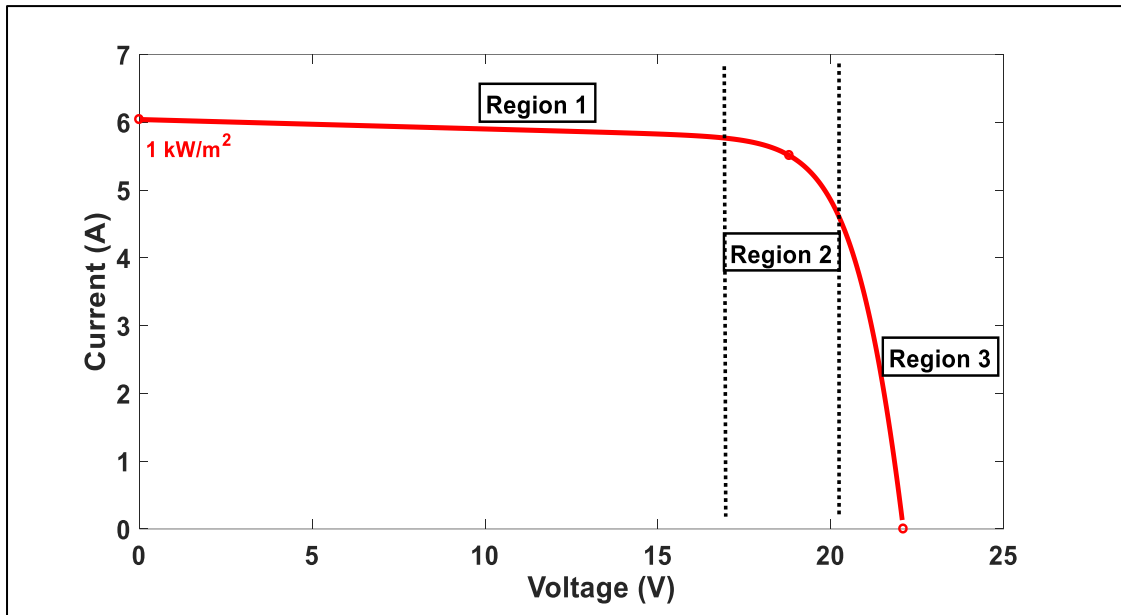
Figure 2.2 I-V Curves of PV Solar Panel
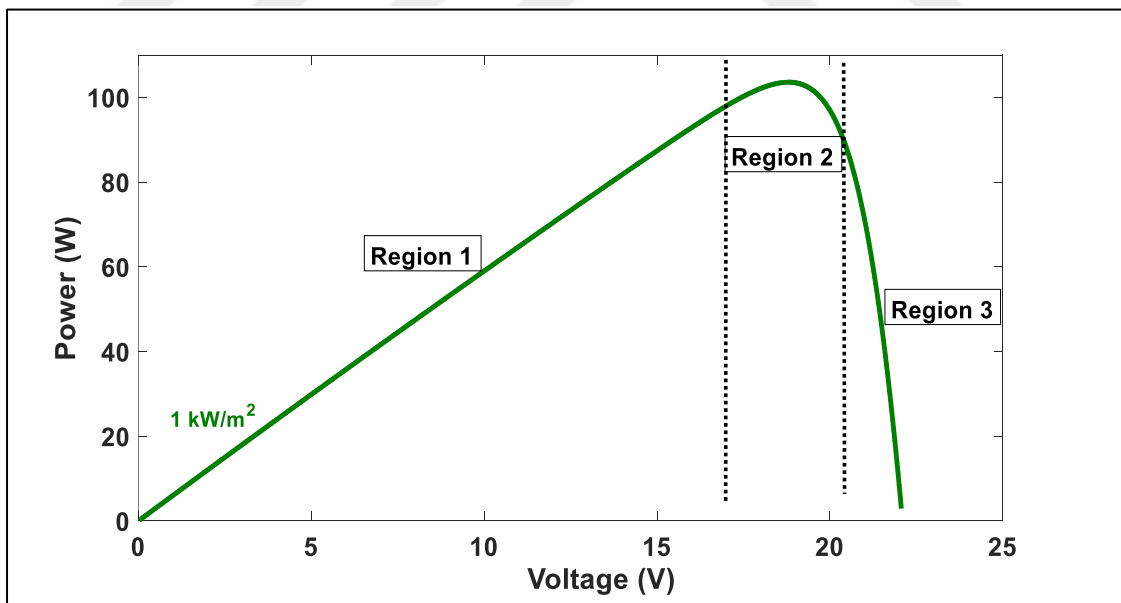
Figure 2.3 P-V Curves of PV Solar Panel

These curves depend on environmental conditions where PV panel is located. The main factors of environmental conditions that affect P-V and I-V curves are temperature and level of irradiance of sun. The change of PV curves with change of environment temperature can be shown in Figures 2.4 and 2.5.
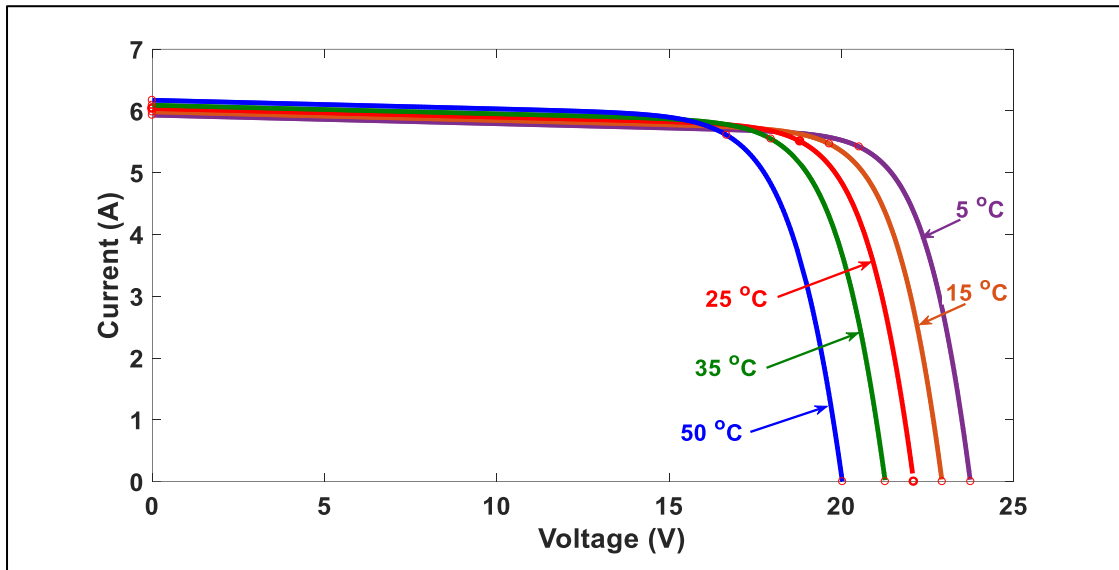
Figure 2.4 Effect of Temperature on I-V Curves
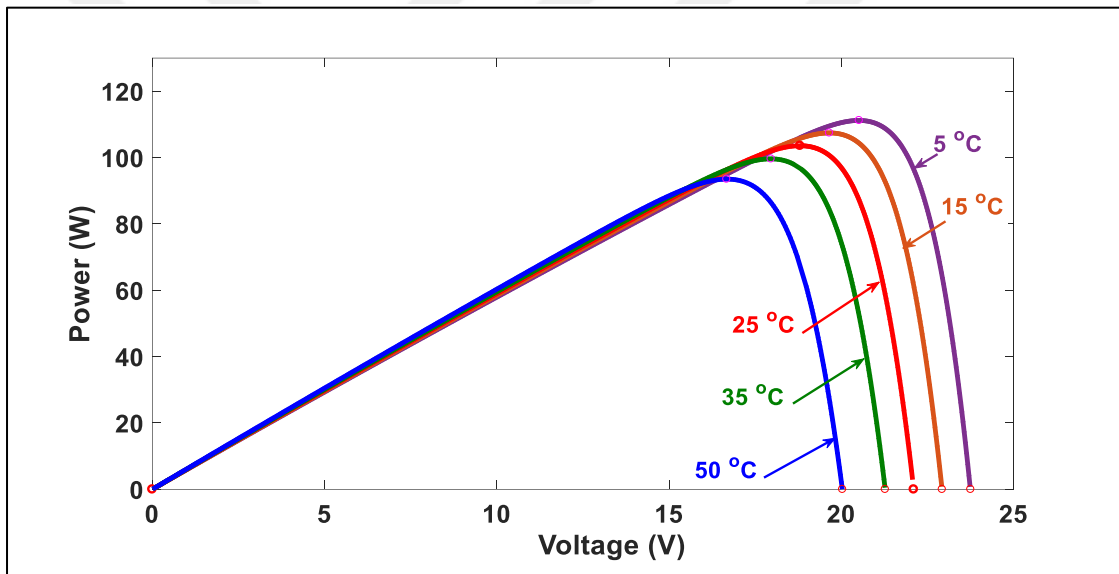
Figure 2.5 Effect of Temperature on P-V Curves

As shown in these figures, the open circuit voltage is affected hardly by changing of temperature. However, small change of short circuit current of PV panel is observed during variation of environment. Consequently, MPP of PV panel moves as shown in the Figure 2.5. As can be shown, this moving of MPP is limited over the operating range temperatures and level of power that can be extracted is not affected hardly. Therefore, the effect of temperature on the performance PV panel curves can be neglected, approximately, over the range of operating temperature.

Figures 2.6 and 2.7 show the effect of changing irradiance level on PV curves. As can be shown from this Figure, changing of irradiance level affects short circuit current

hardly compared to small change in open circuit voltage of PV panel. This change results in moving of maximum power point of PV panel as shown in the Figure. This moving of maximum power point changes considerably the level of power that can be extracted from PV panel. Therefore, the effect of changing irradiance on the performance PV panel curves should be considered carefully, over the range of irradiance levels of interest.
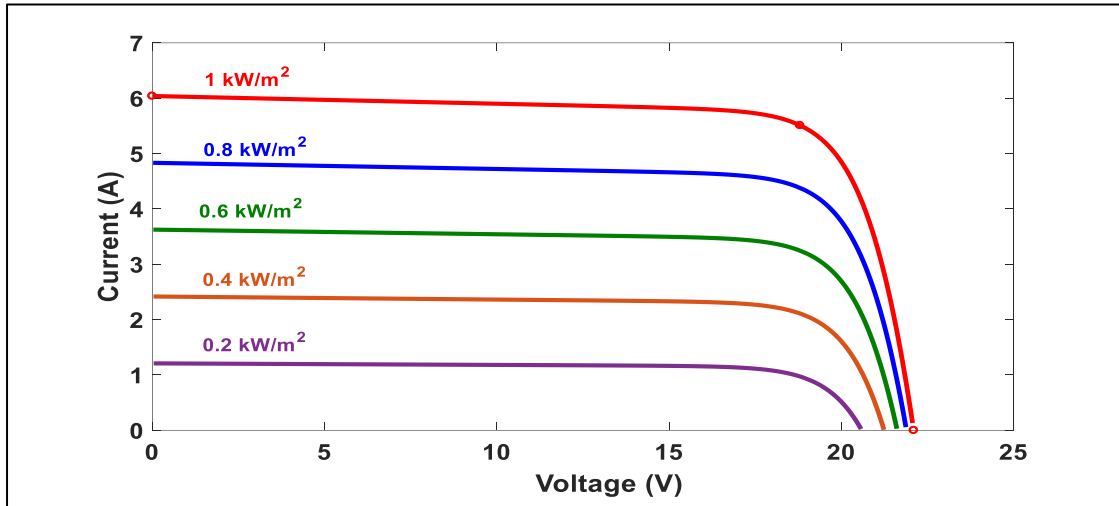
Figure 2.6 Effect of Irradiance on I-V Curves
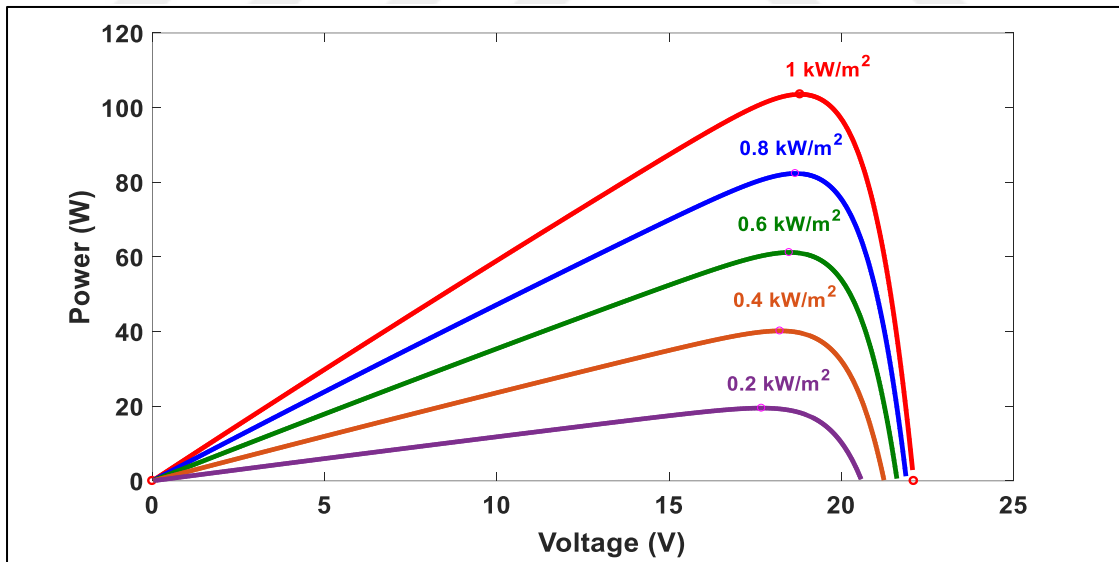
Figure 2.7 Effect of Irradiance on P-V Curves

2.2 MPPT Algorithms

As shown in Figure 2.5 and 2.7, the maximum power point of PV panel moves according to change in environmental conditions. In order to track continuously the maximum power point of PV panel in different environmental conditions, MPPT

11

algorithms have been proposed. These algorithms perform this function by observing the operation point of PV panel and determining the optimum operating point that corresponds to the maximum power point of panel through number of iterations. The number of iterations that are required to reach the MPP depends on the used algorithm. In literature, Numerous MPPT techniques have been presented. These techniques differ in terms of complexity, convergence speed, steady state oscillations, cost, effectiveness and flexibility. MPPT algorithms can be systematically categorized into three main groups. These groups of MPPT algorithms are Hill Climbing, Soft Computing, Approximate algorithms [13].

2.2.1 Hill Climbing Algorithms

The most important algorithms of this group are Perturb and Observe (P&O) and Incremental Conductance (InC) that are shown in Figures 2.8 and 2.9 respectively.
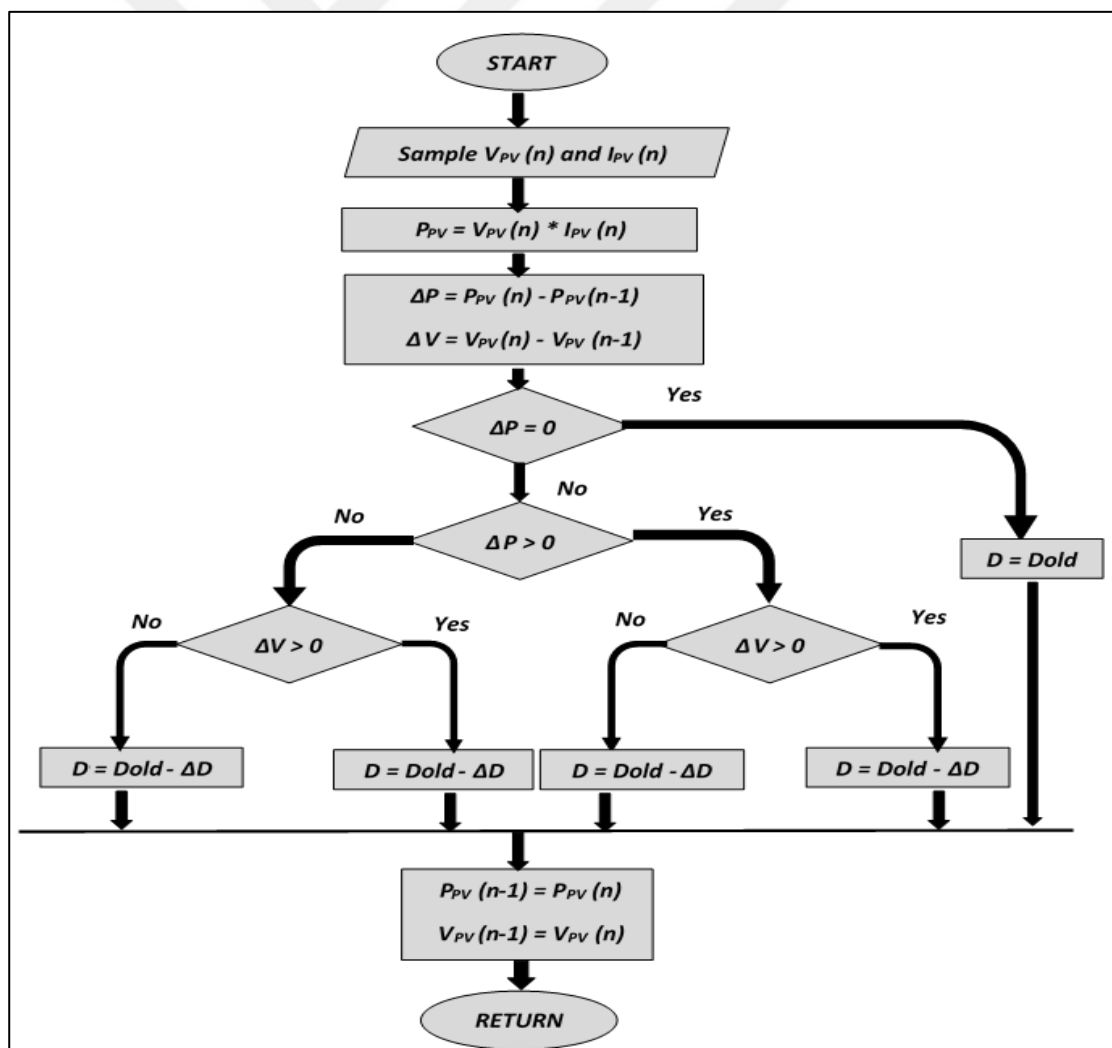
Figure 2.8 Hill Climbing Algorithms: Perturb and Observe (P&O)
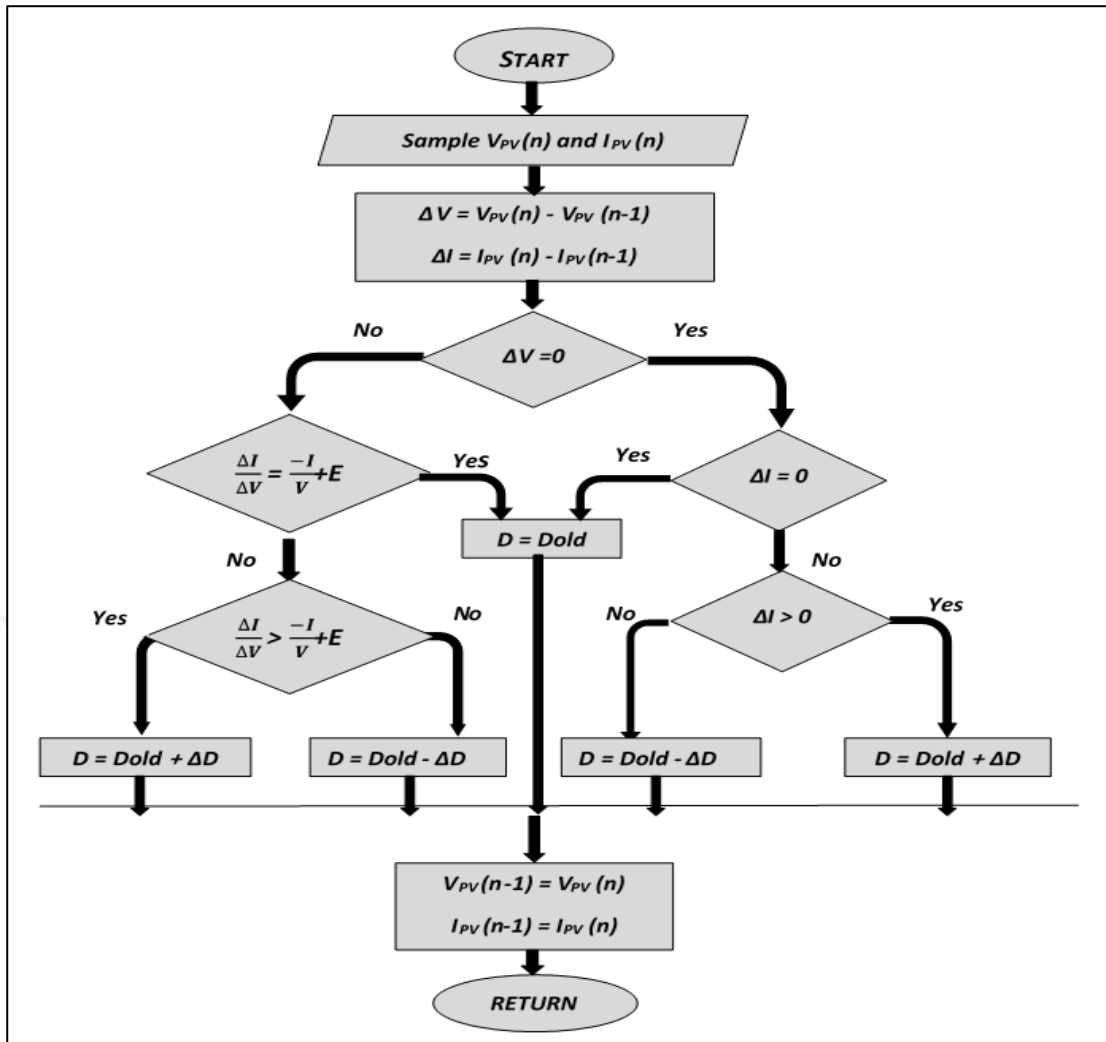
Figure 2.9 Hill Climbing Algorithms: Incremental Conductance (InC)

The operation of P&O algorithm depends on fact that the difference of power at maximum power point is zero ($\Delta P = 0$). The operation of this algorithm is initialized by observing the current operating point of PV panel at instant (n) as V(n) and I(n). PV power at instant (n) is calculated as P(n) = V(n) * I(n). Then, the operating point is perturbed in certain direction along P-V curve of PV panel. The new operating point at (n+1) is observed as V(n+1) and I(n+1). The power at instant (n+1) is calculated as P(n+1). The operating point at instants (n) and (n+1) are compared and ΔV and ΔP between them are calculated. Depending on the signs of ΔP and ΔV the direction of new perturbation is determined. This process continues until ΔP reaches zero. In practical, there is steady state oscillation of power around MPP; thus, MPP is detected when ΔP is within the tolerance band [14].

In the InC algorithm, the operation depends on the fact that the derivative of conductance at MPP is equal to the negative instantaneous conductance. The operation

13

of this algorithm is initialized by sensing the operating point of PV panel at successive (n) and (n+1) instants [15].

Depending on these operating points, the incremental conductance is calculated as (ΔI / ΔV) and compared to the instantaneous conductance (I /V). The process continues until the incremental conductance equals the negative instantaneous conductance ((ΔI / ΔV) = (-I /V)). In practical, there is steady state oscillation of power around MPP; thus, MPP is detected when ((ΔI / ΔV) + (I /V)) is within the tolerance band [15].

- Advantages
  - These algorithms are the most popular used MPPT algorithms for low power applications. This is because of their low cost due the acceptable number of sensors that are required. In addition, the implementation of these algorithms can be performed easily [14].
  - These algorithms have an acceptable speed of tracking under normal environment. The speed of tracking can be improved by adjusting step size of tracking. However, adjusting step size affects oscillation of power around MPP. Therefore, when step size is chosen, there should be a trade-off between speed of tracking and oscillation of power [15].
- Disadvantage
  - These algorithms have oscillatory behavior around the MPP, which results in decreasing the tracking efficiency of these algorithms. In addition, these oscillation causes instability in the output power [14].
  - These algorithms have unacceptable performance in some special cases of environmental conditions such as rapid changing and partial shading conditions [15].

2.2.2 Soft Computing Algorithms

The most important algorithms of this group are Fuzzy Logic Controller (FLC) and Artificial Neural Network (ANN) that are shown in Figures 2.10 and 2.11 respectively. The fuzzy logic MPPT controller consists of fuzzification, fuzzy inference, and de-fuzzification processes. In the fuzzification process, the input to FLC is mapped into fuzzy sets. These inputs can be ΔP and ΔV of PV pane. In fuzzy inference process, the fuzzy sets are related through fuzzy rule table. The table of rule should be provided by expertise who can construct it from experience and practical measurements [16].
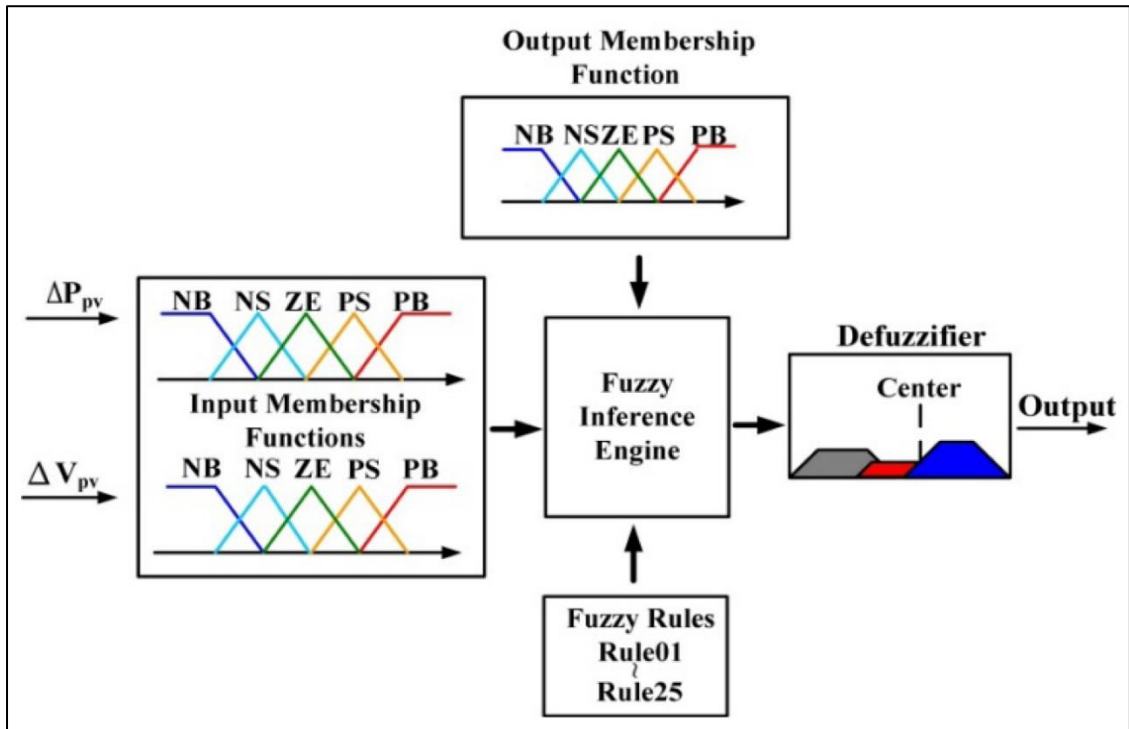
Figure 2.10 Soft Computing Algorithms: Fuzzy Logic Controller (FLC). [17]
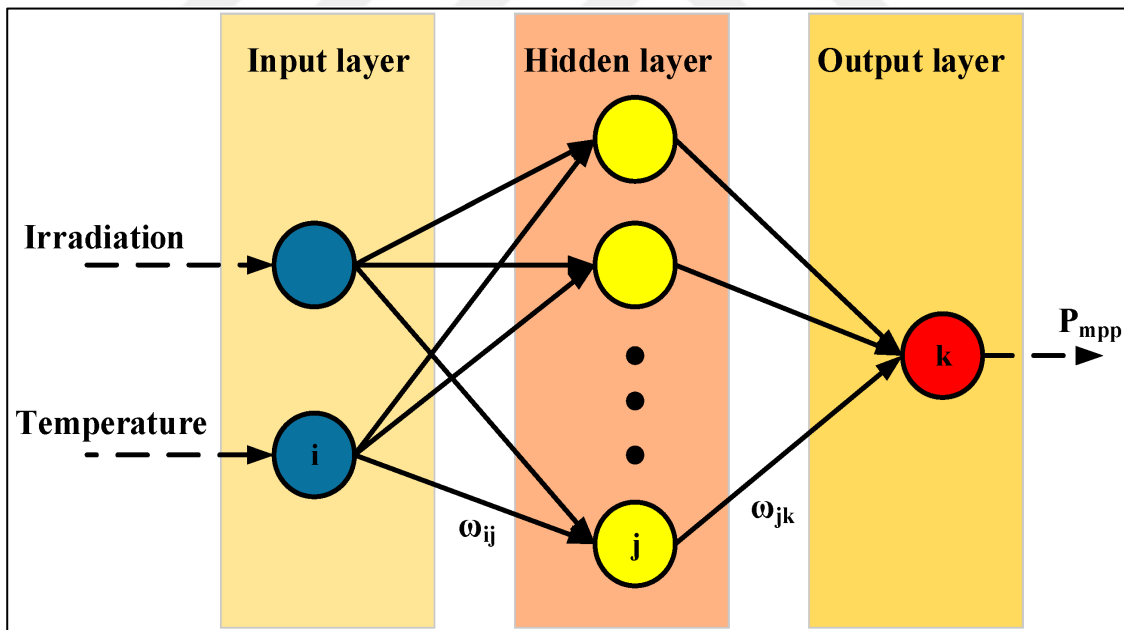
Figure 2.11 Soft Computing Algorithms: Artificial Neural Network (ANN). [18]

Depending on this rule, the fuzzy set of inferred control signals are determined. In defuzzification, the fuzzy sets of inferred control signals are mapped into unfuzzy control signals which can be used to control the operating point of system in a way that

ensures the working of PV panel at MPP. This controller provides high tracking speed with reduced oscillation of power [16].

Artificial Neural network consists of three layer which are feedforward neuron input layer, intermediate hidden layer, and output layer. The neurons in each layer are connected fully to other neurons in the successive layer. The operation of ANN controller depends mainly on learning process of ANN. In the learning process, the network is provided with training data that represent the possible cases of inputs and associated outputs. Inputs data can be PV panel parameters and environmental conditions. The training data is provided by expertise who can obtain them from experience or measurements. This controller provides robust performance with high tracking speed [19].

- Advantages:
  - These algorithms have more robust, flexible, efficient, and stable performance among other MPPT algorithms. In addition, these algorithms have a fast tracking capability [16], [19].
  - These algorithms represent high performance under some special cases of environmental conditions such as fast changing and partial shading conditions [16], [19].
- Disadvantage
  - These accuracy and efficiency of these algorithms depends on the data that should be provided by expertise. Therefore, the application of these algorithms requires experience [19], [20].
  - The implementation of these algorithms is tricky and expensive. This can be shown through the number of sensors and complex algorithms that are required [19], [20].

2.2.3 Approximate Algorithms

The most important algorithms of this group are Fractional Short Circuit (FSC) and Fractional Open Circuit Voltage (FOV) that are shown in Figures 2.12 and 2.13 respectively. The operation of these algorithms depend on approximating the maximum power point (MPP) of P-V curve by percentage of short circuit current (I_{SC}) and open circuit voltage (V_{OC}) of PV panel respectively. The selection of the value of percentage of I_{SC} and V_{OC}, is depending on experience and practical measurements.
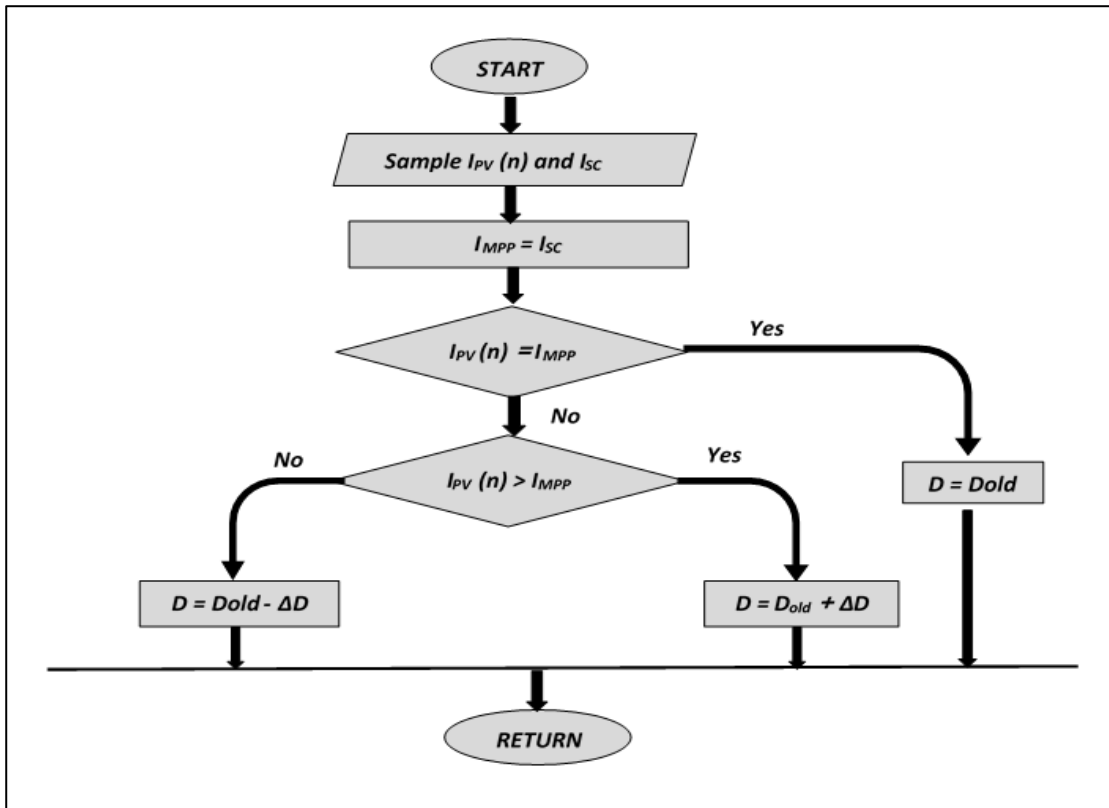
Figure 2.12 Approximate Algorithms: Fractional Short Circuit (FSC)
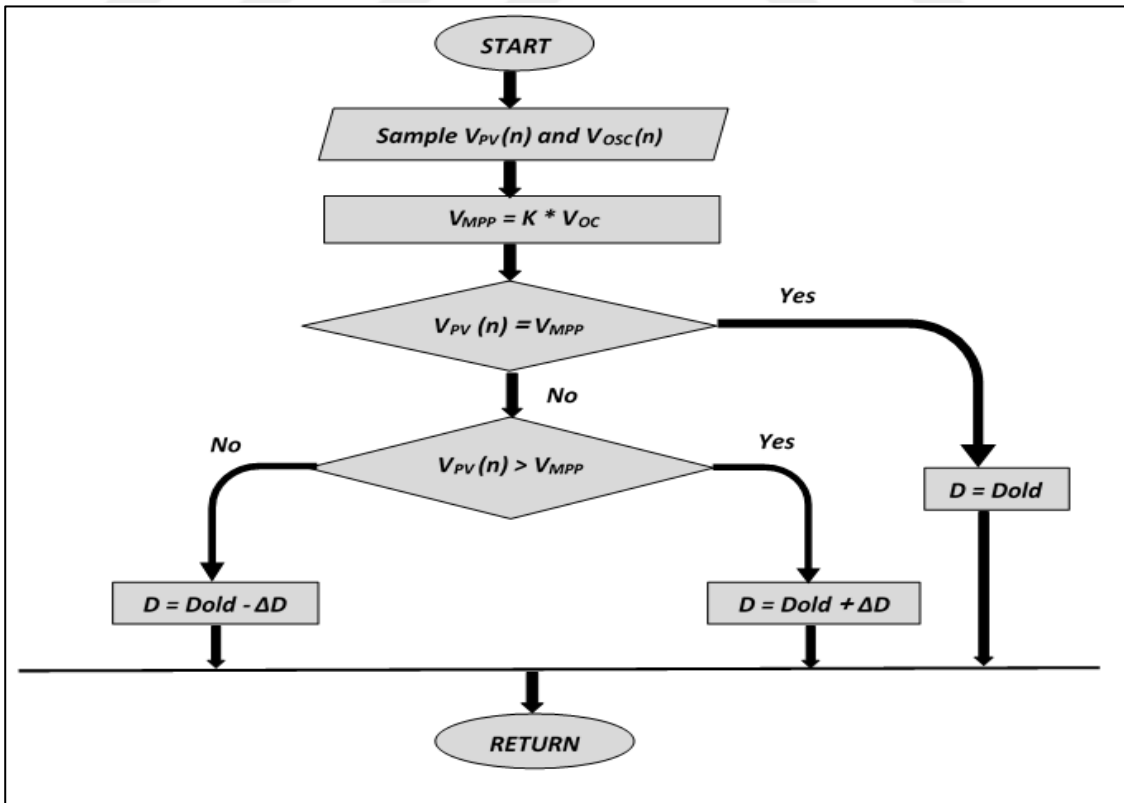
Figure 2.13 Approximate Algorithms: Fractional Open Circuit Voltage (FOV)

In FSC algorithm, the operation is initialized by sensing the I_{SC} and I_{PV} at instant (n). The maximum power current (I_{MPP}) is determined as equal to I_{SC}, and is compared to I_{PV}. This process continues until maximum power current equals the current of PV panel ($I_{MPP} = I_{PV}$) [21].

In FOV algorithm, the operation is initialized by sensing the V_{OC} and V_{PV} at instant (n). The maximum power voltage (V_{MPP}) is determined as percentage (K) of V_{OC}, and is compared to V_{PV}. This process continues until maximum power point voltage equals the voltage of PV panel ($V_{MPP} = V_{PV}$). The measure of I_{SC} of PV panel require that terminals of PV panel to be shorted, which means the loss of supplied PV power temporarily [22].

- Advantages:
  - These algorithms do offer a reliable and lower cost solution because of fewer sensors and simpler algorithm required for implementation [21], [22].
  - These algorithms have advantage on low irradiance conditions, where the P-V curve is flat and determination of maximum power point is hard [21], [22].
- Disadvantage
  - These algorithms have a lower tracking efficiency in environmental conditions under consideration. In addition, they have bad performance in some special cases of environmental conditions such as fast changing or partial shading conditions [21], [22].
  - These algorithms cause a temporary loss of the power that is supplied to load by PV system. This is because of measurements of ISC and VOC that require the PV panel terminals to be short circuited and open circuited respectively [21], [22].

2.2.4 Comparison of Different MPPT Algorithms

Table 3.1 shows a general comparison between different groups of MPPT algorithms that have been discussed. This comparison depends on the discussion that have been done in previous section. As can be shown in this table, the Hill Climbing algorithms represent a good choice because of its low cost and acceptable performance as compared to other categories of algorithms, especially for low power applications. The other categories represent a perfect choice in certain conditions of environments, such as shading and low irradiance conditions.

Table 2.2 Comparison of Different MPPT Algorithms

Items	Hill Climbing Algorithms	Soft Computing Algorithms	Approximate Algorithms
Complexity of Algorithm	Moderate Complexity	High Complexity	Low complexity
Implementation of Algorithm	Implementation is Easy	Implementation is Hard	Implementation is Easy
Tracking speed of MPP	Moderate tracking Speed	High Tracking Speed	NOT Track MPP
Steady State Oscillation	High Oscillation around MPP	Low Oscillation around MPP	NOT Work at MPP
Performance under Shading conditions	Low Performance	High Performance	Bad Performance
Cost of implementation	Moderate Cost	High Cost	Low Cost

2.3 DC-DC Converter

In this research, DC-DC converter is used as interface unit between PV panel and battery bank. It has the capability of working as MPPT tracker or battery charger system depending on the required mode of operation. According to the required mode of operation, the duty cycle of DC-DC converter is adjusted, continuously, by considering the optimum operating point that is determined by MPPT algorithm, charging algorithm, or combined algorithm of them. In the following sections a brief discussion on the most important types of topologies of DC-DC converter is presented.

2.3.1 DC-DC Converter Topology

There are many types of topologies that can be used in PV system. The selection of a certain topology depends mainly on the application under consideration. These topologies can be categorized basically into isolated and non-isolated DC-DC converters. This categorization relays on capability of DC-DC converter in providing an electrical isolation between input and output of it. In this research, the considered application does not have isolation requirements. So, non-isolated DC-DC converter is investigated in more details.

Several topologies of non-isolated DC-DC converter can be used in PV system application. The most common types of these topologies are Buck, Boost, Buck-Boost, Cuk, and SPEIC converters. These converters differ in term of conversion efficiency, range of work, MPPT capability, number of required switches, requirements of required filters, complexity, ease of implementation, and cost [23].

Figures 2.14 and 2.15 shows the equivalent circuits of Buck and Boost topologies of DC-DC converter. As can be shown, these topologies require single diode and single active switch in performing their functions. The main difference between these topologies is the range of work. The range of work of boost converter is in voltages that are higher than input source voltage, whereas, buck converter works in range of voltage that are lower than input source voltage. In addition, filter requirements of boost converter are high in the output side as compared to input side, because of the inductor that is found in the input side. However, filter requirements of buck converter are high in input side as compared to output side, because of the inductor that is found in the output side [23].
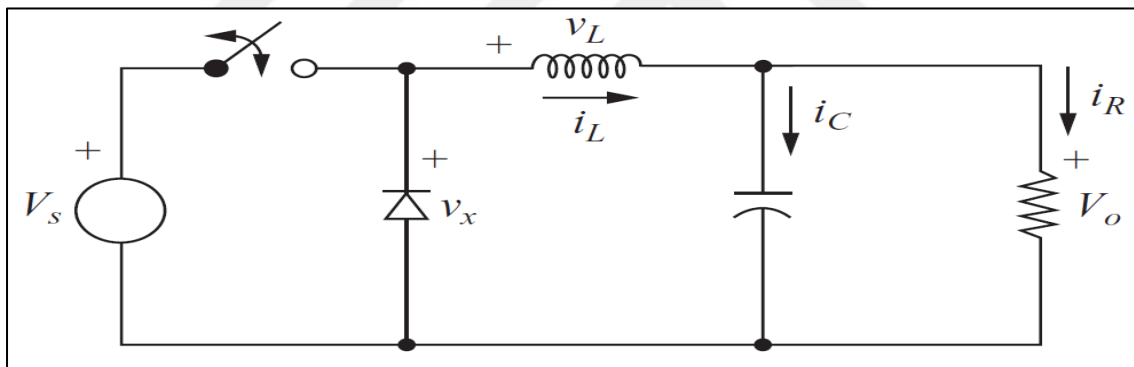
Figure 2.14 Equivalent circuit of Buck DC-DC Converter Topology
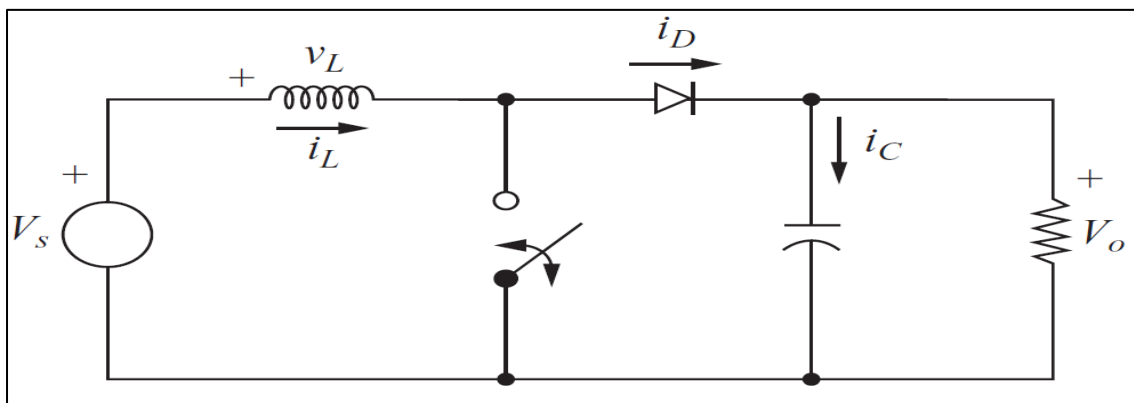
Figure 2.15 Equivalent circuit of DC-DC .Boost Converter Topology.

The advantages of Buck and Boost converters can be combined in single topology that is called Buck-Boost topology as shown in Figure 2.16. This topology require single diode and single active switch in performing its function. In addition, it has the capability of working in range of voltage that can be lower of higher than input source voltage. Furthermore, filter requirements are high in input and output side because of the location of inductor in middle of the circuit. The main disadvantage of this topology is the reverse polarity of output voltage, which may not be accepted in some application [23].
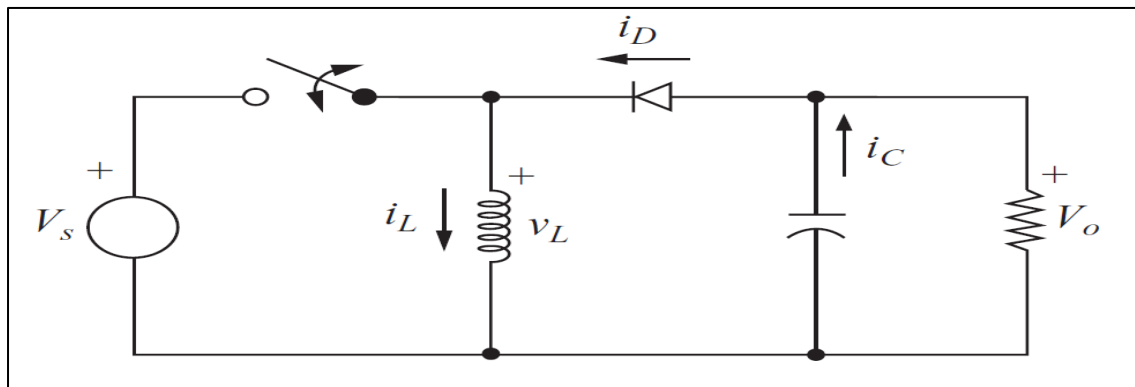
Figure 2.26 Equivalent circuit of DC-DC Buck-Boost Converter Topology

In order to decrease the filter requirements of Buck-Boost converter, Cuk converter have been proposed, which has equivalent circuit as shown in Figure 2.17. It has the same range of work of voltage and reverse polarity of output voltage as Buck-Boost converter. The main difference of Cuk converter is the existence of an inductor in both side of converter that decrease the ripples in input and output circuits. In addition, this topology uses an extra capacitor as storage energy instead of inductor, which increases the number of components of this topology [23].
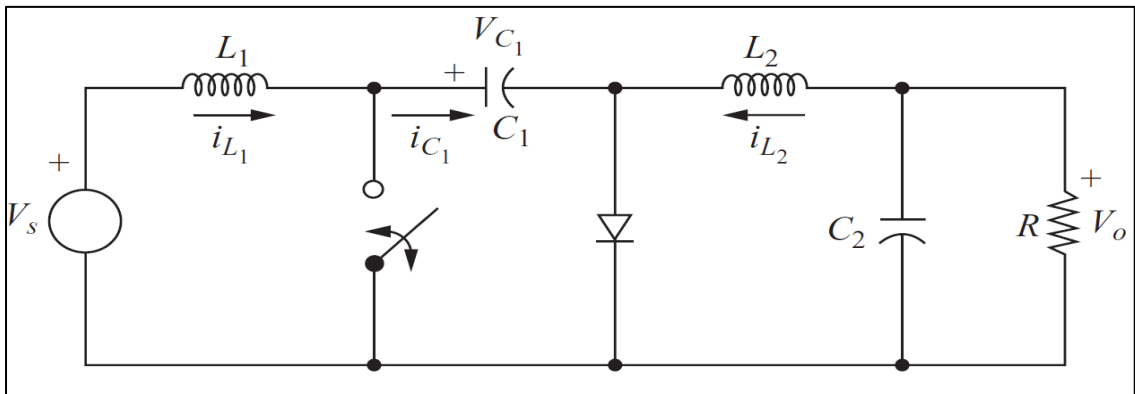
Figure 2.17 Equivalent circuit of DC-DC Cuk Converter Topology.

21

Figure 2.18 shows the equivalent circuit of SEPIC converter that is considered as improved topology of Cuk converter. The main advantage of this topology is the non-reversed polarity of output voltage as compared to input voltage. In addition, the filter requirements of SEPIC converter are lower than Cuk converter [23].
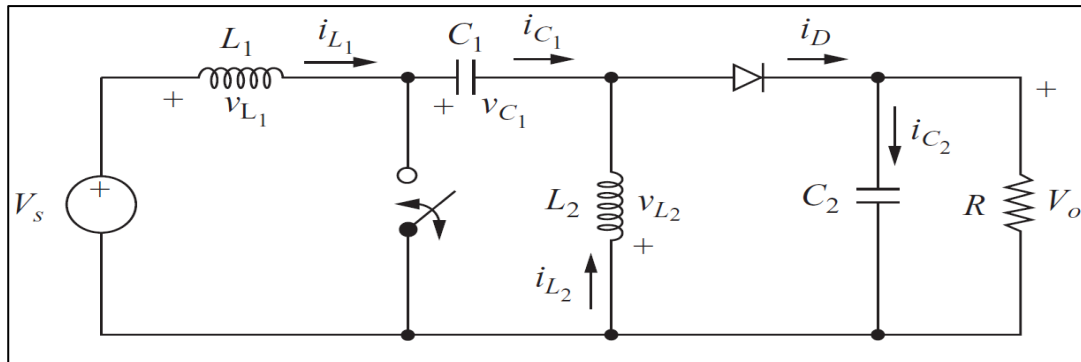
Figure 2.38 Equivalent circuit of DC-DC SEPIC Converter Topology

2.3.2 Comparison of Different Converter Topologies

In literature, many comparative studies have been made between different topologies of non-isolated DC-DC converter that can be used in PV system. In [24], a comparative analysis has presented a comparison between Boost and Buck converters that are applied as MPPT tracker in PV system. The comparison has focused on the tracking and conversion efficiencies of these topologies under different MPPT algorithms. According to this comparison, Boost converter has superiority on buck converters; since it can track MPP with distinct tracking efficiency, and higher conversion efficiency.

Another comparison between buck, boost, and buck-boost converters has been presented in [25].This comparison has focused on the capability of DC-DC converter topologies in tracking MPP of PV panel under different conditions of load. According to this comparison, Buck-Bust converters has preference on Boost and Buck converters; since it can track MPP under different conditions, regardless of operating point of load that can range from V_{OC} to I_{SC} along I-V curve of PV panel. However, Boost and Buck converters have limited capability of tracking that can range from I_{SC} to MPP along I-V curve for Boost converter, and V_{OC} to MPP along I-V curve for buck converter.

In [26], a comparison between boost, Cuk, and SEPIC converters has been presented. This comparison has focused on performance of these converters as MPP tracker under different conditions. In this comparison, the performance of DC-DC converter has been determined depending on tracking speed, stability of output power, and ripple of PV

power factors. According to this comparison, SEPIC converter provides a high stability of output power with less ripples as compared to other converters. Whereas, Boost converter provides a fast speed of tracking of MPP with good stability of output power. In the contrary, Cuk converter provides output power that is unstable. In addition, it provides reversed-polarity output with high ripples as compared to other converters.

Table 2.2 shows a general comparison between different types of non-isolated DC-DC converter that have been discussed. This comparison depends on previous comparative studies that have listed above, and the discussion that have been done previously.

Table 2.2 Comparison of Different DC-DC Converter

Item	Buck Converter	Boost Converter	Buck-Boost Converter	Cuk Converter	SEPIC Converter
Number of component	less Number	less Number	less Number	More Number	More Number
Range of Work of Voltage	Lower than input voltage	Higher than input voltage	Higher or lower than input voltage	Higher or lower than input voltage	Higher or lower than input voltage
Filter Requirement	High in input side	High in output side	High in both side	low in both side	High in both side
Reverse of output voltage	Not-reversed	Not-reversed	reversed	reversed	Not-reversed
Stability of output power	Low stability	High stability	Low stability	Low stability	High stability
Tracking Efficiency	Low Tacking efficiency	High Tacking efficiency	High Tacking efficiency	Low Tacking efficiency	High Tacking efficiency
Conversion Efficiency	Low conversion efficiency	High conversion efficiency	Low conversion efficiency	Low conversion efficiency	High conversion efficiency
Range of MPPT Tracking along I-V Curve	MPPT can be tracked in the range from I_{SC} to MPP	MPPT can be tracked in the range from V_{OC} to MPP	MPPT can be tracked in the range from I_{SC} to V_{OC}	MPPT can be tracked in the range from I_{SC} to V_{OC}	MPPT can be tracked in the range from I_{SC} to V_{OC}
Cost	Low cost	Low cost	Low cost	High cost	High cost

2.4　Battery

2.4.1　Overview

Generally, level of solar radiation changes during a sunny day. In accordance with this changing of solar radiation, the power that can be extracted from PV panel gets affected. Consequently, when PV panel is used to supply a certain load, PV power may be greater or lower than the required power of load according to the level of radiation. This may result in reducing performance of load during low radiation level condition. In order to maintain the required performance of load and increase reliability of PV system in providing the required power under different level of condition, rechargeable battery is used in PV supply system as a secondary sources of energy as shown in Figure 2.19. In this system, battery is charged when generated power is higher than load power, and discharged to the load when generated power is lower than load power [27].
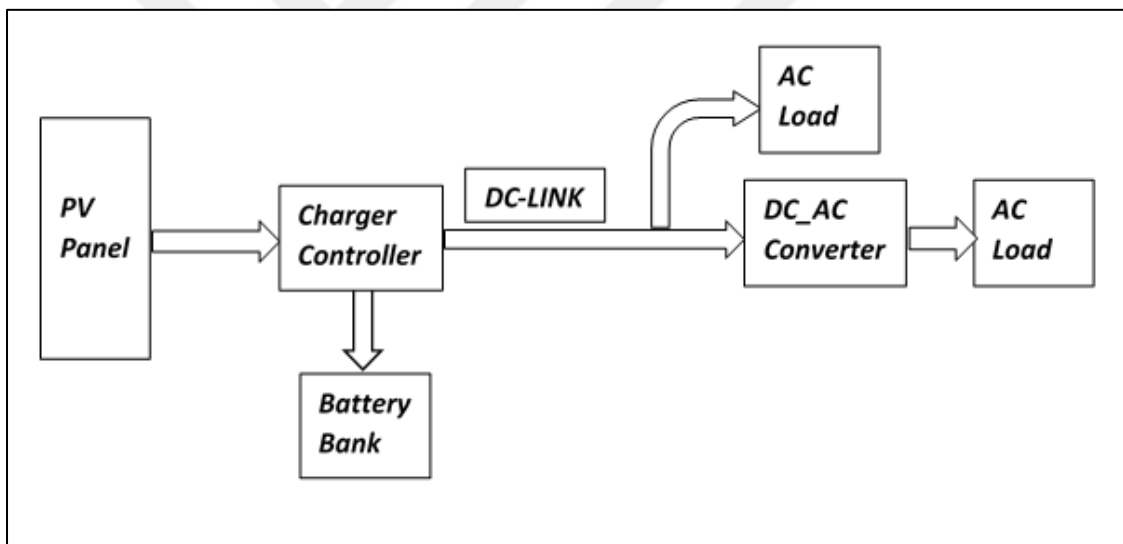
Figure 2.49 Connection of Battery in Stand-Alone PV System as Secondary Source of Energy

In addition, in most low power application, battery is used to get rid of voltage stresses of DC-link that feed inverter and increase reliability of system. In this case, battery is connected as a main source of energy as shown in Figure 2.20. In these system, battery is considered as source of power that supplies DC and AC load [28].

As can be shown in Figure 2.20, battery is charged by PV panel through charger controller which is used to meet charging requirements of battery. Therefore, including battery charger controller in the design process of PV system is essential in order to

improve the performance of battery, and reduce cost of maintenance and replacement of battery that may be required in case of improper charging and damage of battery.
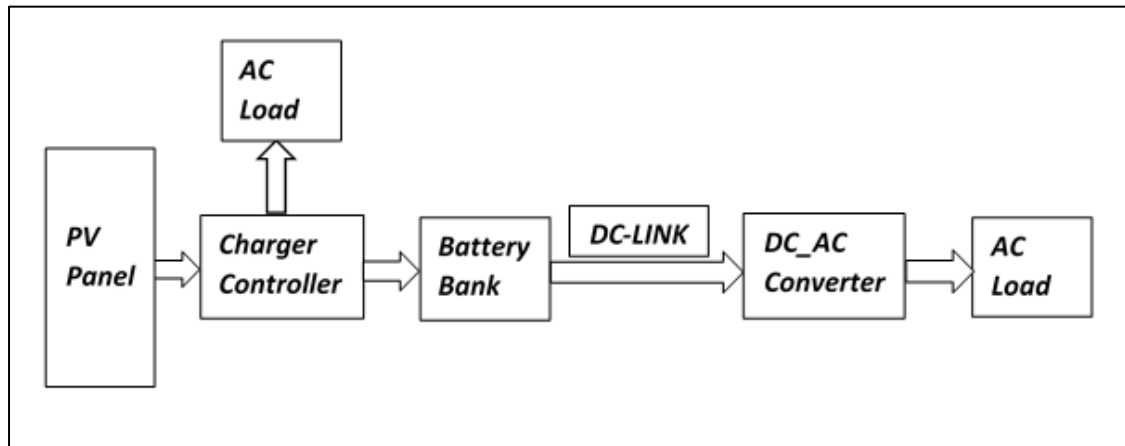
Figure 2.20 Connection of Battery in Stand-Alone PV System as Maın Source of Energy

There are several types of batteries that are used in different field of applications. These types of batteries differ in terms of materials of manufacturing, power density/kg, and power density/m3, ability of recharge, life cycle, and cost. In the field of solar PV system, four types of batteries are dominated which are Lead Acid, Nickel Cadmium (Ni-Cd), Nickel Metal Hydride (Ni-MH), and Lithium Ion (Li-ion) batteries [27], [28].

In practice, Lead Acid battery is the very common in PV application. This is because of its low cost and acceptable performance in most applications. However, Lead Acid battery has many limitations and requirements of charging process that should be taken into account when designing PV system. These requirements emphasize fully charged condition and protect battery from degradation and damage [8], [29].

In this research, Lead Acid battery will be considered in more details. Parameters that can affect the proper operation of Lead Acid battery will be analyzed and the essential requirements of charging will be determined. This analysis is important in order to develop a proper charge controller that can be applied in PV system.

2.4.2 Battery Parameters Analysis

Performance of rechargeable battery is determined mainly by number of parameters. Some of these parameters are related to battery charging process and others are related to battery discharging process. In this research, charging of battery by PV solar system is under consideration. Therefore, parameters that affect the charging process of Lead

Acid battery taken into account when battery charger is designed in order to insure the high performance of battery and protect it from degradation and damage. These parameters are explained in the following points.

2.4.2.1 Battery Charging Voltage

Battery voltage is critical on performance of Lead Acid batteries because of its effects on chemical process of these batteries. So, battery voltage should be considered carefully during charging process of battery. Figure 2.21 shows normal charging profile of Lead Acid battery. As can be shown, battery voltage increases during charging process from minimum value to maximum value. These minimum and maximum values represent fully discharge state and fully charge state of battery respectively. The rate of increase of battery voltage depends of the value of charging current; thus the value of maximum battery voltage is affected by charging current [29], [30].
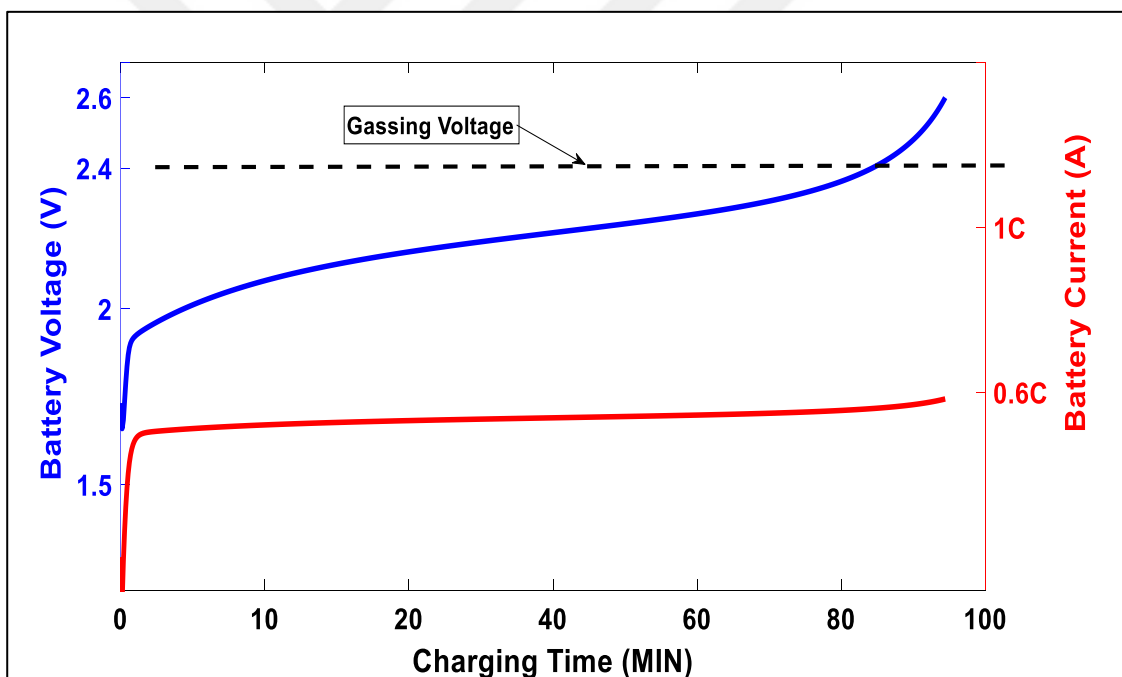
Figure 2.21 Normal Charging Profile of Lead Acid battery

The maximum value of battery voltage has an important role in performance of rechargeable battery. For Lead Acid battery, the maximum value of battery voltage should not exceed the gassing voltage value which represent the value at which gases form in chemistry of battery. Charging of battery to maximum value that is larger than gassing voltage results in increasing temperature, watering process, gassing and corrosion of battery. In the contrary, charging of battery to maximum value that is lower

than gassing voltage increases sulfation of battery, which takes place when a Lead Acid battery is deprived of being a full charged for a long time. In addition, ripples of maximum value of battery voltage should be limited to be within allowed limits that are provided by manufacturers; otherwise, they may affect battery hardly [29], [30], [31].

2.4.2.2 Battery Charging Current

As stated previously, the performance of battery voltage is determined basically by charging current. When charging current is high, the maximum value of battery voltage increases and charging time decreases. However, high charge current causes an increase in cell temperature, which may cause damage of battery [30], [31].

Normally, battery manufactures provide recommended values of charge current for different types of batteries. For Lead Acid battery, these values is ranging from 0.3C to 1C; where C-rate is the ability of battery to deliver the stored energy over a given period [30], [32].

Practically, the level of charging current is affected by temperature of environment. However, in this research, effect of environment temperature has been ignored on PV characteristics curves. As a result, the level of charging current is assumed to be constant irrespective of environment temperature

Figure 2.22 shows charge profile of Lead Acid battery under different value of charge currents. As shown in this figure, when charge current decreases, the voltage of battery decrease with respect of it. This decrease in battery voltage results in increasing time required to reach maximum value; so, charging process time is increased.
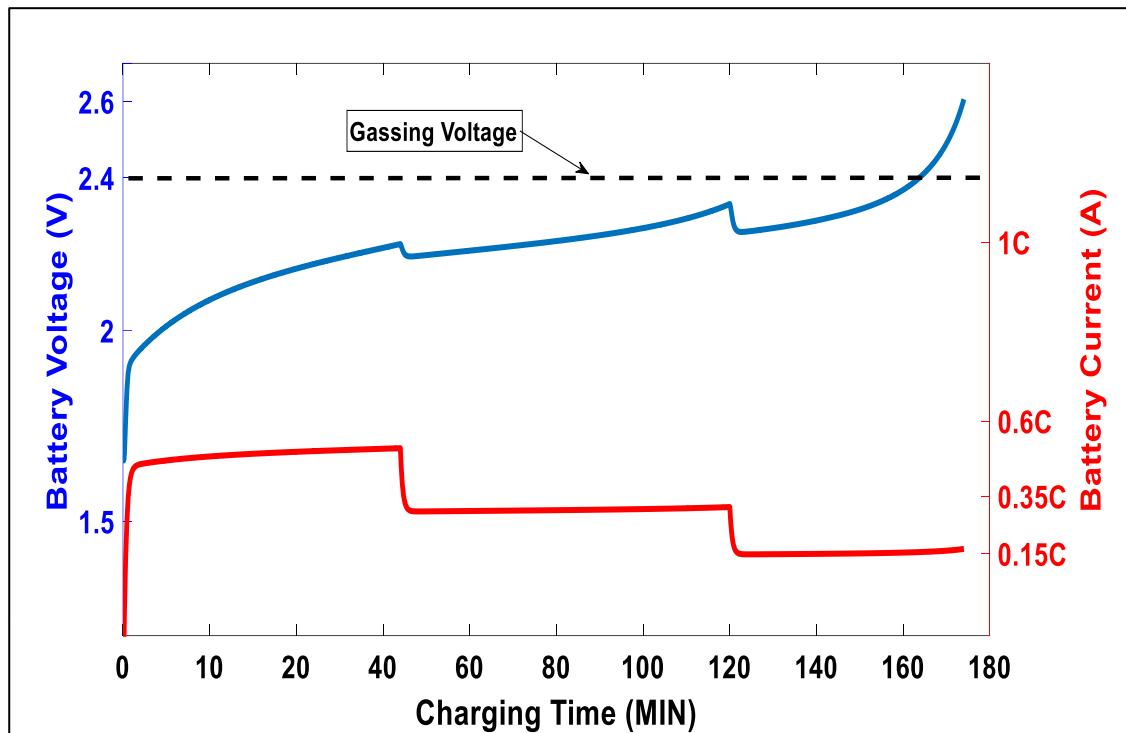
Figure 2.22 Charge Profile of Lead Acid Battery under variable Charge Currents

2.4.2.3 Battery State of Charge (SOC)

As stated previously, the charge process of batteries is performed over a period of time. Through this period, the voltage of battery changes with respect to the level of charge of battery. Consequentially, it is essential to indicate the level of charge of battery at any moment; in order to determine the effect of battery voltage value on charging process of battery. An important parameter that is used to describe the level of charge is State of Charge (SOC) of battery. SOC is defined as the rate of available battery capacity in specific moment in relative to rated capacity of battery under consideration. SOC of battery is ranging from 0% to 100% for fully discharged and fully charged battery respectively [32].

Figure 2.23 shows the relation between battery voltage, charge current, and SOC of Lead Acid battery. As can be shown in this figure, at specific SOC of battery, increasing the charge current results in increasing the voltage of battery and versa vice. In addition, at specific charge current of battery, increasing SOC results in increasing the battery voltage and versa vice. Furthermore, at specific charge voltage of battery, increasing charge current results in increasing the SOC of battery voltage and versa vice.

28
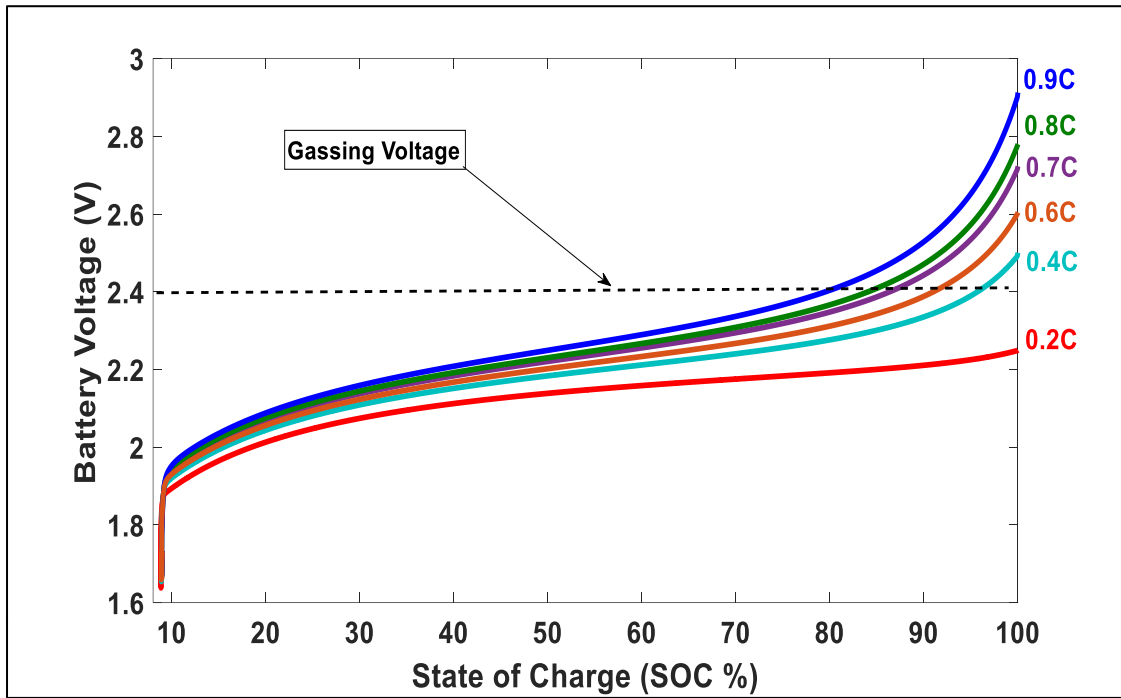
Figure 2.23 Relation between Charge Voltage, Charge Current, and State of Charge of Lead Acid Battery

In addition, increasing charging current results in decreasing charging time and increasing maximum value of battery voltage that corresponds to fully charge of battery (100% SOC). When maximum value of battery voltage is larger than gassing voltage, the battery voltage reaches the gassing value before fully charged state is reached. In this case, further charging of battery over gassing value to reach fully charged state causes overcharging and damage of battery.

2.4.3   Charging Algorithms of Battery

As stated previously, the charging process of battery should be controlled according to parameters that have been explained; in order to ensure the fully charge of battery and protect it from damage. The control of charging process is performed by using algorithm that performs the required charging of battery.

In literature, many charging algorithms of battery have been proposed for different types of batteries as in [33], [34], and [35]. These algorithms differ in terms of complexity, number of required sensors, detection of full SOC, cost, and effectiveness. For Lead Acid batteries, the most applicable algorithm for charging battery is Constant Current and Constant Voltage (CC-CV).

Figure 2.24 shows the charging profile of practical CC-CV charging algorithm that will be used in this research. This algorithm consists of three successive stages that are pre-charging, constant current, and constant voltage stages [33].
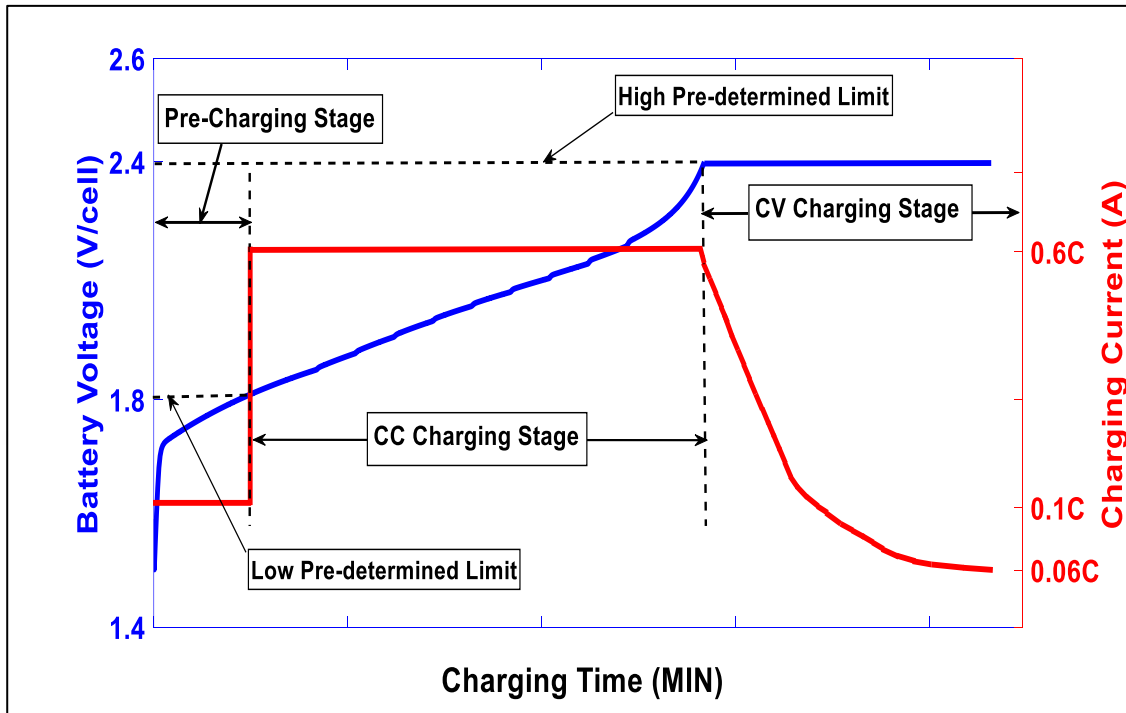
Figure 2.24 Practical Charging Profile of CC-CV Charging Algorithm

As can be shown in Figure 2.24, there are two predetermined limits of battery voltage that determine the activated stage of CC-CV algorithm. These limits are low pre-determined limit (V_{low_limit}) and high pre-determined limit (V_{high_limit}) which are generally provided by manufacturers and ranging from 1,75 to 1,85 per cell for V_{low_limit}, and from 2,3 to 2,45 per cell for V_{high_limit} [36], [37].

Pre-charging stage is activated when battery voltage is lower than V_{low_limit}. In this stage, the battery is deep discharged, so it is required to restore charge slowly in order to ensure the safe operation of system. Therefore, the battery is charged with minimum value of charging current that increases battery voltage slowly. The value of minimum charging current has a value ranging from (1/100) C to (1/500) C depending on manufacturer. This stage ends up when battery voltage reaches low predetermined voltage V_{low_limit}, and leaves battery with SOC of 10-20% [36], [37].

Constant current stage is activated when battery voltage is between V_{low_limit} and V_{high_limit}. In this stage, the battery is charged with maximum available charge current which causes battery voltage increases gradually. This stage ends up when battery

voltage reaches high predetermined limit V_{high_limit}, and leaves battery with SOC of 75-85%. The remaining of SOC of battery is provided by applying constant voltage stage of charging algorithm [36], [37].

Constant voltage stage is activated when battery voltage is higher than V_{high_limit}. In this stage, the battery is charged with constant voltage, which is high predetermined limit of voltage. Through this stage, current of battery decreases gradually with increase of SOC. This stage ends up when battery current reaches minimum value that is normally 10% of charge current in CC stage, and leaves battery with SOC of 100% [36], [37].

2.5 Connections and Charging Requirements of Battery Charged By PV Solar System

Availability of energy storage system, such as batteries, enables PV panels to be used in stand-alone solar system. These batteries store energy, which is supplied by PV system, in order to either supply load when PV panel has not enough energy, because of low irradiance, or supply load continuously as source of energy. In both case of application, battery will be charged by PV system for high performance and reliability of stand-alone system. However, charging process of battery by using PV panel should be considered carefully; otherwise battery performance might be degraded hardly and, in some cases, battery could be damaged [27].

As stated previously, charge process of battery should be performed fully and safely. This can be ensured by using changing algorithms that take into account parameters that affect the performance of battery. However, the application of these algorithms directly in PV system without considering nonlinearity of variables of PV panel could affect the performance of the whole stand-alone system. In consequence, charging of battery in stand-alone PV system should be analyzed carefully in order to determine the requirements of charging that ensure both the fully and safely charging of battery and the high performance of the whole stand-alone PV system [38].

The requirements of battery charging in PV solar System can be extracted by considering different cases of connection of battery in PV system. In this research, three connections of battery with PV panel will be considered which are direct connection of battery, connection of battery through charging system, and connection of battery through MPPT system

2.5.1 Connection of Battery Directly

Figure 2.25 shows the direct connection of battery to PV panels. In this connection, battery charger controller is not provided. As a consequence, charging process of battery is not under control, and charging algorithm is not applied in this design. The charging of battery is performed by supplying the maximum available current of PV panel into battery. The charging process ends up when battery voltage reaches maximum limited value of voltage, and leaves battery with 75-80% SOC [38].

Figure 2.25 Direct Connection of Battery to PV Panel

In addition, MPPT tracker controller is not provided in direct connection design. Therefore, operating point of battery must be compatible with MPP of PV panel in order to extract maximum power from PV panel. However, the operating point of battery through charging process is not constant because of changing of battery voltage. So, the operation of PV panel at MPP is restricted, and loss of PV power is resulted. This loss of PV power increases under changing environmental conditions [30], [38].

Charging of Lead Acid battery in this design has many disadvantages which are increase of battery sulfation, increase of battery charging time, decrease of battery cycle life, and decrease of efficiency of whole system. The main advantages of this design are low cost and ease of implementation [38].

2.5.2 Connection of Battery through Charger System

Figure 2.26 shows the connection of battery to PV panels through battery charger controller. In this connection, charging process of battery is under control, and charging algorithm is applied in this design. The charging of battery is performed by supplying the maximum available current of PV panel into battery through constant current stage. In this stage of charging, battery voltage increases until reaches maximum limited value. At this point, charging of battery continues with constant voltage stage. The charging

process ends up when battery current reaches minimum limited value, and leaves battery with 100% SOC [27], [38].
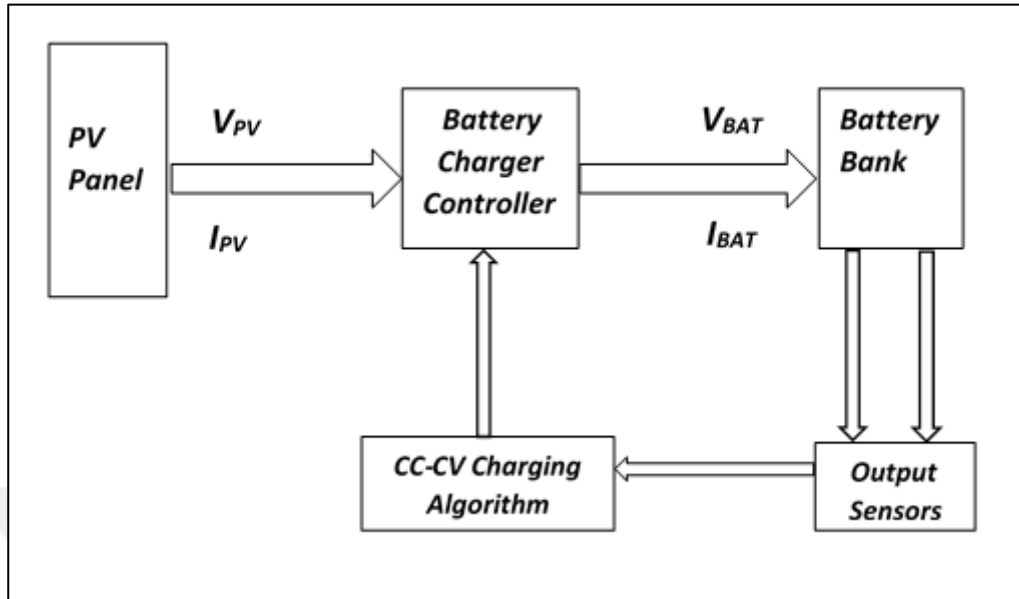
Figure 2.26 Connection of Battery to PV Panels through Battery Charger Controller

However, MPPT tracker controller is not provided in this design. Therefore, operating point of battery must be compatible with maximum power point of PV panel in order to extract maximum power from PV panel. However, because of the application of charging algorithm in this design, the operating point of battery through charging process is not constant. So, PV panel does not operate at maximum power point, and loss of PV power is resulted. This loss of PV power increases under changing environmental conditions [27].

Charging of Lead Acid battery in this design has disadvantages that are increase of charging time of battery and decrease of efficiency of whole system. The main advantages of this design are acceptable cost and increase of life of battery [38].

2.5.3   Connection of Battery through MPPT System

Figure 2.27 shows the connection of battery to PV panels through MPPT tracker controller. In this connection, battery charger controller is not provided. As a consequence, charging process of battery is not under control, and charging algorithm is not applied in this design. The charging of battery is performed by supplying the maximum available current of PV panel into battery. The charging process ends up when battery voltage reaches maximum limited value of voltage, and leaves battery with 75-80% SOC [8], [38].
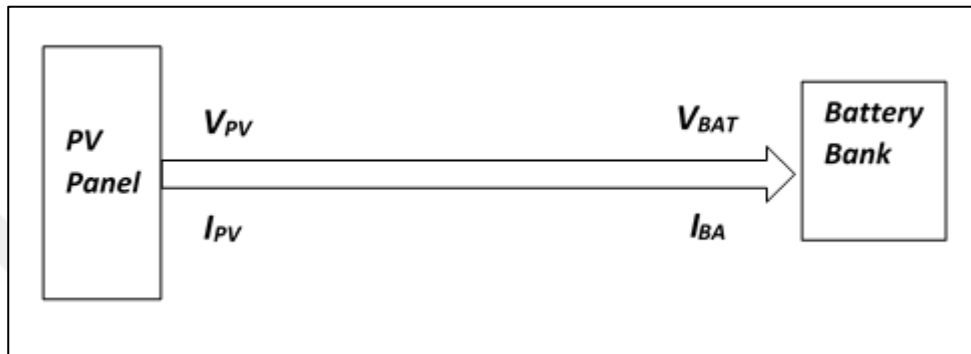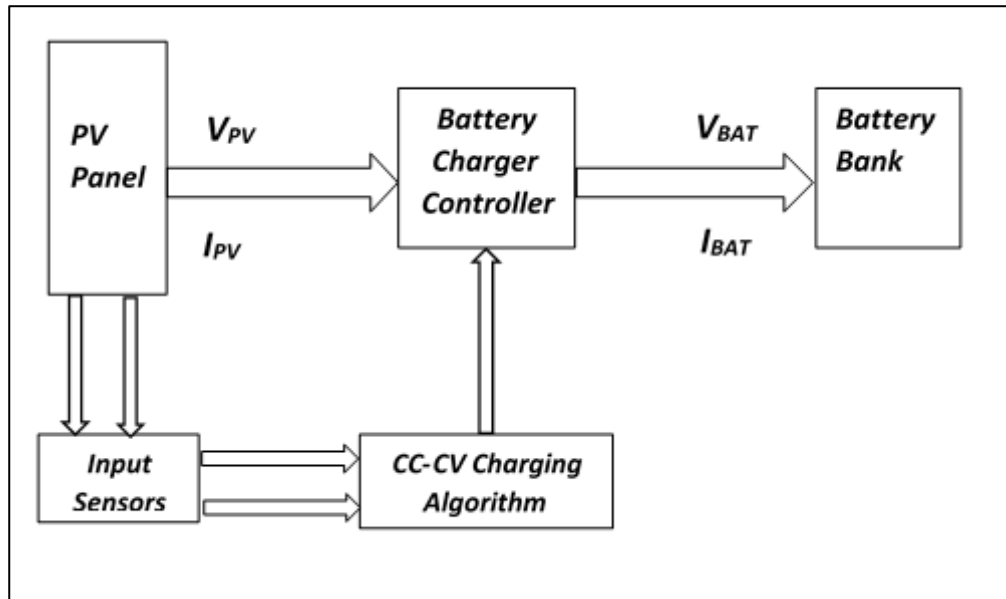
Figure 2.27 Connection of Battery to PV Panels through MPPT Controller

MPPT tracker controller is provided in this design. As a consequence, PV panel operates in maximum power point under different environmental conditions regardless of operating point of battery. Therefore, the maximum power available from PV panel is supplied continuously without losses [8].

Charging of Lead Acid battery in this design has many advantages of reducing charging time of battery and increasing efficiency of whole system. The main disadvantages of this design are higher cost and possibility of sulfation of battery [8], [38].

2.5.4   Main Requirements of Battery charging By PV Solar System

Depending on the analysis that have been done on performance of battery under different connections to PV system, the main requirements of charging of Lead-Acid battery from PV panels can be summarized in the following points:

1. The supplied PV power should be maximum under different environmental conditions in order to avoid sulfation of battery, reduce charging time, and increase efficiency of stand-alone system.
2. The charging process should be controlled in a way that ensures proper and full charging of battery without damage or degradation. In addition, control of charging process should not affect performance of PV panel and stand-alone system.

The implementation of these requirements in the design of battery charging system is topic of interest. In this research, design of MPPT controlled DC-DC converter that can

perform these requirements will be considered thoroughly. A compromise between different requirements is required in order to accomplish an accepted design of charging system as will be shown in coming chapters

DEVELOPMENT OF MPPT CONTROLLED DC-DC CONVERTER FOR SOLAR CHARGER SYSTEM

As stated in the previous chapter, the requirements of extracting maximum power of PV panel and proper charging of battery can be performed by MPPT and Charging algorithms respectively. These algorithms adjust duty cycle of DC-DC converter that controls the operating point of the stand-alone PV system. In general, the DC-DC converter is controlled to achieve either MPPT or charging function. In order to perform the MPPT and charging functions, it is required to use two stage DC-DC converters in the stand-alone system. The first stage performs MPPT function and the second stage performs the proper charging of battery. In two stage converters system, MPPT and charging algorithms are operated simultaneously and separately from each other at the expense of cost and efficiency of whole stand-alone system.

On the contrary, single stage DC-DC converter, which is called DC-DC converter simply, can be controlled to perform MPPT and charging functions with some restrictions. In this single stage system, the MPPT and charging algorithms are merged into a single algorithm that can be applied to control the single stage DC-DC converter. The operation of merged algorithm is based on the requirements that ensure the high efficiency and performance of stand-alone system. The limitations of using this single stage system can be shown through the restricted operation of DC-DC converter in performing the MPPT function through the whole duration of operation. In addition, the proper charging of battery is limited to some degree. These limitations are compensated with low cost and high efficiency of stand-alone of system. Practically, the design of single stage DC-DC converter to implement the MPPT and charging functions is restricted to the requirement of application under consideration and the acceptance of the limitations that are imposed on the operation of MPPT and charging functions.

3.1 Design requirements of MPPT controlled DC-DC converter used in charger systems

Depending on what have been discussed in previous chapters, the main requirements that have to be met during design process of MPPT controlled DC-DC converter used in solar charger system are summarized in the following points:

- The deigned system is required to have the ability of tracking maximum power point (MPP) of PV panel under different environmental conditions rapidly and efficiently. In order to accomplish that, the applied MPPT algorithm should be characterized by ease of implementation, less number of sensors, stability at steady state, high tracking efficiency ,and less costly.

- The designed system is required to charge battery bank rapidly and properly under different environmental conditions. In order to accomplish that, the applied charging algorithm should take into consideration charging of battery under low voltage and high voltage conditions of battery voltage as well as the end of charging process.

- The designed system is required to be implemented easily and low costly. In order to accomplish that low cost and efficient components should be used in the design process. In addition, control algorithm should be implemented easily and low costly.

3.2 Design Process of Developed MPPT controlled DC-DC Converter for Solar charger System

In this research, MPPT controlled DC-DC boost converter for solar battery charger system is proposed. The design of the proposed system depends on requirements that have been determined in the previous section. In this design, in order to meet the requirements of MPPT tracker and battery charger systems, an expanded MPPT algorithm is developed. The developed algorithm comprises Incremental conductance MPPT algorithm which is expanded to incorporate CC-CV charging algorithm. In addition, the design of DC-DC boost converter is based on taking into account the parameters that affect the performance of battery and PV system. The system surrounded by red lines in Figure 3.1 shows components of proposed MPPT controlled DC-DC boost converter, which is used as battery charger system. In this system, boost

DC-DC converter is used to implement the MPPT and charging functions together according to the developed algorithm.
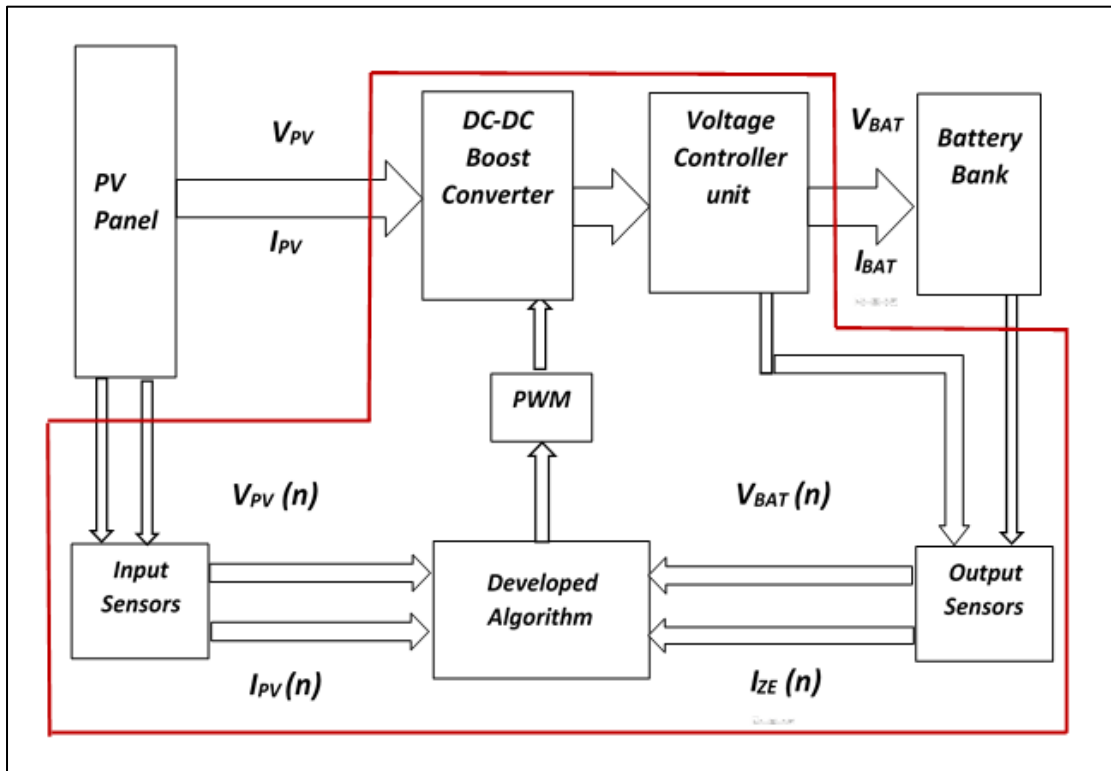
Figure 5.1 Main Components of Designed MPPT Controlled DC-DC Boost Converter for Solar Battery Charger System

The duty cycle of boost converter is adjusted directly by new developed algorithm in order to control the operating point of PV panel. Additional auxiliary components are used in this design, as shown in Figure 3.1, in order to ensure the optimum operation of developed algorithm. These auxiliary components are voltage controller unit, current sensor, and voltage sensor. The design process and operation of this proposed system are illustrated in details in the following sections.

3.2.1   Boost DC-DC Converter

According to the discussion that have been made in the types of DC-DC converter in pervious chapter, Boost converter topology is selected in this proposed system. As mention, boost converter has the ability of processing power through it with high efficiency. Furthermore, it has less rate of input ripples due to the existence of inductor in input side; thus the requirement of input filter is reduced. In addition, boost converter can be implemented easily and less costly.

The proposed boost converter is limited for applications that require higher voltage than input voltage. So, the ability of MPPT function to track the maximum power point of PV panel is restricted to the constant current portion of I-V curve of PV panel. That means variation of environmental conditions that results in operating point at constant current region of I-V curve can be tracked successfully. The model and design process of boost DC-DC converter are covered thoroughly in the following two sections.

3.2.1.1 Boost Converter Model

Boost topology is chosen for DC-DC converter since it is capable of transferring maximum energy from PV panel to load irrespective of different irradiation of sun through the day. The topology of converter is shown in Figure 3.2. It consists of dc source V_g, inductor L, power switch T, diode Di, output capacitor C, and output load R. When the switch T is in the on state, inductor stores energy that is supplied by source and the diode is off, so the load is supplied totally by the output capacitor. When the switch T is turned into off state, both the source and the stored energy in the inductor are transferred through the diode to the output load and output capacitor is charged [39].
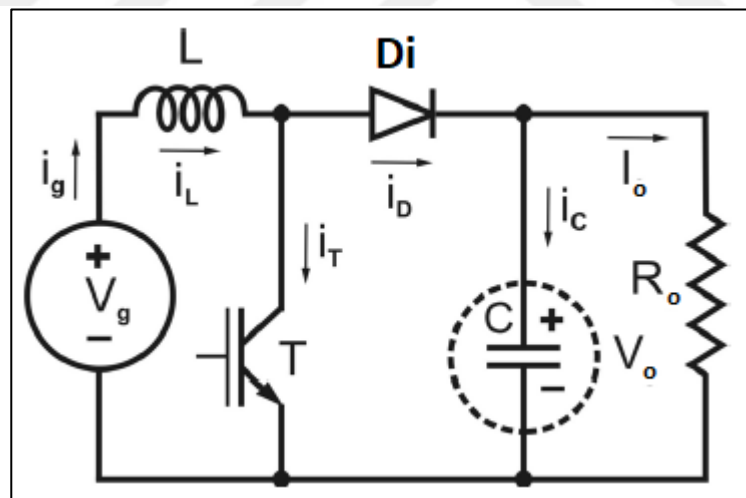
Figure 3.2 Equivalent Circuit of DC-DC Boost Converter. [40]

The waveforms of boost converter in the CCM are presented in Figure 3.3. As shown in waveform of inductor voltage and current, the inductor is supplied with source voltage V_g in the period of operation, so the current of inductor increases linearly. In the second period voltage (V_g-V_O) with reversed polarity, where V_O is the output voltage of boost converter, is induced across the inductor in order to maintain the current through inductor in the same direction, so current of inductor decreases linearly [39].

The change of inductor currents in both periods of operation (ΔILP and ΔILN) are written as in (3.1) and (3.2).

$$\Delta I_{LP} = (V_g/L)DT \qquad\qquad (3.1)$$

$$\Delta I_{LN} = (V_O - V_g/L)(1 - D)T \qquad\qquad (3.2)$$
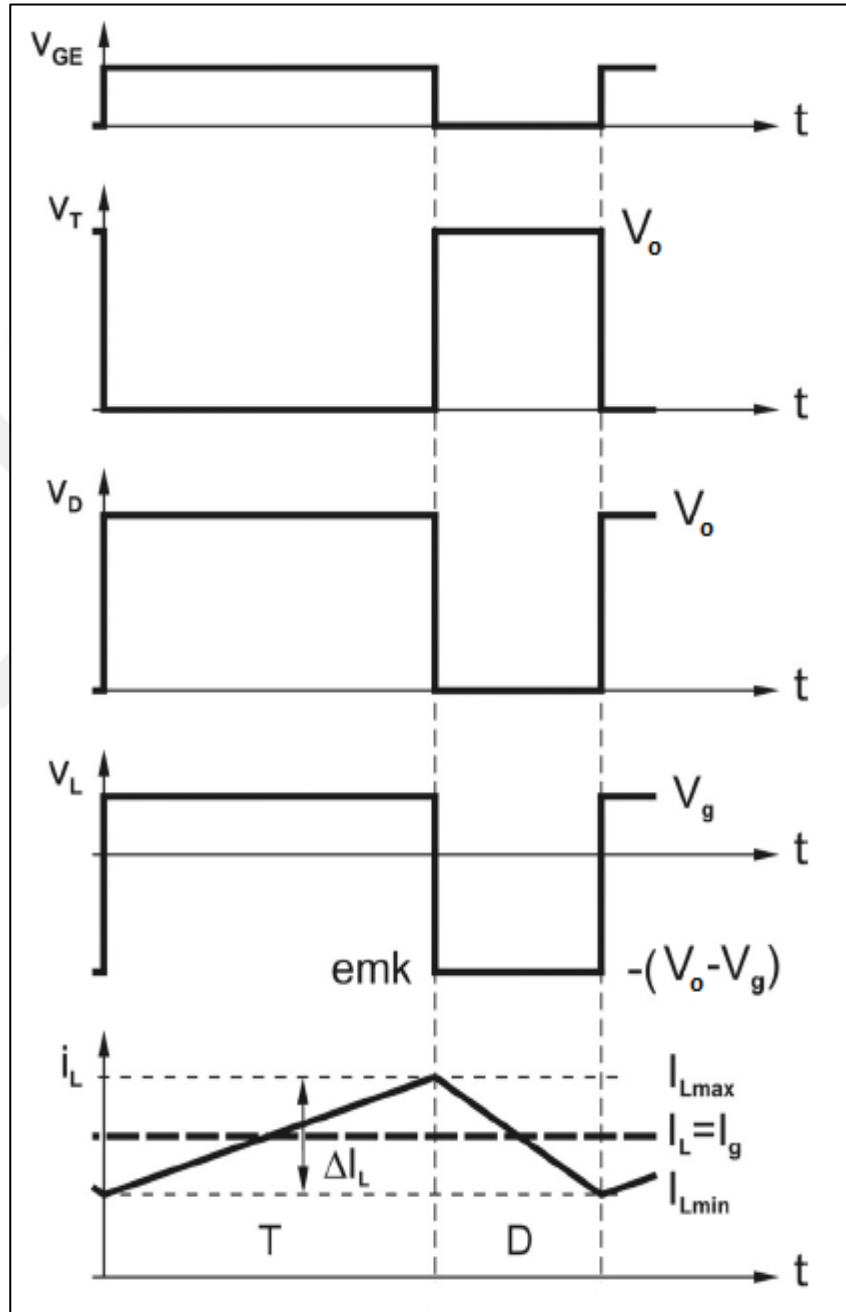
Figure 3.6 Waveform of DC-DC Boost Converter. [40]

Where D is the duty cycle of boost converter. In steady state operation, inductor voltage in both periods of operation are equal; so, the rate of change of inductor current during on-state period is equal to the rate of change during off-state period. Accordingly, (3.1)

40

and (3.2) are equal to each other and can be written as shown in (3.3).

$$V_S \, DT = (\, V_O - V_g)(1 - D)T \tag{3.3}$$

From (3.3) the average output voltage of DC-DC boost converter can be obtained as in equation (3.4).

$$V_O = (1/(1 - D)) \, V_g \tag{3.4}$$

The output voltage of the converter can be controlled between $V_S < V_O < V_{max}$, where V_{max} is the maximum required output voltage [39].

3.2.1.2 Boost Converter Design Process

To design and size the components of boost converters, many factors should be considered such as, input voltage to converter, output voltage magnitude, DC-DC converter efficiency, output voltage ripple, input power, desired output power, input current, output current and duty cycle of PWM controller. In this research, five components will be considered and chosen when boost converter is designed. These components are power switching device, diode, inductor, output capacitor, and input capacitor [39].

- Power switching device: The main switching device must withstand the maximum current and voltage stresses and also operate at the desired frequency [39].

- Diode: Diode must be characterized by capability of withstanding the required reversed off–state voltage stress as well as the maximum and average current. In addition, it must have low forward voltage drop, reduced reverse–recovery, and fast switching capability [41].

- Inductor: the design of boost inductor depends on the maximum required ripple current which is determined at minimum duty cycle and maximum input voltage. The value of boost inductor is determined for specific load as shown in (3.5), where Fs is the operating switching frequency.

$$L = (V_S * (\, V_O - V_S\,))/(\Delta I_{LP} * F_S * V_O\,) \tag{3.5}$$

Regarding the current flowing in inductor boost converter has two mode of operation depending on the value of inductance. The first mode is called continuous current mode (CCM), in which boost converter has high value of

41

inductance that is enough to produce continuous current through switching process. The other mode is called discontinuous current mode (DCM), in which boost converter has small value of inductance that produces discontinuous current through switching process. For CCM of operation, the minimum inductance required (Lmin) is calculated as in (3.6).

$$L_{MIN} = (V_S * (V_O - V_S))/(2 * I_s * F_S * V_O)$$ (3.6)

Where Is is the source current. When Fs is selected, there should be a trade-of between minimizing the size of the inductor and limiting the loss of the power switching device. Generally, high-frequency of Fs is imposed and it should be checked if the current ripple is correct by low frequency [39], [41].

- Output capacitor: Output capacitor must be designed carefully to perform two important functions. Firstly, it must limit the output voltage ripple as well as withstand the required ripple current stress. The second function, it must supply the required output current to the load when the diode in off state. The minimum value of the output capacitance that provides the specified voltage ripple (ΔV_O) is calculated as in (3.7). In addition, the required ESR that give the required voltage ripple could be determined as in (3.8) [39], [41].

$$C_{min} = (Io * D)/(F_S * \Delta Vo)$$ (3.7)

$$ESR \leq \Delta Vo/((I_S + (\Delta I_{LP})/2))$$ (3.8)

- Input capacitor: The minimum value of input capacitor is necessary to regulate the input voltage due to the current requirement of power supply. This minimum value can be increased in case of noisy input [39].

3.2.2 Auxiliary Components

The implementation of developed algorithm of proposed MPPT controlled DC-DC boost converter depends mainly on additional auxiliary components. The performance of these components affect the operation of whole system; thus, they should be considered carefully. These components are voltage controller unit, input sensors, and output sensors.

3.2.2.1 Voltage Controller Unit

Voltage controller unit consists of Zener diode which is operated as voltage regulator. Zener diode is p-n junction semiconductor device that has symbol and characteristic curve as shown in Figure 3.4. As shown from characteristic curve, Zener diode has the same characteristic of normal diode when it is forward biased. It contacts forward current with a forward voltage drop of 0,7 volt [42].
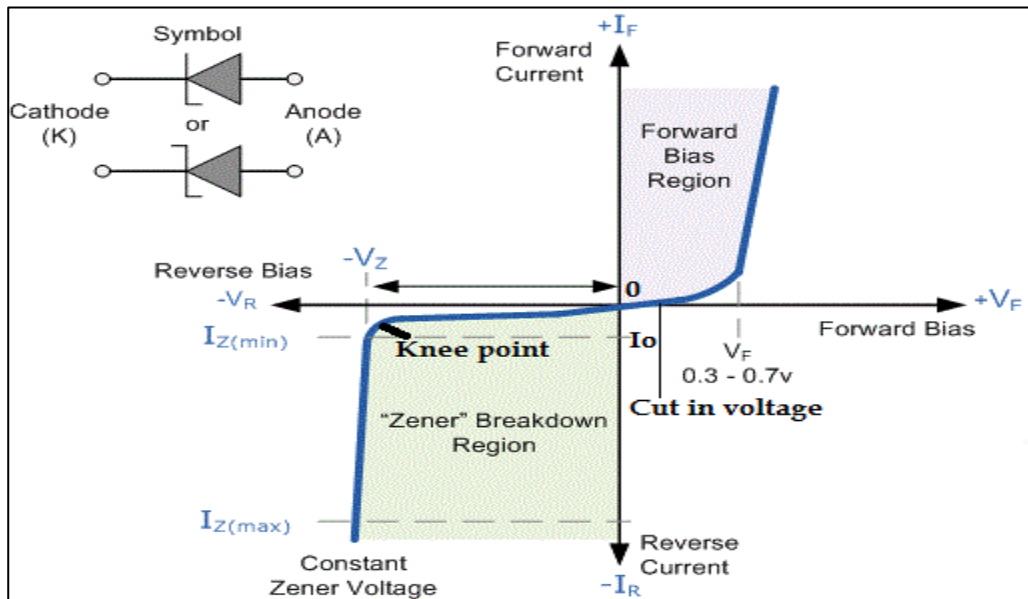
Figure 3.4 Symbol and Characteristic Curve of Zener Diode. [43]

The main difference between Zener diode and normal diode is the characteristic in the reversed direction. When Zener diode is backward biased, the flow of current is blocked through the diode, except of small leakage current through p-n junction of diode, until the voltage across the diode terminals reaches specific value which is called Zener voltage. At this specific value of voltage, the current through diode increases gradually and the voltage drop across diode remains at Zener voltage value nearly [42].

The level of current through Zener diode should be limited based on the maximum power rating of Zener diode. Maximum power rating provides the safe level of current that can be passed without risk of high temperature rise that may destroy the diode [42].

There are many manufactured Zener diodes in market that have rating of Zener voltage ranging from few Volts to hundreds of Volts, and rating of maximum power ranging from few Milliwatt to 50 Watt. Practically, backward-biased Zener diode is used rather than forward-biased Zener diode. This is because forward-biased Zener diode is replaced by p-n normal diode that has identical characteristic with lower cost.

The most important applications of backward-biased Zener diode are voltage clipping and voltage regulation applications. In this research, the Zener diode is used as voltage regulator in order to implement the constant voltage mode of charging process. Figure 3.5 illustrates the operation of backward-biased Zener diode as regulator [44].
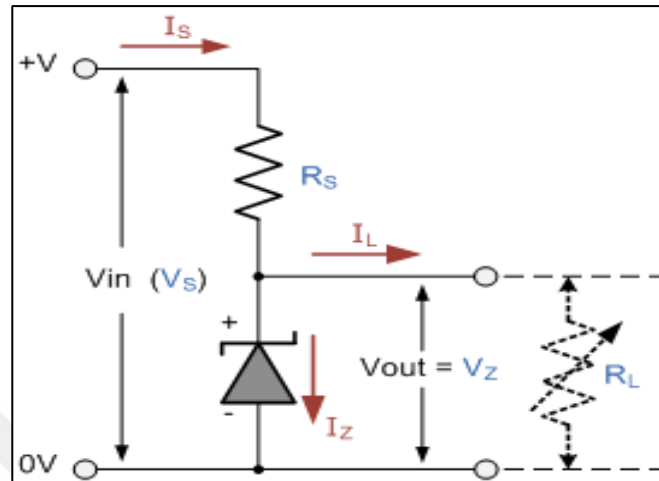
Figure 3.5 Operation of Zener Diode as Regulator. [43]

As shown in Figure 3.5, Zener diode is connected across load terminal in the reverse direction, and separated from input source by current-limiting resistor (R_S). When voltage across Zener diode reaches Zener voltage (V_{ZE}), current starts to flow through it. The level of Zener current is limited by R_S resistor depending on the maximum power rating of Zener diode. In addition, the voltage drop across resistor R_S is the difference between input source voltage and Zener voltage [44].

When changes of input voltage or output load occur, the Zener diode regulates the output voltage around V_{ZE} as the Zener current within allowed limit. That means Zener diode regulates voltage by increasing or decreasing the flow of current across it, in order to maintain the voltage drop across the output load mostly constant. These concepts of Zener diode regulator operation will be used in this research to ensure the charging of battery properly [44].

3.2.2.2 Voltage and Current Sensors

The operation of developed algorithm in this research depends mainly on the data that should be fed continuously and accurately into the controller of the proposed system. As shown in Figure 3.1, sensors are used to perform this function of getting the required data from system under consideration. In this research, two types of sensor are used to

obtain the required data for operation of developed algorithm; these types of sensor are current sensors and voltage sensors.

As shown in figure 3.1, current sensors are used to measure the current of PV panel as well as the current of Zener diode, and voltage sensors are used to measure the voltage of PV panel as well as the voltage of battery that is charged. In addition, these sensors are required to adjust the measured value in order to be within the limited rating of controller that implements the developed algorithm.

In this research, the performance of voltage and current sensors can be measured by accuracy and response time. Accuracy of sensor determines the errors that are introduced by sensors in measuring required data. This factor should be high as possible in order to ensure low errors in the measured value. The response time of sensor determines the time that is required by sensors to track the changing of measured value. This factor has the effect of delaying the operation of developed algorithm in performing the right action; so it should be as minimum as possible [45].

3.3 New Developed Algorithm

As stated previously, the duty cycle of proposed MPPT controlled DC-DC boost converter is adjusted by new developed algorithm that consists mainly of InC MPPT algorithm which is expanded to include CC-CV charging algorithm.

Figure 3.6 shows the main chart of developed algorithm that is used in this research. As can be shown, the developed algorithm consists of three main blocks which are pre-charging, MPPT-CC charging, and CV charging blocks. These blocks represent different operation modes of designed system. During pre-charging and CV charging blocks, designed system is operated in charger mode which takes into consideration the charging of battery during low battery voltage and high battery voltage conditions respectively. In contrast, during MPPT-CC charging block, the designed system is operated in MPPT tracker mode which supplies battery with maximum available power of PV panel. As shown in Figure 3.6, the developed algorithm is initiated by measuring values of PV voltage, PV current, battery voltage, and Zener current. The activation of each block of developed algorithm depends on comparing the measured value of battery voltage with low and high predetermined limits of battery voltage which have been discussed in section 2.4.3. The operation and chart of each block are illustrated thoroughly in following sections.
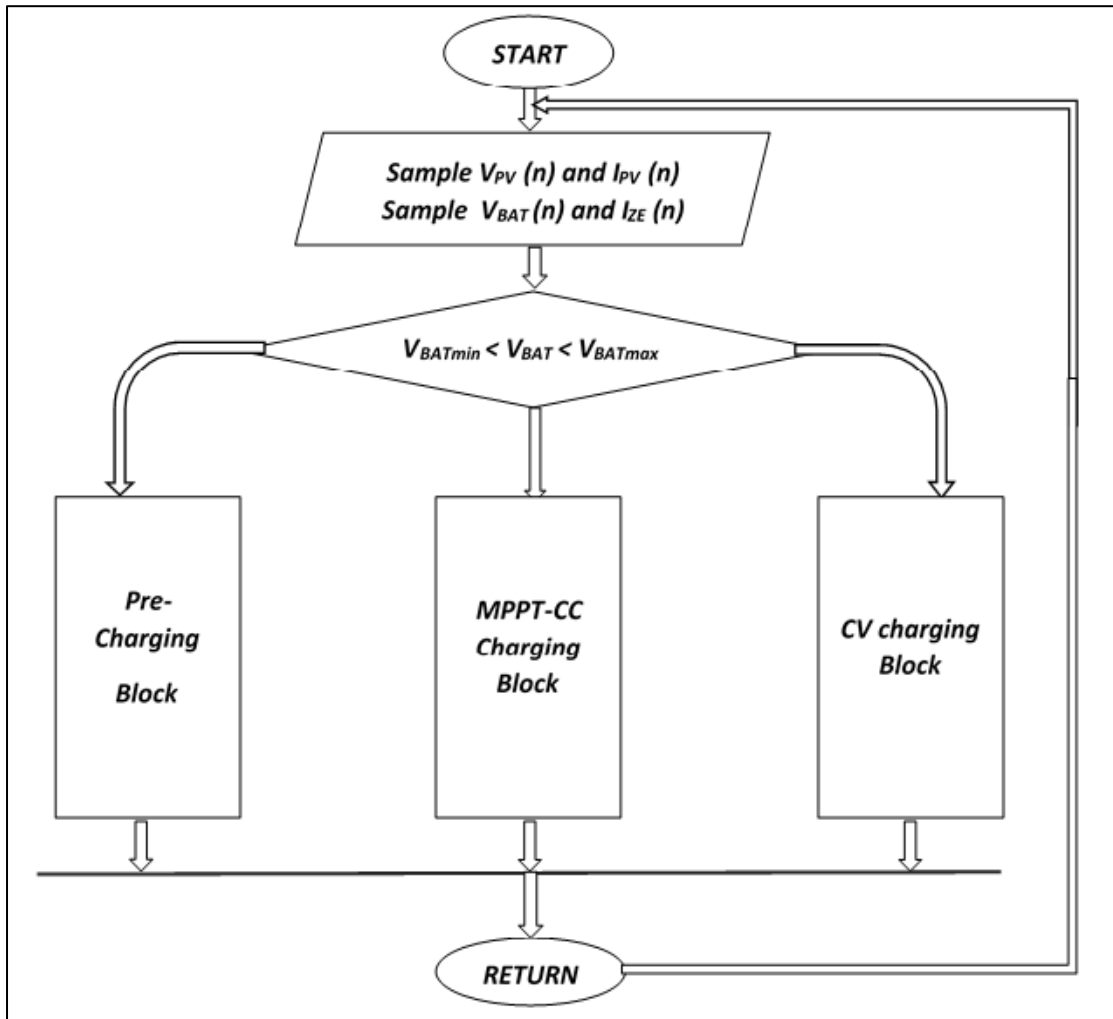
Figure 3.6 Main Chart of Developed Algorithm of Designed MPPT Controller DC-DC Boost Converter

3.3.1 Pre-Charging Block of Developed Algorithm

This block of developed algorithm is activated when measured value of battery voltage is less than low predetermined limit. In this block, battery is charged with minimum constant charging current until battery voltage reaches low predetermined limit. That means, during this stage, charging current remains constant with slowly increase of battery voltage. This characteristics of charging process are similar to characteristics of constant current region of I-V curve of PV panel; in which, current is mostly constant with slowly increase of PV voltage. As a result, pre-charging block of developed algorithm depends on operating PV panel at constant current region of I-V curve as shown in Figure 3.7. As shown, the developed algorithm adjusts the operating point of PV panel in the direction of increasing of PV power.

Figure 3.7 Region of Operation of Pre-charging Block of Developed Algorithm along Curves of 100W PV Panel

Figure 3.8 shows chart of pre-charging block of developed algorithm. This chart is initiated by computing PV power P_{PV} and battery power P_{BAT} at specific instant (n) as in (3.9) and (3.10) respectively.

$$P_{PV}(n) = V_{PV}(n) * I_{PV}(n) \tag{3.9}$$

$$P_{BAT}(n) = V_{BAT}(n) * I_{BAT} \tag{3.10}$$

Where $V_{PV}(n)$ is PV voltage at instant (n), $I_{PV}(n)$ is PV current at instant (n), $V_{BAT}(n)$ is battery voltage at instant (n), and I_{BAT} represents minimum charging current of Lead Acid battery which is provided by manufacturer.

As can be shown in Figure 3.8, the operation of this chart depends on comparing the calculated values of P_{PV} and P_{BAT}. According to the result of this comparison, the duty cycle of boost converter is adjusted directly.

When P_{PV} is greater than P_{BAT}, duty cycle of boost converter is increased. In the contrary, when P_{PV} is less than P_{BAT}, the duty cycle is decreased. The process of adjusting duty cycle continues until PV power P_{PV} equals the battery power P_{BAT} (P_{PV} = P_{BAT}). When PV power is identical with battery power, the duty cycle remains unchanged. In this case, battery is charged with required current of I_{BAT} ,and battery voltage is increased slowly. With increasing V_{BAT}, P_{BAT} increases correspondingly and duty cycle decreases in order to increase P_{PV} until equals P_{BAT}.

47
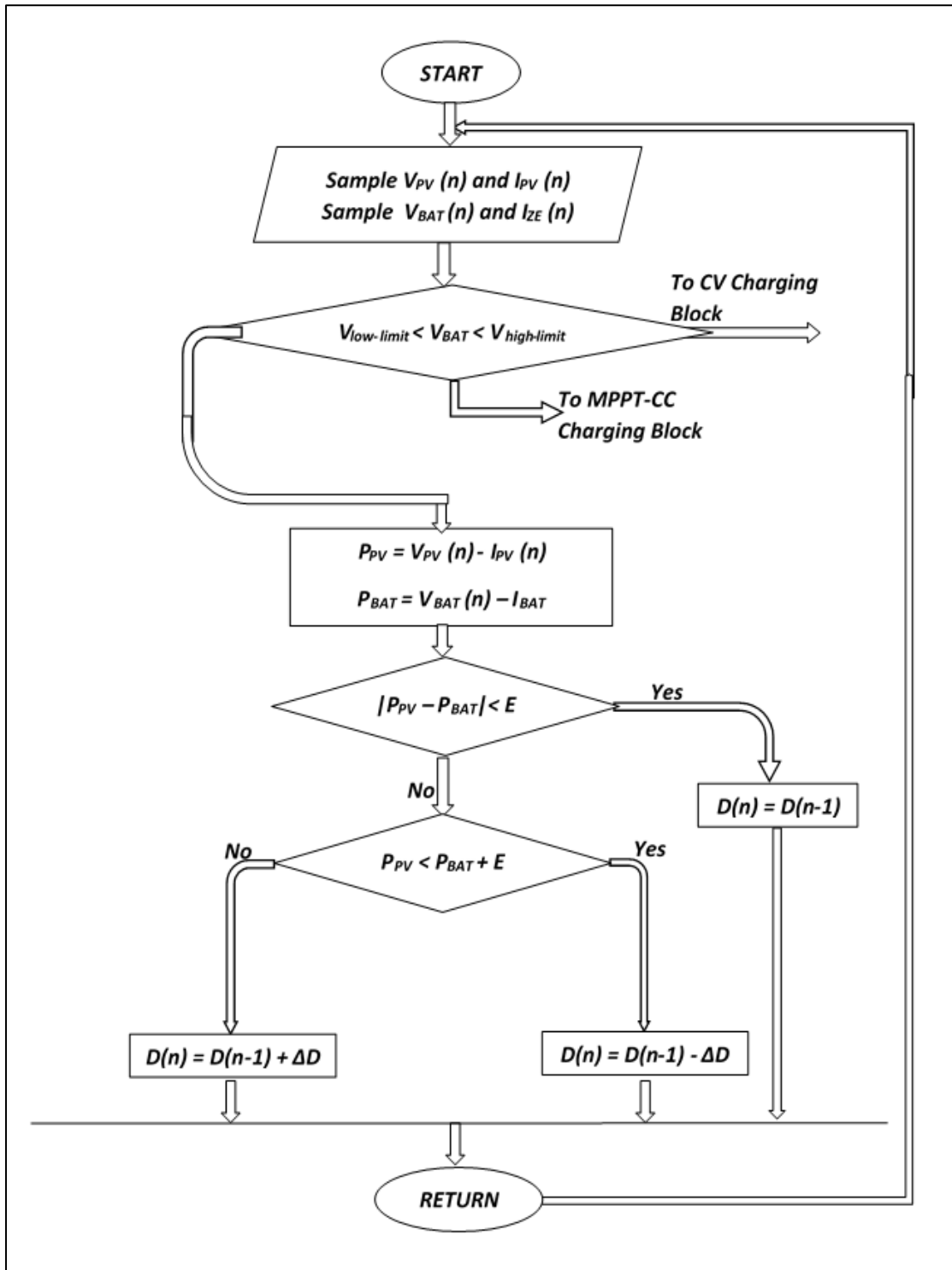
Figure 3.8 Chart of Pre-Charging Block of Developed Algorithm

In practice, because of inaccuracy of sensors and performance of boost converter, equality between PV and battery powers is detected within specific tolerance (ε), as $|P_{PV}-P_{BAT}| < \varepsilon$

Equality between PV and battery powers ($P_P = P_{BAT}$) can be detected at two points along P-V curve of PV panel. One of this point at constant current region and the other point

at open voltage region of P-V curve of PV panel. The chart of this block of developed algorithm ensures the operation at constant current region by controlling initial value of duty cycle. As a consequence, the initial value of duty cycle should be equal to or greater than D_{MPP} that corresponds to maximum power point of PV panel.

3.3.2 MPPT-CC Charging Block of Developed Algorithm

This block of developed algorithm is activated when measured value of battery voltage is between low predetermined limit (V_{low_limit}) and high predetermined limit (V_{high_limit}). In this block, battery is charged with maximum charging current until battery voltage reaches the high predetermined value. During this stage, battery should be charged with most of its energy within minimum charging time. This requires PV power to be maximum under different environmental conditions. As a result, MPPT-CC charging block of developed algorithm in this research depends on operating PV panel at maximum power point of I-V curve as shown in Figure 3.9.
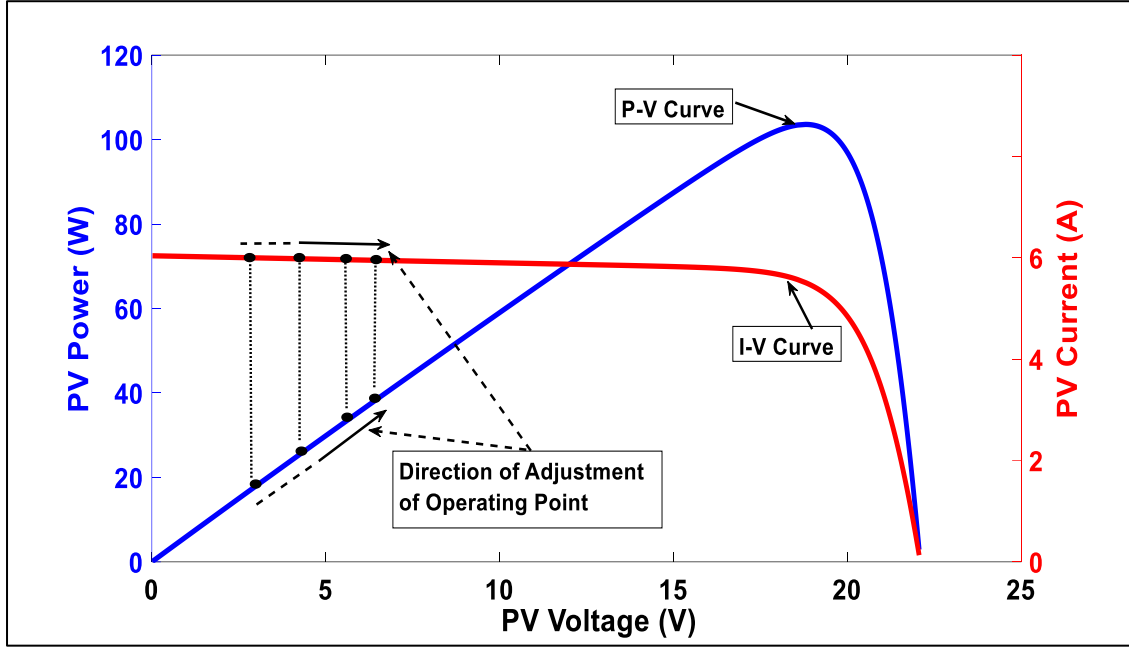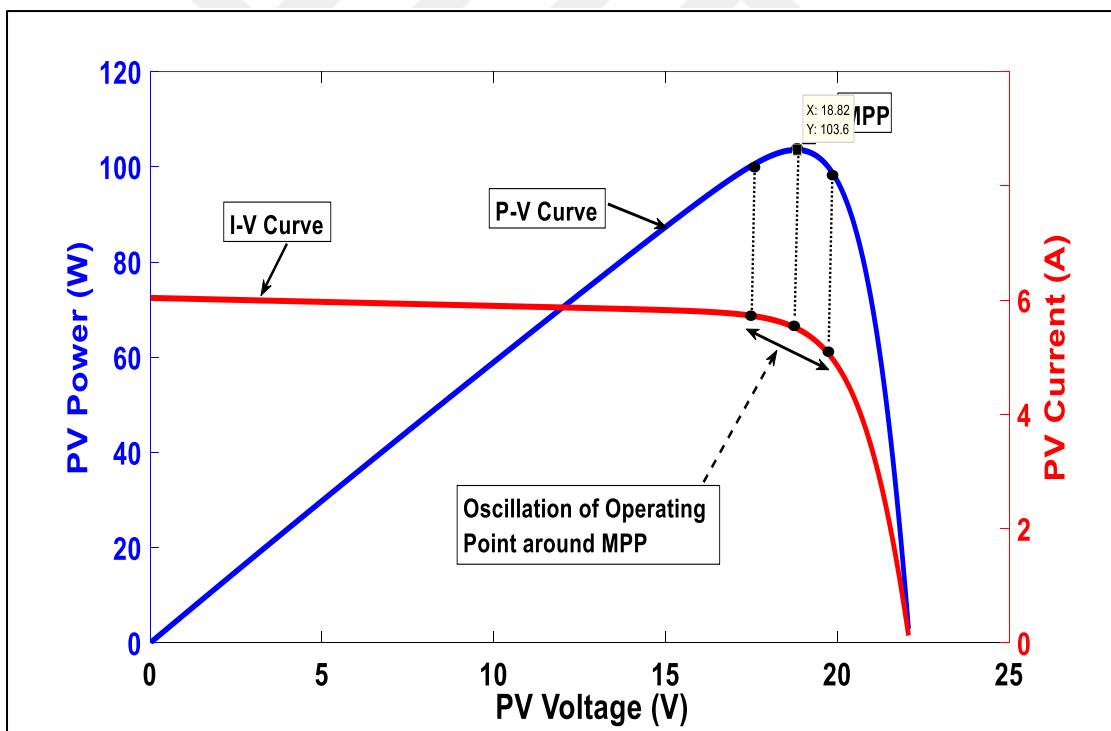

Figure 7.9 Region of Operation of MPPT-CC Charging Block of Developed Algorithm along Curves of 100W PV Panel

Figure 3.10 shows chart of MPPT-CC charging block of developed algorithm. As can be shown, this chart represents incremental conductance (InC) MPPT algorithm which ensures operation of PV panel at maximum power point.

InC algorithm depends on the fact that derivative of PV power with respect to PV voltage (dP_{PV}/dV_{PV}) is equal to zero when operating point of system is at MPP of P-V curve. When operating point is at right side of P-V curve, the (dP_{PV}/dV_{PV}) is less than zero. However, when operating point in the left side of P-V curve, the (dP_{PV}/dV_{PV}) is greater than zero.

Depending on this fact, the main rules of InC algorithm can be derived by replacing $P_{PV}= V_{PV} I_{PV}$ in (dP_{PV}/dV_{PV}) as shown in (3.11).

$$\frac{dP_{PV}}{dV_{PV}} = \frac{d(V_{PV} I_{PV})}{dV_{PV}} \tag{3.11}$$

The derivative of (33) can be performed by applying chain rule as in (3.12).

$$\frac{d(V_{PV} I_{PV})}{dV_{PV}} = V_{PV} \frac{dI_{PV}}{dV_{PV}} + I_{PV} \tag{3.12}$$

Using these equations, the rules of InC algorithm are derived and summarized as in (3.13), (3.14), and (3.15).

$$\frac{dI_{PV}}{dV_{PV}} \approx \frac{\Delta I_{PV}}{\Delta V_{PV}} = -\frac{I_{PV}}{V_{PV}} \qquad \text{At MPP} \tag{3.13}$$

$$\frac{dI_{PV}}{dV_{PV}} \approx \frac{\Delta I_{PV}}{\Delta V_{PV}} > -\frac{I_{PV}}{V_{PV}} \qquad \text{At Left Side} \tag{3.14}$$

$$\frac{dI_{PV}}{dV_{PV}} \approx \frac{\Delta I_{PV}}{\Delta V_{PV}} < -\frac{I_{PV}}{V_{PV}} \qquad \text{At Right Side} \tag{3.15}$$

These rules state that the incremental conductance (dI / dV) of PV panel is equal to negative instantaneous conductance (-dI /dV) at MPP of P-V curve. In addition, (dI /dV) is lower and higher of (- dI / dV) at right and left side of P-V curve respectively.

Generally, the chart of InC algorithm is initiated by measuring PV voltage (V_{PV}) and PV current (I_{PV}) at successive (n-1) and (n) instants. Using these measured values, incremental conductance of PV panel is calculated as incremental voltage (ΔV_{PV}) and incremental current (ΔI_{PV}) that are shown in (3.16) and (3.17) respectively.

$$\Delta V_{PV} = V_{PV} (n) * V_{PV}(n-1) \tag{3.16}$$

$$\Delta I_{PV} = I_{PV} (n) * I_{PV}(n-1) \tag{3.17}$$

As can be shown in Fıgure 3.10, the operation of this chart depends on verifying of the rules of Incremental Conductance algorithm. According to the result of this verification, the duty cycle of boost converter is adjusted directly.
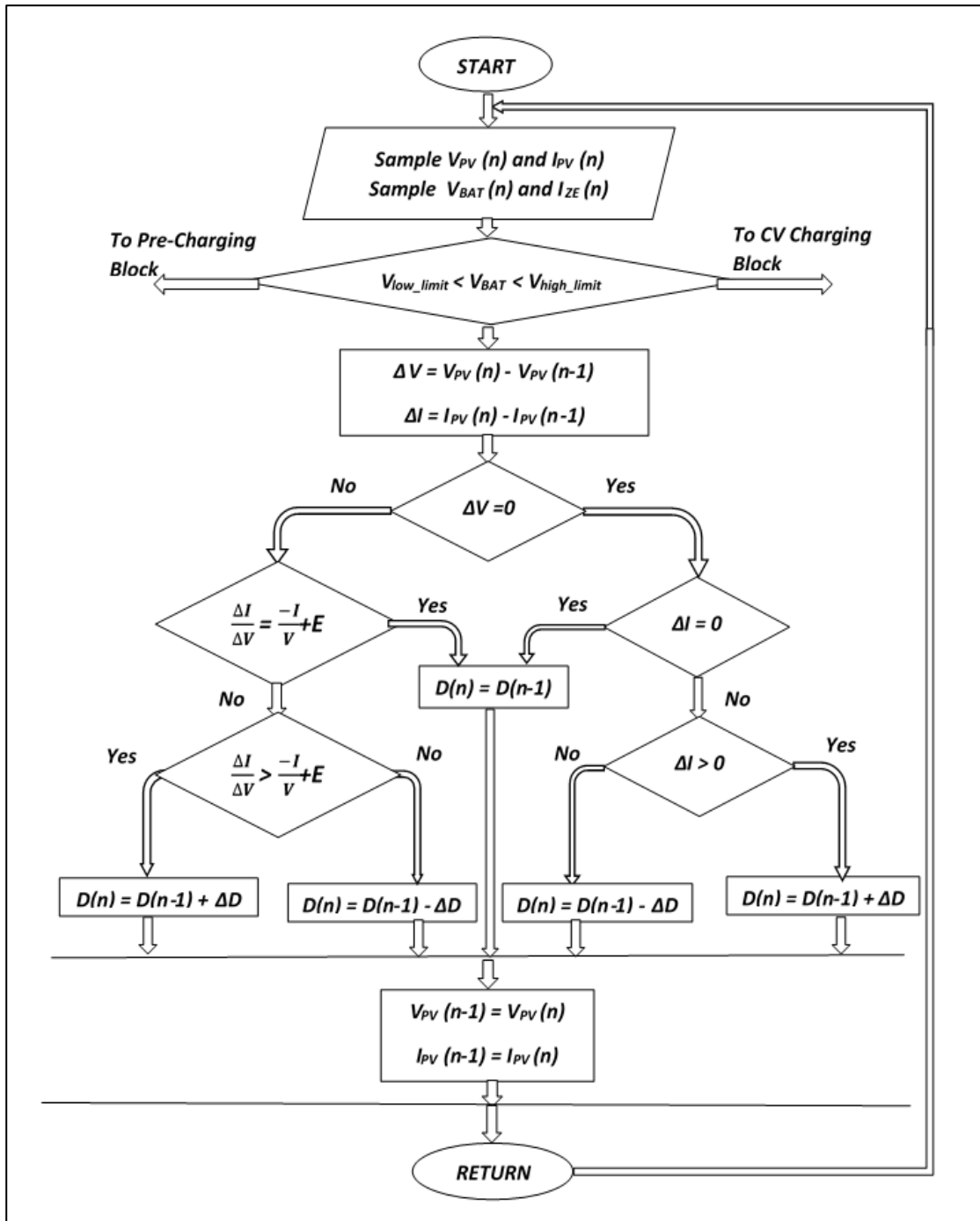
Figure 3.10 Chart of MPPT-CC Charging Block of Developed Algorithm

When $(\Delta I_{PV} / \Delta V_{PV}) > (- I_{PV} / V_{PV})$ is verified, duty cycle of boost converter is increased. In the contrary, when $(\Delta I_{PV} / \Delta V_{PV}) < (- I_{PV} / V_{PV})$ is verified, the duty cycle is decreased. The process of adjusting duty cycle continues until $(\Delta I_{PV} / \Delta V_{PV}) = (- I_{PV} / V_{PV})$ is verified in which the duty cycle remains unchanged. In this case, PV panel operates at maximum power point (MPP) and battery is charged with maximum available current IBAT while battery voltage is increased gradually. With increasing V_{BAT}, operating point of PV panel changes correspondingly and duty cycle changes in

order to maintain PV panel at MPP. In practice, because of inaccuracy of sensors and performance of boost converter, equality between incremental and instantaneous conductance of PV panel is detected within specific tolerance (ε), which can be shown as $| (\Delta I_{PV} / \Delta V_{PV}) + (- I_{PV} / V_{PV}) | < \varepsilon$.

As can be shown from (3.16), incremental voltage ΔV_{PV} is calculated as the difference of PV voltage between successive instants of measurement. So, when PV voltage of these successive points remains constant, incremental voltage ΔV_{PV} equals to zero. This causes mistake in program that applies InC algorithm as ($\Delta I_{PV} / \Delta V_{PV}$) will be unknown. In order to avoid this mistake in controller program, it is essential to ensure that incremental voltage ΔV_{PV} do not equal to zero in advance as shown in Figure 3.10. When ΔV_{PV} equals to zero, there are two cases of operating point of system should be considered. The first case occurs when environmental conditions remains unchanged through step size of successive instants. In this case, the operating point of system remains unchanged and ΔI_{PV} equals to zero. As a result, duty cycle of boost converter remains unchanged. The other case results from changing of environmental condition through step size of successive instants of measurement. In this case, the operating point of system and ΔI_{PV} changes according to changing of environmental conditions. As a result, duty cycle is adjusted according to sign of ΔI_{PV}. This process continues until either MPP is met or change in ΔV_{PV} is detected at which algorithm continues as shown in Figure 3.10.

3.3.3 CV Charging Block of Developed Algorithm

This block of developed algorithm is activated when measured value of battery voltage reaches high predetermined limit. In this block, battery voltage is kept constant at high predetermined limit. As a consequence of constant battery voltage, battery current decreases gradually until reaches lower specified value of current at which battery is detected to be fully charged. This characteristics of charging is similar to characteristics of constant voltage region of I-V curve of PV panel; in which, voltage is mostly constant with decreasing of PV current. As a result, CV charging block of Developed Algorithm depends on operating PV panel at constant voltage region of I-V curve as shown in Figure 3.11. As shown, the developed algorithm adjusts the operating point of PV panel in the direction of decreasing of PV power.
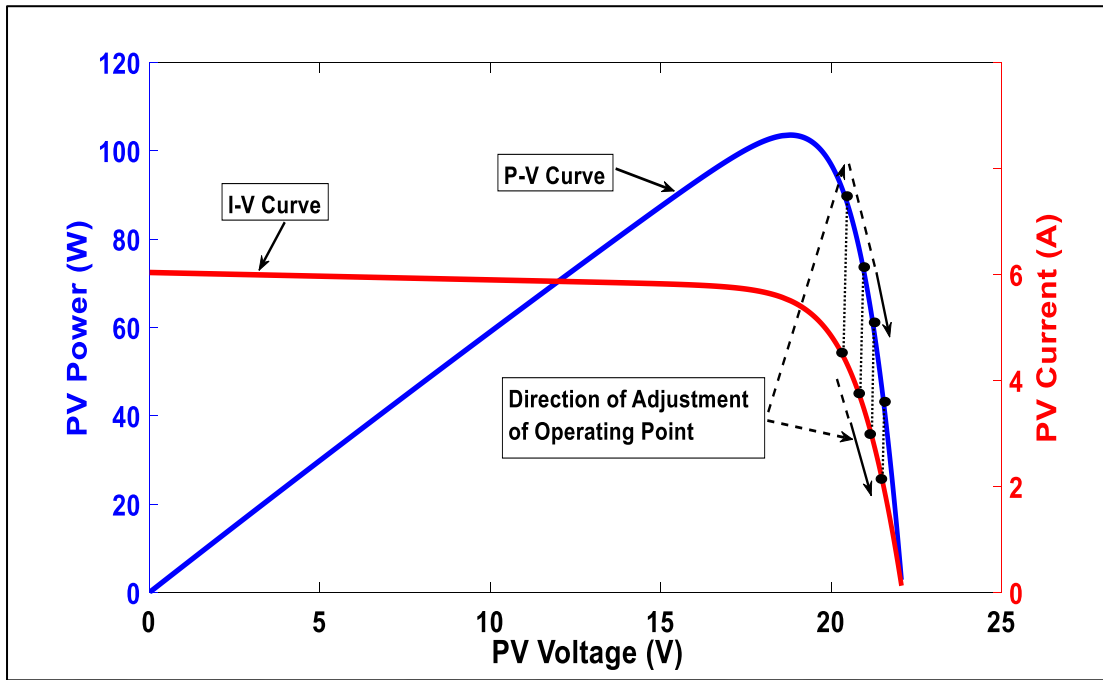
Figure 3.11 Region of Operation of CV Charging Block of Developed Algorithm along Curves of 100W PV Panel

The implementation of CV Charging block of developed algorithm depends basically on using of voltage controller unit. The voltage controller unit consists of Zener diode that is connected directly across battery terminals in order to regulate its voltage around Zener voltage. Generally, the Zener voltage is chosen to be nearly equal to high predetermined limit ($V_{high\text{-}limit}$) of battery voltage. Therefore, when battery voltage reaches Zener voltage, Zener diode starts contacting current across its impedance; in order to regulate the voltage across terminal of battery. Since battery voltage remains constant at Zener voltage, then charging current of battery decreases gradually with increasing of level of charge. As current that is supplied by boost converter is still constant at specific duty cycle, then decreasing of charging current results in increasing of Zener current and power. Therefore, in order to limit current and power of Zener diode, it is essential to decrease the current supplied by boost converter.

These requirements of charging process can be accomplished by adjusting duty cycle of boost converter; so as to ensure the operating of PV panel at constant voltage region of I-V curve of PV panel. In this control of duty cycle, the operation point of PV panel is moved into constant voltage region gradually in accordance with increasing of current and power of Zener diode. The purpose of control in this block of developed algorithm is to maintain the power of Zener diode within allowed limits while battery charging current decreases in response of constant voltage charging.

53

Figure 3.12 shows chart of CV charging block of developed algorithm. This chart is initiated by computing PV power P_{PV} and Zener power P_{ZE} at specific instant (n). P_{ZE} is calculated as in (3.18).

$$P_{ZE}(n) = V_{ZE}(n) * I_{ZE}(n) \tag{3.18}$$

Where V_{ZE} (n) is Zener voltage at instant (n), I_{ZE} (n) is Zener current at instant (n). As can be shown in Figure 3.12, the operation of this chart depends on comparing the calculated value of P_{ZE} with selected thresholds of Zener power under. These thresholds are selected in a way that gives developed controller enough time to recover P_{ZE} within allowed limits before damage of diode is occurred.

The developed algorithm is started by comparing P_{ZE} with P_{ZEH} and P_{ZEL}. Where P_{ZEH} represents first high threshold value of Zener power and P_{ZEL} represents first low threshold value of Zener power. According to the result of comparison, the duty cycle of boost converter is adjusted directly. When P_{ZE} is greater than P_{ZEH}, duty cycle of boost converter is decreased in order to move operating point of PV panel further into constant voltage region. In the contrary, when P_{ZE} is lower than P_{ZEL}, the duty cycle is increased in order to maintain power that is supplied to battery. In addition to P_{ZEH} and P_{ZEL} limits of Zener diode, there are additional two cases are detected in developed algorithm as shown in Figure 3.12. The first case is when current through Zener diode increases rapidly over threshold value. As a result, P_{ZE} increases over P_{ZEH} substantially, which may destroy Zener diode because of resulted high temperature. In order to protect Zener diode from damage, the duty cycle of boost converter should be decreased with larger step size to recover P_{ZEH} within limits through minimum time. . In order to specify this condition, second high threshold value (P_{ZEHH}), which is larger than P_{ZEH}, is used. Accordingly, when P_{ZE} is larger than P_{ZEHH}, larger step size of duty cycle is used.

The other case detected in this algorithm is when environmental conditions change through charging process which results in decreasing supplied PV power into battery. These changes decrease current supplied by boost converter; and thus decrease current of Zener diode. As result, the calculated power of Zener diode P_{ZE} decreases largely more than P_{ZEL} and duty cycle is increased correspondingly. This may change the operating point of PV panel along I-V curve from constant voltage region into constant current region when environmental conditions change largely. Therefore, it is essential to differentiate between decreasing of P_{ZE} as a result of charging process control and that result from changing of environmental conditions.
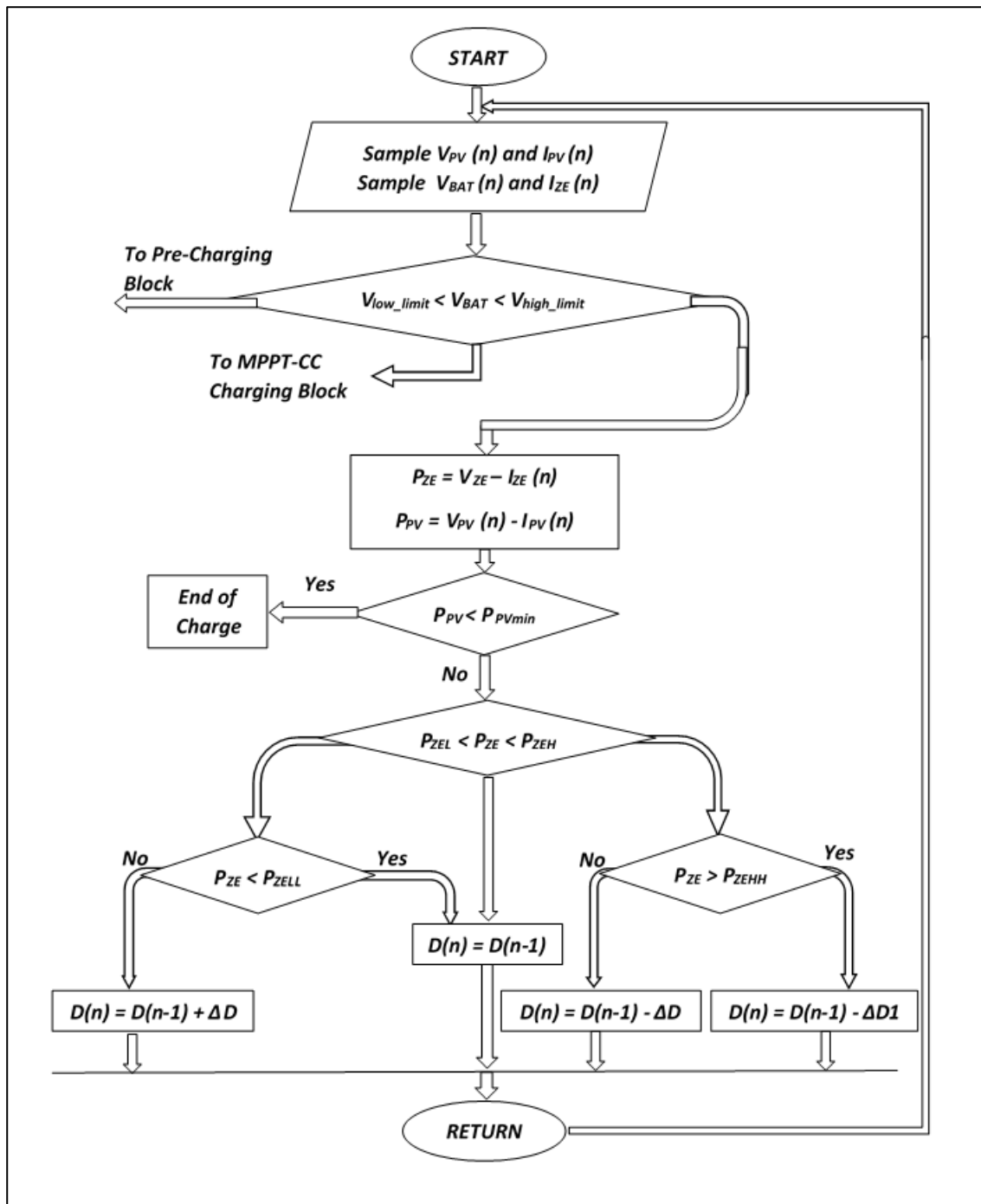
Figure 3.12 Chart of CV-Charging Block of Developed Algorithm

In this developed algorithm, this requirement is accomplished by detecting second low threshold value (P_{ZELL}) that is lower than P_{ZEL} as an indication of changing environmental conditions. Therefore, when P_{ZE} is lower than P_{ZELL}, duty cycle is kept unchanged in order to decrease charging current of battery, and thus decrease battery voltage which moves the operation of algorithm from CV charging block to the MPPT-CC Charging Block of developed algorithm. In this case, the algorithm searches for maximum power point of new environmental conditions and start to charge battery at

new charging current until voltage reaches Zener voltage again and process continues as explained before.

Normally, the detection of end of charge in CC-CV algorithm is performed by measuring charging current of battery which decreases gradually until reaches a low predetermined value that is equivalent to full SOC. In this research, since measurement of charging current is not provided, the end of charge process is detected by measuring PV power which is decreased in response to decreasing charging current. This relation of PV power and charging current can be explained by observing that PV power at any instant is equal to summation of Zener and battery powers. The Zener power can be considered constant because is controlled by algorithm to have a constant value approximately. In the contrary, battery power decreases gradually because of as a result of constant voltage charging. So, decreasing of PV power can be considered as equivalent to decreasing charging current of battery. Therefore, the end of charge is detected by reaching a minimum value of PV power (P_{PVmin}) that can be calculate as (3.19).

$$P_{PVmin} = P_{ZE} + (V_{ZE} * I_{BAT-min})$$
(3.19)

Where P_{ZE} is Zener power, V_{ZE} is Zener voltage, and $I_{BAT-min}$ is low specific value of charging current that is equivalent to full SOC. The value of $I_{BAT-min}$ can be calculated from charging requirements of Lead Acid battery under consideration.

SIMULATION AND ANALYSIS

In this chapter, the developed MPPT controlled DC-DC boost converter for solar charger system, which has been described in previous chapter, is validated by SIMULINK-MATLAB program. During this validation process, detailed operation and performance of the developed charger system under different conditions of charging and environment are investigated and analyzed thoroughly.

In order to accomplish the validation process of developed system properly, it is required to simulate the developed controller within overall stand-alone charger system that consists of PV panel, the developed charger controller, and battery bank. Hence, in this chapter, the overall stand-alone charger system shown in Figure 3.1 is designed and build in SIMULINK-MATLAB program completely.

Later in section 4.1, the design of overall stand-alone charger system, which will be built in SIMULINK-MATLAB program, will be presented. The detailed operation of developed MPPT controlled DC-DC converter as solar charger will be simulated and presented in section 4.2. Finally, the performance of developed charger system will be presented in section 4.3 thoroughly.

4.1   Design Process of Simulated Stand-Alone charger System

Generally, the design of stand-alone solar charger system depends mainly on requirements of battery under charge. Therefore, in this research, the design process of simulated stand-alone charger system shown in Figure 3.1 is performed according to specifications of battery that are shown in Table 4.1.The battery bank consists of two POWER SONIC DCG 12-24 battery.

In the following sections, the design process is initiated by sizing and selecting PV panel that supplies energy to battery bank through developed charger controller.

Table 4.3 Specification of 24 V battery bank

Parameter	Value	Remarks
Number of cells in battery bank (N)	12 cell	Connected In series
Normal voltage of battery bank (V_{BAT})	24 V	2 V /cell
Charge Voltage of Battery bank ($V_{Charging}$)	28 V	2.35 V /cell
Capacity of Battery Bank (AH)	24 AH	At C20
Maximum allowable current of battery bank	7,2 A	At intial condition
Maximum Charging current of battery bank ($I_{BAT,MAX}$)	4,8 A	At continuous condition (Chosen)
Output voltage ripples ($V_{BAT,RIPPLE}$)	1,4 V	5% of $V_{Chargin}$

Depending on specifications of selected PV panel and battery, the design process of boost converter, Zener diode, and developed algorithms is performed. The outputs of this design process are used to build and simulate the overall stand-alone charger system in SIMULINK-MATLAB program.

4.1.1 Sizing of PV Panel of Stand-Alone Solar Charger System

The size of PV panel depends mainly on specification of battery bank under charge process. Consequently, the sizing process of PV panel is performed according to specifications of battery listed in Table 4.1.

Sizing process of PV panel is initiated by finding total amount of energy that is required to be supplied by PV panel to battery bank. This energy of battery (E_{BAT}) can be calculated as in (4.1).

$$E_{BAT} = V_{BAT} * \text{Capacity} = 24\ (V) * 24\ (AH) = 546\ (WH) \tag{4.1}$$

In addition to the energy of battery, PV panel should supply the dissipated energy as losses in developed charge controller and connections of system. In this research, an overall system efficiency of 90 % between PV panel and battery bank is proposed for

purpose of sizing PV panel. Hence, the total amount of energy that should be provided daily by PV panel under STC of environment can be calculated as in (4.2).

$$E_{PV} = \frac{E_{BAT}}{\text{Overall Effeciency}} = \frac{576}{0.9} = 640 \text{ (WH)} \qquad (4.2)$$

In practice, capacity of PV panel is characterized by maximum power (P_{MAX}) that can be extracted under STC of environment. Therefore, in order to determine the number of PV panels required to supply the total amount of energy calculated in (4.2), it is essential to calculate the total amount of power needed to be supplied by PV panel. The total amount of power can be concluded from total amount of energy of (4.2) by considering the number of Sun hours of environment at which PV panel is installed. Sun hours represent number of hours through which PV panel operates at STC of environment. In this research, Sun hours is assumed to be 6 hours. As a result, the total amount of power (P_{PV}) can be calculated as in (4.3).

$$P_{PV} = \frac{E_{PV}}{\text{Sun Hours}} = \frac{640}{6} = 106{,}7 \text{ (W)} \qquad (4.3)$$

In this research, PV panel that has maximum power of 100 W and specification listed in Table 4.2 is selected as building block of PV solar source. So, the number of 100 W panels, which are required to supply the total amount of power calculated in (4.3), is determined as in (4.4)

$$N_{Panel} = \frac{P_{PV}}{P_{max}} = \frac{106.7}{100} = 1{,}06 \approx 1 \text{ panel} \qquad (4.4)$$

Table 4.2 Specification of 100 W PV panel at 25 C^O

Parameter	Value
Nominal Maximum Power (P_{MAX})	100 W
Optimum Operating Voltage (V_{MPP})	18,8 V
Optimum Operating Current (I_{MPP})	5,51 A
Open Circuit Voltage (V_{OC})	22,1 V
Short Circuit Current (I_{SC})	6,04 A

4.1.2 Design of Boost DC-DC converter

Depending on specifications of battery bank and PV panel that are listed in Table 4.1 and 4.2 respectively, the design specifications of boost converter are determined and listed in Table 4.3. These specifications are used in conjunction with equations (3.4-3.8) during design process of boost converter

Table 4.3 Design Specification of DC-DC Boost Converter

Parameter	Value	Remarks
Switching Frequency of Switch (F_S)	25 KHz	Chosen
Maximum output voltage ($V_{OUT,MAX}$)	28 V	$V_{Charging}$ of Battery
Maximum output voltage ripple ($V_{OUT,RIPPLE}$)	1,4 V	5% of $V_{Charging}$
Maximum Output Current ($I_{OUT,MAX}$)	6 A	125 % of ($I_{BAT,MAX}$)
Range of Input voltage ($V_{IN,MAX} \sim V_{IN,MIN}$)	(22,1~17,5) V	Range of change of V_{OC} due to irradiance
Maximum Input Current ($I_{IN,MAX}$)	6,04 A	I_{SC} of PV panel
Maximum input current ripple ($I_{IN,RIPPLE}$)	1,2 A	20% of I_{SC}

As stated previously, the design process of DC-DC boost converter includes determination of switch, diode, inductor, input capacitor, and output capacitor components. In this research, the design process of these components is performed ideally. Therefore, power losses of these components will not be analyzed in more details. In the following sections, the Selection process of each component is illustrated thoroughly.

4.1.2.1 Selection of Switch Component

In boost DC-DC converter, the selection of switch depends on the maximum stress of current and voltage under operating frequency. As a result, it is required to calculate maximum voltage and current that switch will experience.

For PV powered Boost Converter, maximum input current that can be supplied by PV panel is short circuit current (I_{SC}) which has ripples depend on the value of inductance of boost converter. In this design, the value of ripples are required to be less than 20 % of I_{SC} as shown in Table 4.3. The distribution of theses ripples around I_{SC} is assumed to be identical; so, half of the ripple value is added to I_{SC} and the other half is subtracted from it. Consequently, the maximum current that can flow through switch is calculated as in (4.5).

$$I_{SW,MAX} = I_{SC} + \frac{I_{IN,RIPPLE}}{2} = 6 + 0,6 = 6,6 \text{ (A)} \qquad (4.5)$$

In addition, the maximum voltage that switsh can experience is maximum voltage of output circuit. In battery charging application, the maximum voltage of battery is gassing voltage of battery which is 28 V as shown in Table 4.3. This voltage has ripples that are controlled by output capacitor. In this design, the value of ripples are required to be less than 5 % of $V_{GASSING}$ as shown in Table 4.3. The distribution of theses ripples around $V_{GASSING}$ is assumed to be identical; so, half of the ripple value is added to $V_{GASSING}$ and the other half is subtracted from it. Consequently, the maximum voltage that switch should withstand is calculated as in (4.6).

$$V_{SW,MAX} = V_{GASSING} + \frac{V_{BAT,RIPPLE}}{2} = 28 + 0,7 = 28,7 \text{ (A)} \qquad (4.6)$$

4.1.2.2 Selection of Diode Component

In order to reduce the losses of switching process, Schottky diode is used in this design. Similar to switch selection, the selection of diode depends on the maximum stress of current and voltage under operating frequency. As a result, it is required to calculate maximum voltage and current that switch will experience.

For boost converter, maximum current that can flow through diode is equal to the maximum input current of the converter. Therefore, the maximum current of diode is similar to that of switch calculated in (4.5). In addition, the maximum voltage that diode can experience is similar to that of switch calculated in (4.6).

4.1.2.3 Selection of Inductor

In this research, the boost converter is designed to operate at CCM. Therefore, the minimum value of inductance that ensure the operation at CCM is calculated as in (4.7).

$$L_{MIN} = \frac{V_{IN,MAX} * (V_O - V_{IN,MAX})}{I_{IN,RIPPLE} * F_S * V_O} = \frac{22,1*(24-22,1)}{1,2*25*1000*24} = 58,32 \text{ (H)} \tag{4.7}$$

4.1.2.4 Selection of Input Capacitor

Due to the existence of inductor in the input circuit of boost converter, minimum value of input capacitor, which has lower ESR, can be chosen to stabilize ripples of input voltage within the given requirements. In case of high noisy source, the value of input capacitor can be increased. In this research, the input capacitor is chosen to stabilize ripples of input voltage within 2% of maximum input voltage value.

4.1.2.5 Selection of Output Capacitor

The minimum value of output capacitor is calculated according to the required ripples ($V_{BAT, RIPPLE}$) at maximum value of battery voltage. In order to perform this calculation, it is necessary to calculate maximum duty cycle (D_{MAX}) of boost converter that corresponds to maximum value of battery voltage as shown in (4.8). Hence, the minimum value of output capacitance and associated ESR, which are required to produce minimum requirement of ripples of battery voltage, are calculated in (4.9) and (4.10) respectively.

$$D_{MAX} = 1 - \frac{V_{IN,MIN}}{V_{BAT,MAX}} = 1 - \frac{17,5}{28,8} = 0,4 \tag{4.8}$$

$$C_{MIN} = \frac{I_O * D_{MAX}}{F_S * V_{BAT,RIPPLE}} = \frac{6* 0,4}{25 *1000*1,4} = 68,5 \text{ (μF)} \tag{4.9}$$

$$ESR <= \frac{V_{BAT,RIPPLE}}{I_S + (\frac{I_{IN,RIPPLE}}{2})} = \frac{1.4}{6+0,6} = 212 \text{ (mΩ)} \tag{4.10}$$

The values of main components of DC-DC boost converter, which have been calculated and determined in previous sections, are summarized in Table 4.4. These values will be used in constructing the model of DC-DC boost converter in SIMULINK-MATLAB program.

As can be shown in Table 4.4, the value of inductor has been chosen greater than calculated value in (4.7) which represents the minimum value of inductor. This selection of inductor value has based on simulation results. In adduction, the value of input capacitor has been chosen depending on the requirements of 2% of maximum input voltage.

Table 4.4 Components of Designed DC-DC Boost Converter

Parameter	Value	Remarks
Switch	$I_{SW,MAK} = 6,6$ A	Equations (4.5) and (4.6)
	$V_{SW,MAK} = 28,7$ V	
Diode	$I_{SW,MAK} = 6,6$ A	Equations (4.5) and (4.6)
	$V_{SW,MAK} = 28,7$ V	
Inductor	$L = 99,18$ µH	It has been chosen greater than calculated value in (4.7)
Input capacitor	$C = 330$ µF	It has been chosen according to required ripple of input voltage (2%)
	$ESR = 40$ mΩ	
Output Capacitor	$C = 68$ µF	Equations (4.9) and (4.10)
	$ESR = 212$ mΩ	

4.1.3 Selection of Zener Diode

In this research, the selection of Zener diode depends mainly on the selection of Zener voltage and power. The selection of Zener voltage depends on the voltage at which battery is charged during CV stage of charging process. In addition, the selection of Zener power depends on the speed of controller in tracking the change of Zener current during charging process. The speed of controller determines time required by controller to follow changes of Zener power so that maximum rating of Zener not to be crossed; thus protects Zener diode from damage.

Depending on Table1 and developed algorithm, 3W Zener diode is chosen to perform regulation action during CV stage of charging algorithm. This diode has a Zener voltage (V_{ZE}) of 28 V which corresponds to gassing voltage of battery. The selection of power has been ensured by simulation process to ensure the protection of Zener diode.

4.1.4 Selection of parameters of developed algorithm

The operation of developed algorithm, which has been illustrated in section 3.3.3, depends on comparing the measured parameters of PV panel and battery bank with predetermined limits through different stages of charging.

The values of these predetermined limits are selected according to the specifications and requirements of different components of stand-alone solar charger system. Table 4.5 lists the values of different predetermined limits that are used in developed algorithms in this research.

Table 4.5 Values of Limits used in Developed Algorithm

Predetermined limits	Value	Remarks
High predetermined limit ($V_{\text{high-limit}}$)	28 V	Table 4.1
Low predetermined limit ($V_{\text{low-limit}}$)	21.6 V	Table 4.1
Minimum charging current (I_{BAT})	1.2 A	Table 4.1
Tolerance error of power during per-charge block (E_{POWER})	0.5 W	Chosen
Step size of duty cycle adjustment during pre-charging block (ΔD)	5e-7	Chosen
Tolerance error of conductance during MPPT block ($E_{conductance}$)	5e-3	Chosen
First lower limit of Zener power (P_{ZEL})	1 W	chosen
First higher limit of Zener power (P_{ZEH})	2 W	chosen
Second lower limit of Zener power (P_{ZELL})	0.85 W	chosen
Second higher limit of Zener power (P_{ZEHH})	2.6 W	chosen

4.1.5 Simulated Stand-Alone Solar Charger System in SIMULINK-MATLAB

Depending on the values given in Table 4.1 ,Table 4.2 ,Table 4.4 , and Table 4.5, the stand-alone solar charger system is built in in SIMULINK-MATLAB program. Figure 4.1 shows the simulated stand-alone solar charger system which consists mainly of PV panel, charge controller, and battery. Charge controller comprises of DC-DC boost converter that is controlled by developed algorithm, and Zener diode. In this simulated system, models of PV panel, boost converter, Zener diode, and battery has been taken

from SIMULINK-MATLAB library. These models give a good approximatopn of performance of these components; but they have limits which may affect operation of whole simulation.
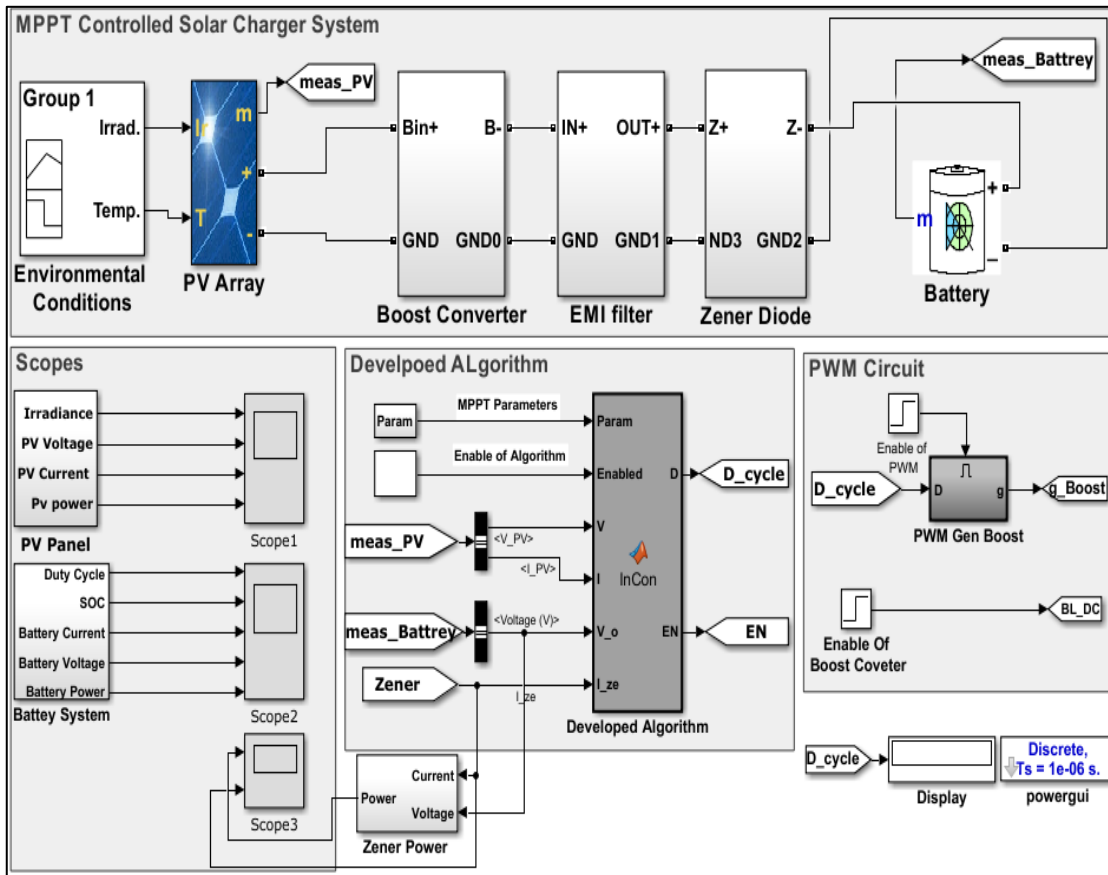

Figure 4.8 Simulated Stand-Alone Solar Charger System in SIMULINK-MATLAB

4.2 Operation of developed MPPT controlled DC-DC Boost converter for Charger System

According to developed algorithm that has been described in section 3.3.3, the proper charging of battery is performed through three stages of charging process that are activated depending on the measured value of battery voltage. These stages are pre-charging, MPPT-CC charging, and CV charging stages. The operating of PV panel at MPP under different environmental conditions is ensured in MPPT-CC charging stage of charging process; so that the maximum available power of PV panel to battery bank is provided. The other two stages of charging process provided by developed algorithm ensures the charging of battery effectively and safely. These functions of developed algorithm is accomplished by MPPT controlled DC-DC boost controller and Zener diode as illustrated previously.

The operation of developed charge controller can be expressed by simulating stand-alone charger system shown in Figure 4.1 in SIMULINK-MATLAB. The simulation of charger system is run for different irradiance levels to simulate the real solar irradiation through a sunny day. The variation of temperature through a day could be taken constant approximately; because the decreasing of open circuit voltage of PV panel is associated with increasing of short circuit current of PV panel. In the following section, the operation of developed controller will be investigated by simulating stand-alone system under STC and changing conditions of environment sequentially.

4.2.1 Operation of Developed Controller under Standard Test Condition of Environment

Under Standard Test Condition of environment, level of irradiance remains constant at 1000 kw/m^2 through the charging period of battery. The operation of developed controller under these conditions of environment is investigated by expressing voltage, current, and power of PV panel and battery bank in the three stages of charging process. In the following sections. The simulation is run over an interval of time equals to 4(s) that is chosen according to capability of computer and version of SIMULINK-MATLAB. Therefore, the simulation time cannot approximate the real charging time of battery. However, it can be used as an indication of the charging time performance under different conditions of environment and charging process; based on the total time of simulation.

4.2.1.1 Operation of Developed Controller during Pre-Charging Stage of Charging Process.

The operation of this stage takes place when battery voltage is less than 21,6. In this simulation, charging process of battery is started with SOC of 11,2% that indicates a battery voltage of 21,33V as shown in Figure 4.2 and 4.3 respectively. Accordingly, the developed controller charges battery bank with the minimum value of charging current which is 1,2 A as shown in Figure 4.4. During this stage of charging process, power of battery is minimum because of minimum charging current as shown in Figure 4.5 which represents battery power of 25,6 W.
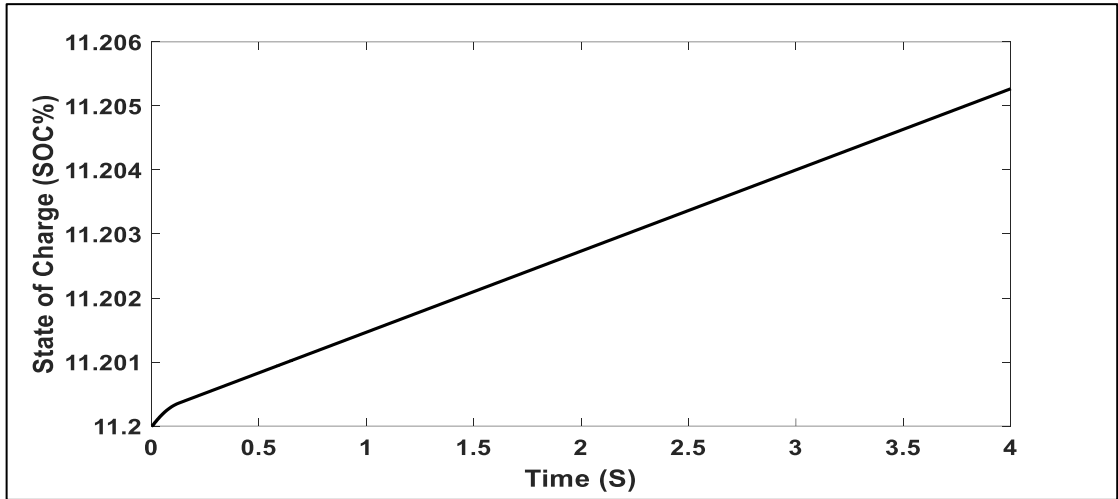
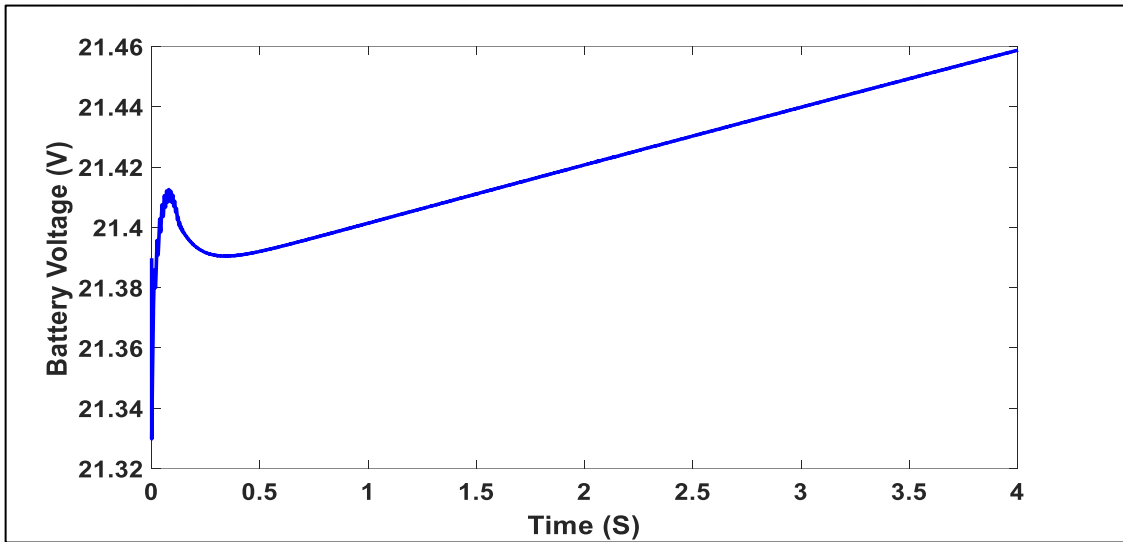Figure 4.2 SOC of Battery during Pre-Charging Stage under STC

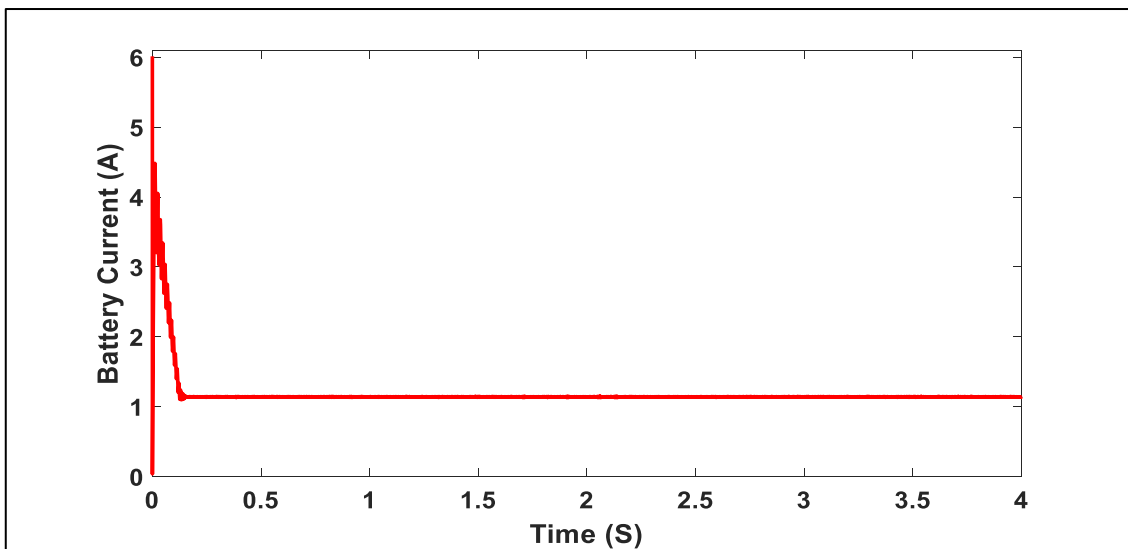Figure 4.3 Battery Voltage during Pre-Charging Stage under STC

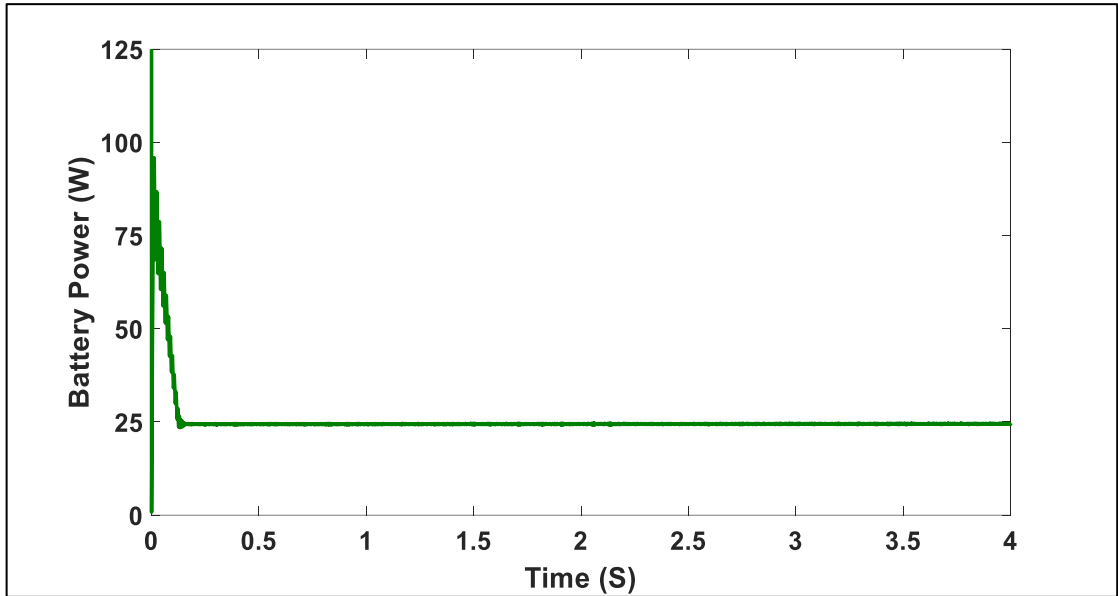Figure 4.4 Battery Current during Pre-Charging Stage under STC

Figure 4.5 Battery Power during Pre-Charging Stage under STC

In order to ensure the charging of battery as stated above, the developed controller operates the PV panel at constant current region of V-I curve. In this region, PV current equals nearly short circuit current of 6 A as shown in Figure 4.6. The determination of PV voltage depends on the required PV power and PV current. The required PV power is equal ideally the power of battery that is 25,6 W as shown in Figure 4.5. The power of PV panel during precharging stage of charging process is shown in Figure 4.7. As a consequence, PV voltage is determined as 4,4V during precharging stage as shown in Figure 4.8.
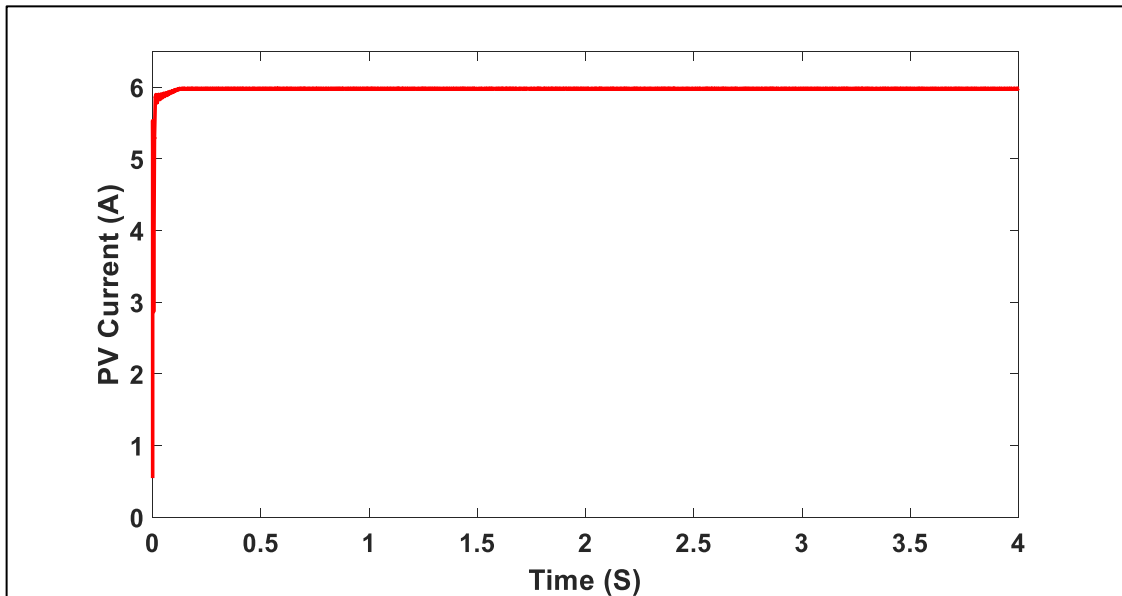
Figure 4.6 PV Current during Pre-Charging Stage under STC
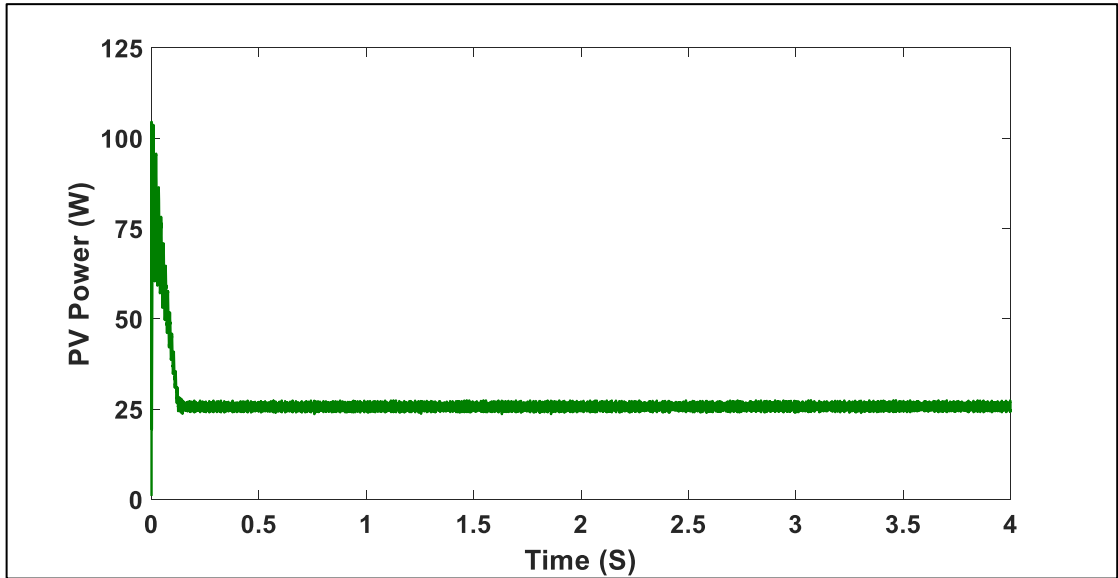
68

Figure 4.7 PV Power during Pre-Charging Stage under STC
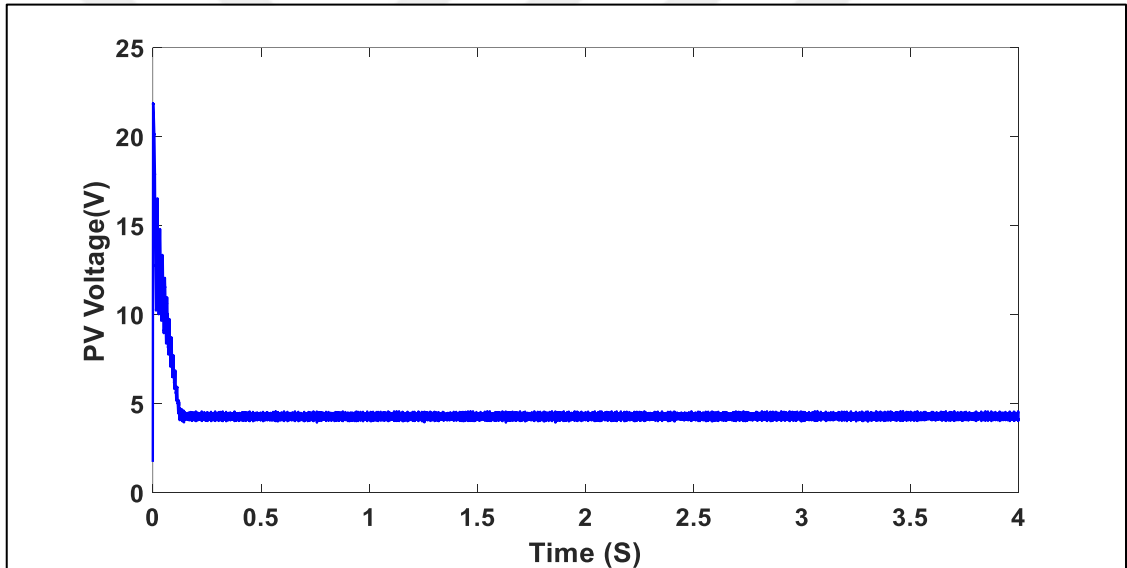

Figure 4.8 PV Voltage during Pre-Charging Stage under STC

As can be shown in above Figures, battery voltage increases gradually during charging process which results in increasing PV voltage by controller in order to maintain powers of battery and PV panel equal nearly.

In addition, charging current of battery decreases slowly because of decreasing PV current as a result of moving of operating point along I-V curve of PV panel. This moving along I-V curves is activatied by the developed controller which continuously adjust duty cycle of boost converter in order to ensure the equality between battery power and PV power . This process continues until battery voltage reaches $V_{low\text{-}limit}$ that is 21,6 V.

4.2.1.2 Operation of Developed Controller during MPPT-CC charging Stage of Charging Process

When battery voltage reaches 21,6V, the developed controller charges battery bank with maximum charging current of 4,8 A. Figure 4.9 and 4.10 shows the voltage and current of battery respectively. As can be shown through transition period, charging current increases from 1,2 A to 4,8 A smoothly within minimum time. Charging of battery with maximum charging current of 4,8A results in increasing the rate of change of state of charge as can be shown in Figure 4.11. Due to the increase of charging current, the required power of battery increases substantially from 25,6 W to 100 W as shown in Figure 4.12.
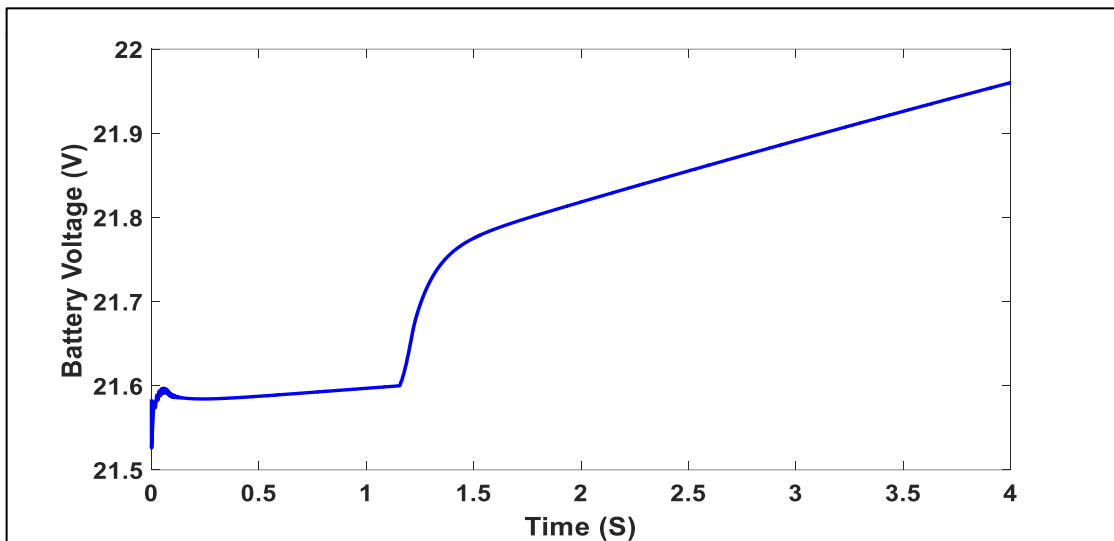

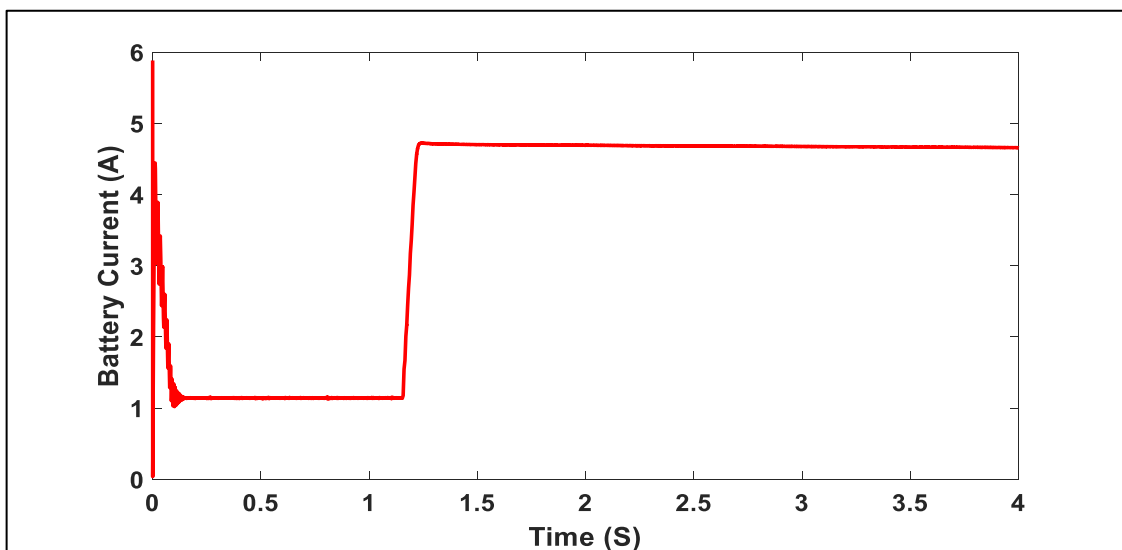Figure 4.9 Battery Voltage during MPPT-CC Charging Stage under STC

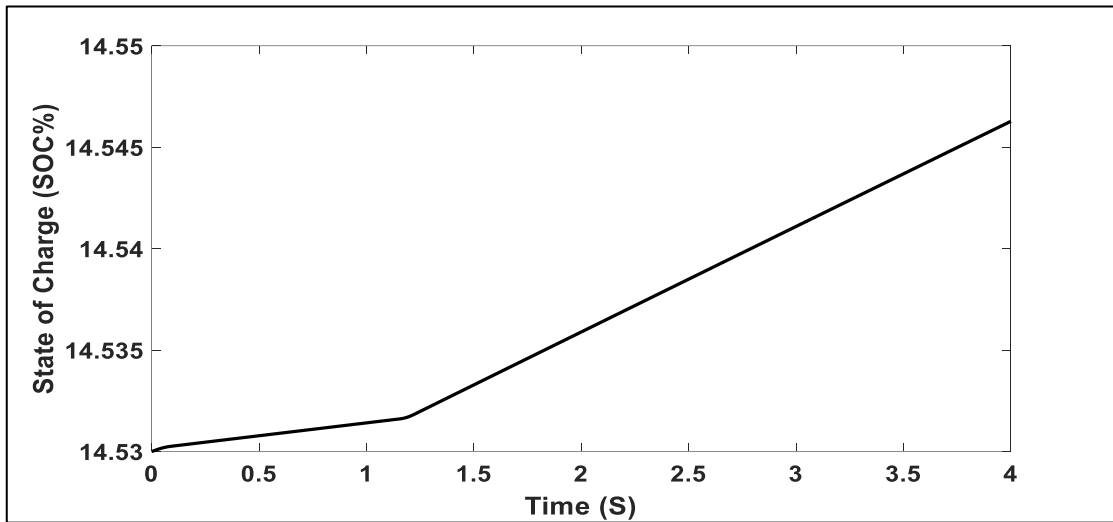Figure 4.10 Battery Current during MPPT-CC Charging Stage under STC

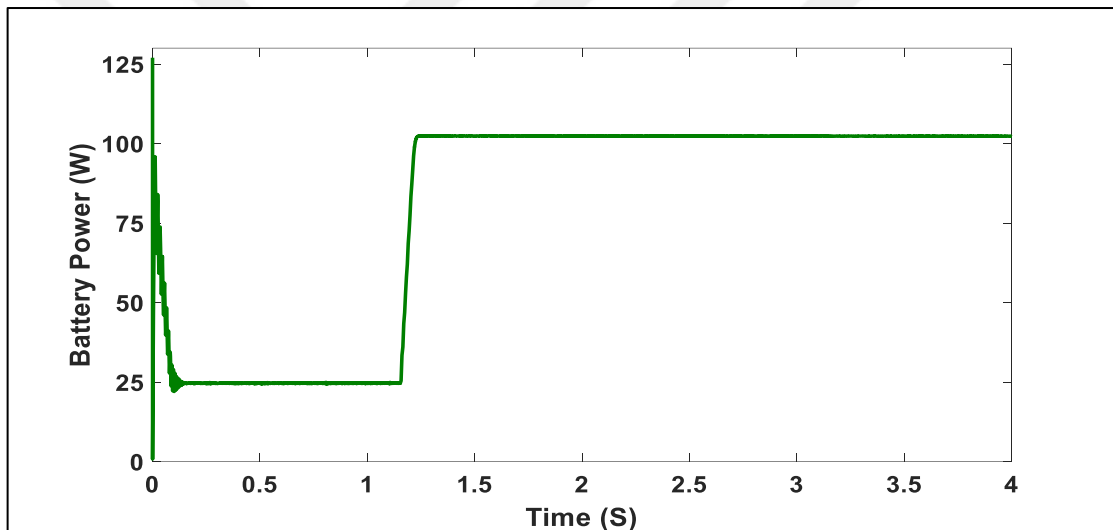Figure 4.19 SOC of Battery during MPPT-CC Charging Stage under STC

Figure 4.102 Battery Power during MPPT-CC Charging Stage under STC

In order to accomplish the above conditions of battery charging, the developed controller operates the PV panel at maximum power point of V-I curve in order to provide maximum available power of PV panel. At MPP, PV panel is operated at maximum power point voltage and maximum power point current of 18,8 V and 5,4 A respectively. Figure 4.13 and 4.14 show the PV voltage and current during MPPT-CC charging stage respectively. Figure 4.15 shows PV power of 100W that is extracted by incremental conductance algorithm under STC of environment. In this stage, developed controller operates as MPPT controller to ensure supplying maximum charging current to the battery continuously; thus this stage represents constant current (CC) stage of charging algorithm.
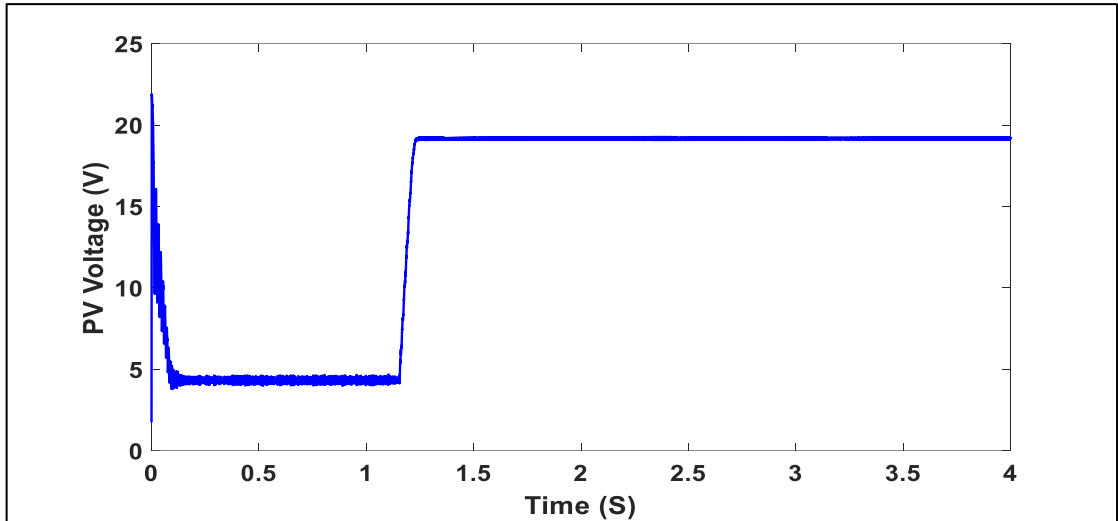
71

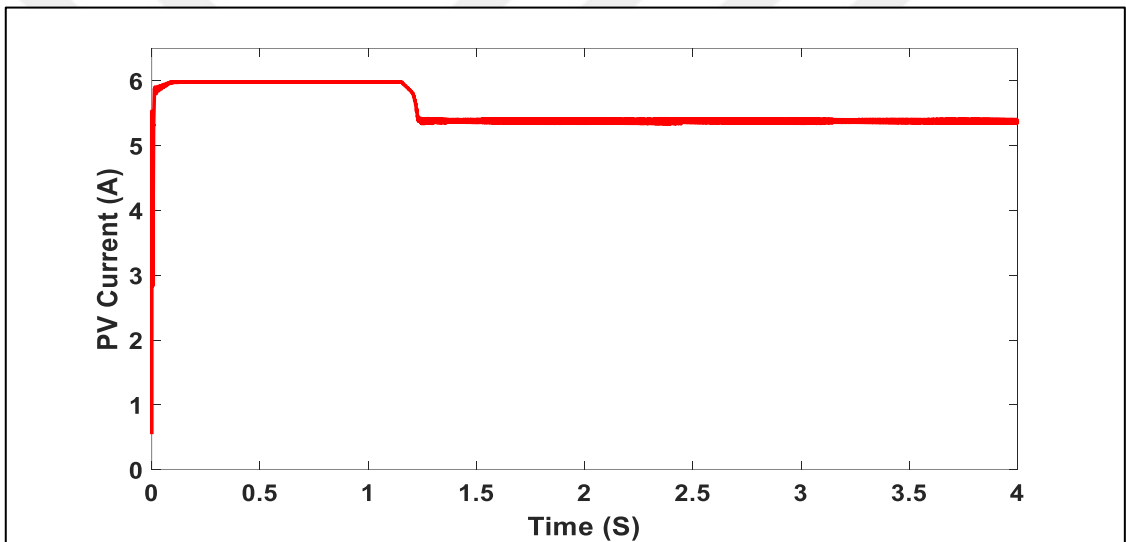Figure 4.113 PV Voltage during MPPT-CC Charging Stage under STC

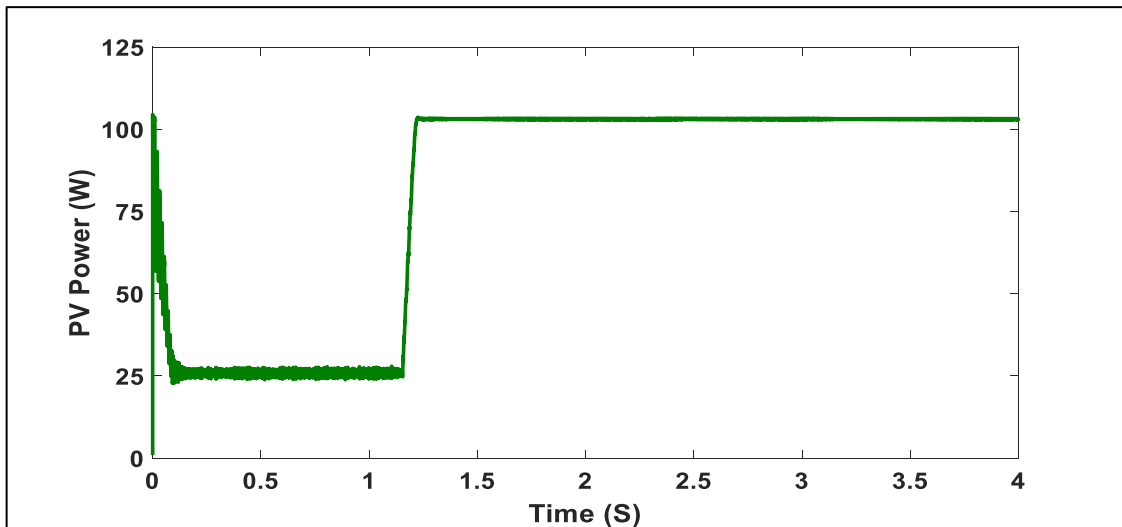Figure 4.14 PV Current during MPPT-CC Charging Stage under STC

Figure 4.125 PV Power during MPPT-CC Charging Stage under STC

In addition, as can be shown from above Figures, battery voltage increases gradually with slow decreasing of battery charging current in order to maintain battery power constant. This condition is resulted from operating the developed controller as MPPT controller which increases PV voltage according to the increase of battery voltage. As a result, PV current decreases slowly in order to extract maximum power from PV panel. This process of extracting maximum power continues until voltage of battery reaches $V_{high\text{-}limit}$ that is 28 V.

4.2.1.3 Operation of Developed Controller during CV Charging Stage of Charging Process

When battery voltage reaches 28 V, the developed controller requlates the voltage across battery terminals at that value of voltage in order to ensure the charging of battery in constant voltage (CV) stage of charging process. This regulation of battey voltage is accomplished by using Zener diode which starts conducting at Zener voltage of 28 V and regulating voltage across battery terminals. Figure 4.16 shows the requlation of battery voltage at the value of Zener voltage during this stage of charging process. Charging of battery with this regulated voltage increases SOC of battery in as shown in Figures 4.17. Figure 4.18 shows battery current that decreases gradually in accordance with increasing of SOC of battery. These conditions of battery charging result in decreasing of battery power as can be shown in Figure 4.19. This decrease of battery power continuses until the end of charge condition is detected.
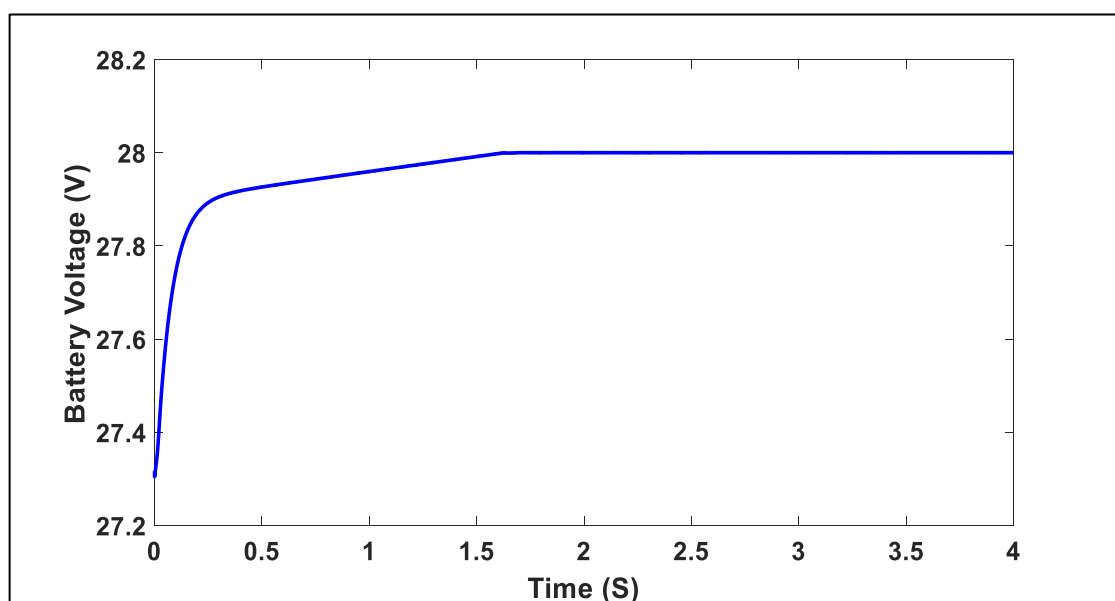

Figure 4.136 Battery Voltage during CV Charging Stage under STC
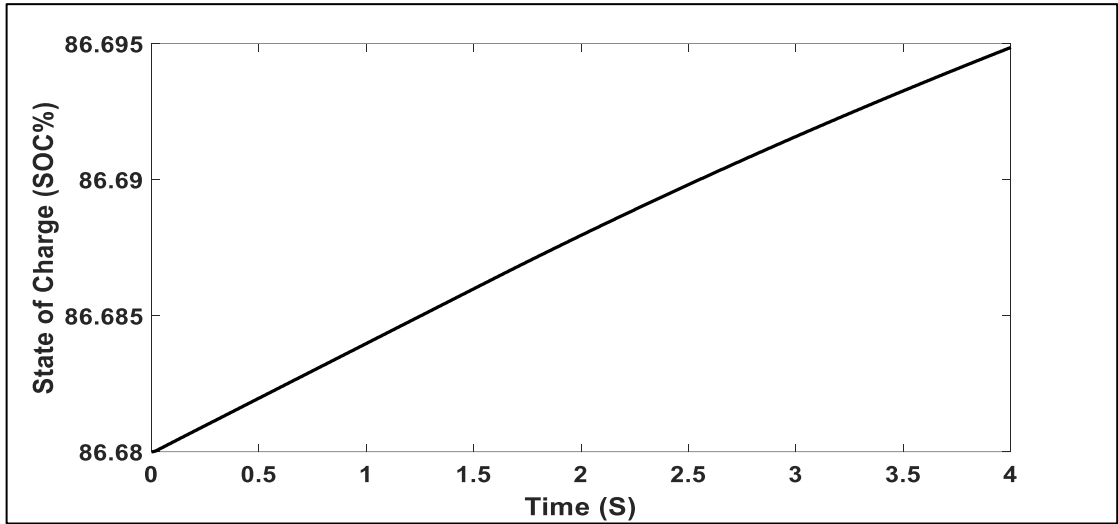
Figure 4.17 SOC of Battery during CV Charging Stage under STC
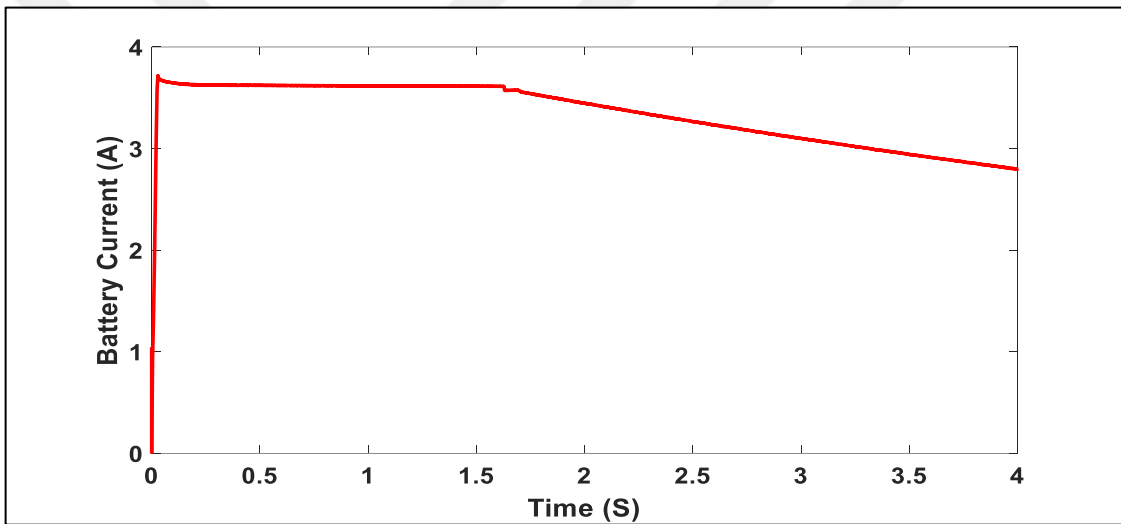

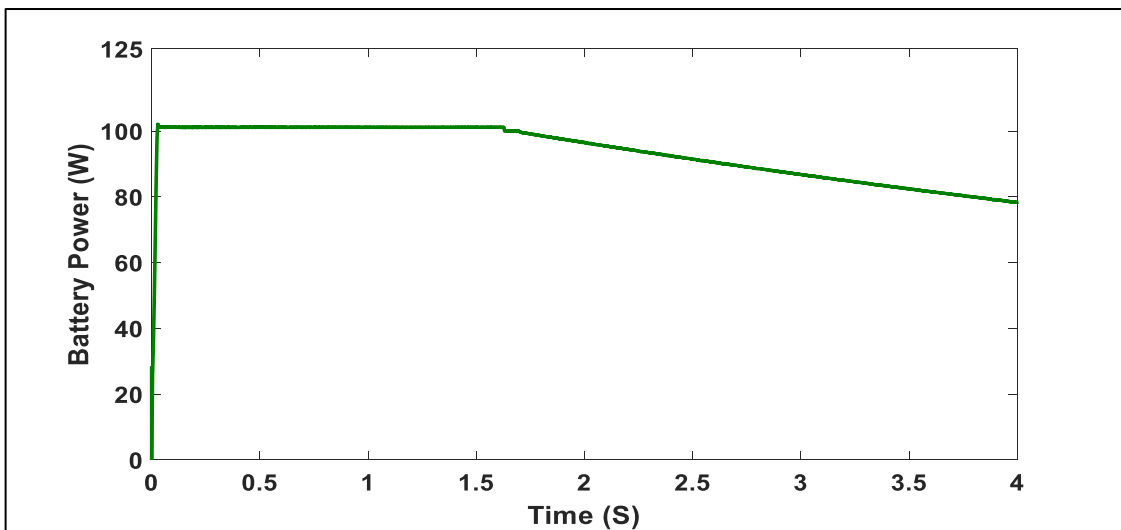Figure 4.148 Battery Current during CV Charging Stage under STC

Figure 4.159 Battery Power during CV Charging Stage under STC

Since power provided by PV panel remains unchanged until duty cycle of boost converter is changed, the decreasing of battery power during CV charging stage results in increasing power of Zener diode as shown in Figure 4.20. The developed charge controller limits this increasing of Zener power by adjusting duty cycle of boost converter in order to reduce the current of PV power in accordance with decreasing current of battery.
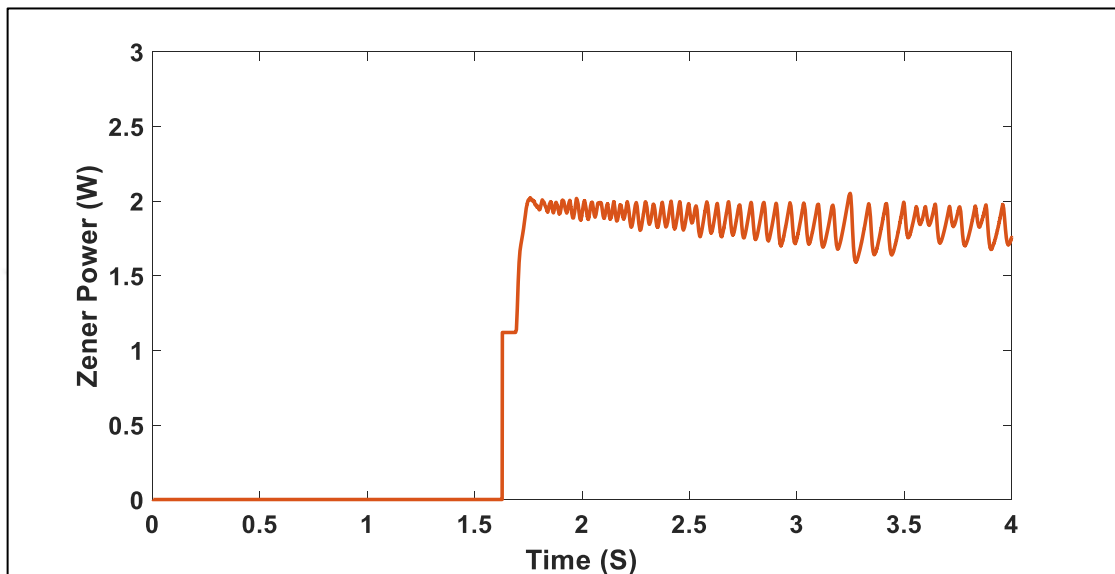

Figure 4.20 Zener Power during CV Charging Stage under STC

In order to accomplish the constant voltage charging of battery, the developed controller operates PV panel at constant voltage region of I-V curve. In this region, the PV voltage is constant nearly as shown in Figure 4.21.
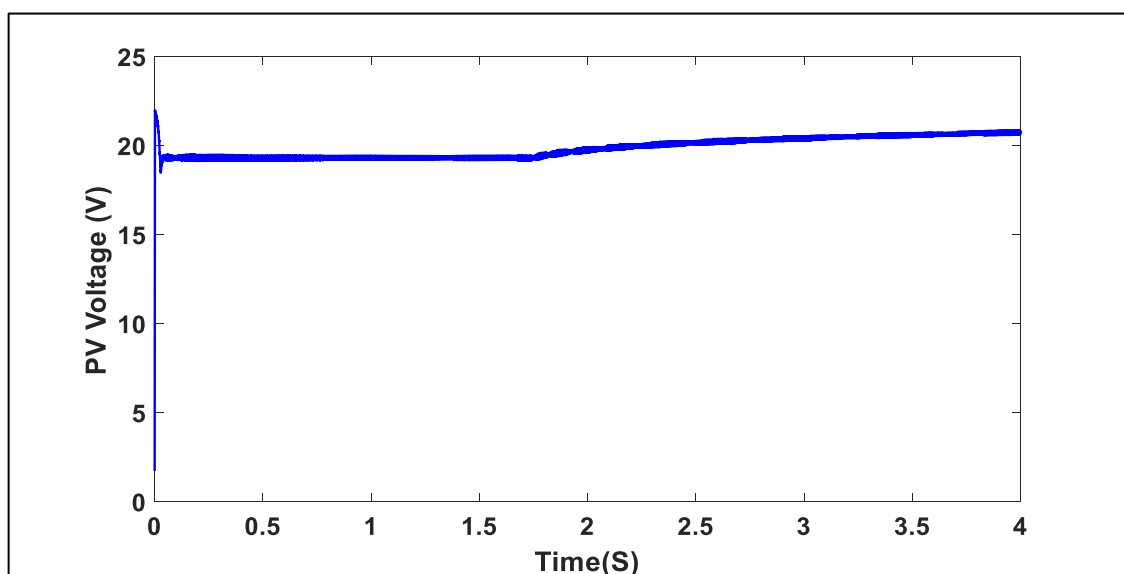

Figure 4.21 PV Voltage during CV Charging Stage under STC

75

However, PV current and power decrease gradually as a result of decreasing current and power of battery as shown in Figures 4.22 and 4.23 respectively. This process continues until PV power reaches 6.72W which is calculated from (3.19) and equivalent to minimum charging current of 0.24A that indicates end of charge of battery.
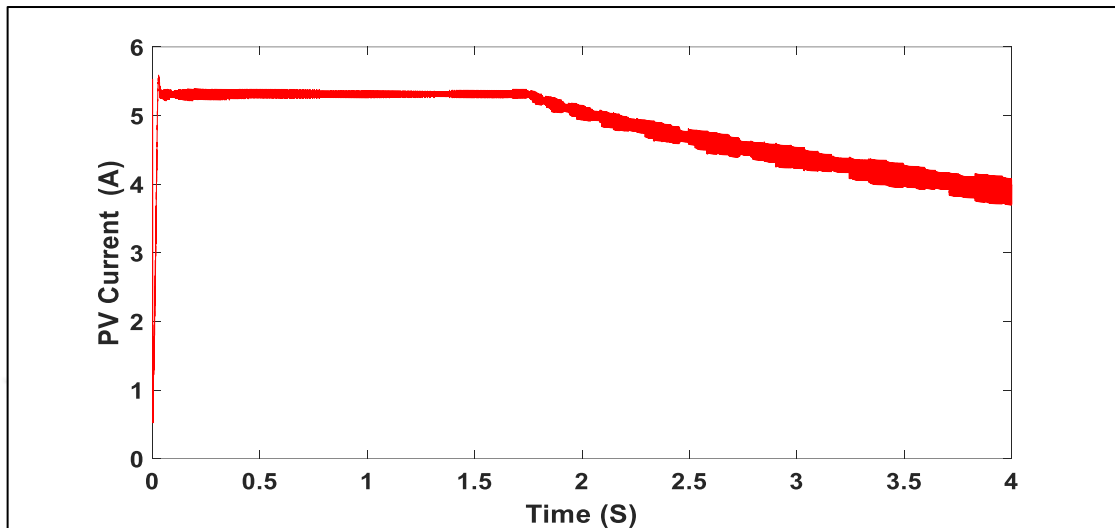
Figure 4.22 PV Current during CV Charging Stage under STC

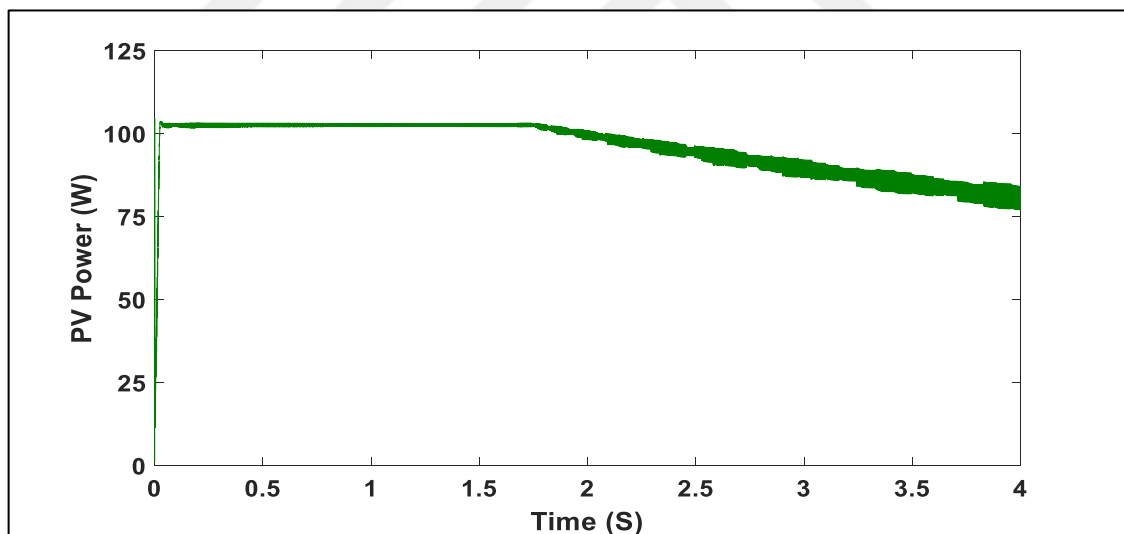

Figure 4.23 PV Power during CV Charging Stage under STC

4.2.2 Operation of Developed Controller under Changing Conditions of Environment

In this simulation, changing environmental conditions are represented by changing levels of irradiance through simulation period with constant temperature. Figure 4.24 shows the changing environmental conditions that will be used in this simulation. It

represents irradiance Levels of (1000, 600, 900, 700, 400) W/m^2. In addition, the transition between these irradiance levels is represented by ramp changing.

In the following sections, the operation of developed controller under changing environment of Figure 4.24 will be investigated in the three stages of charging process.
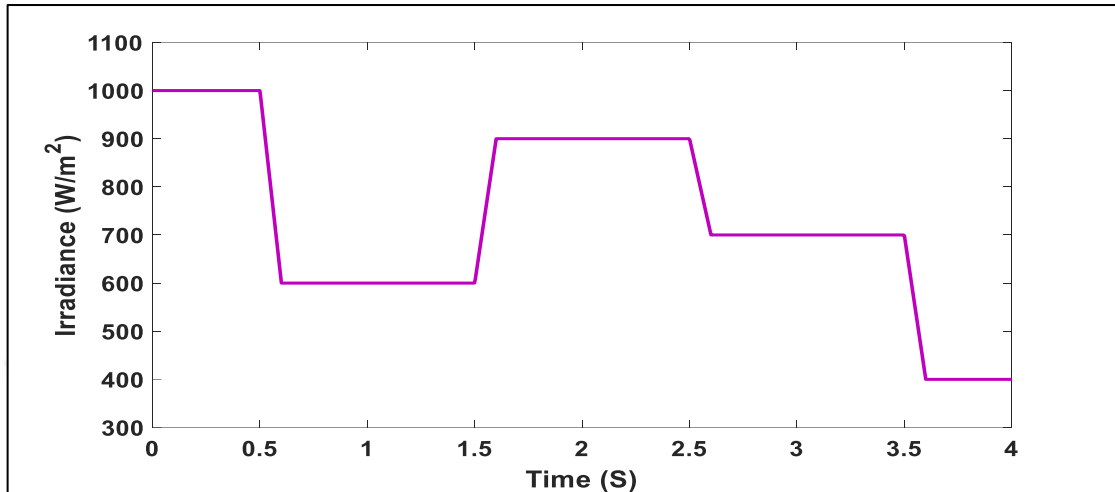
Figure 4.24 Simulated Change of Irradiance Levels

4.2.2.1 Operation of Developed Controller during Pre-Charging Stage of Charging Process

In this stage, the PV panel is operated at constant current region of I-V curve which is affected hardly by changing of environmental conditions. Therefore, changing environmental conditions of Figure 4.24 results in changing of PV current considerably as shown in Figure 4.25.
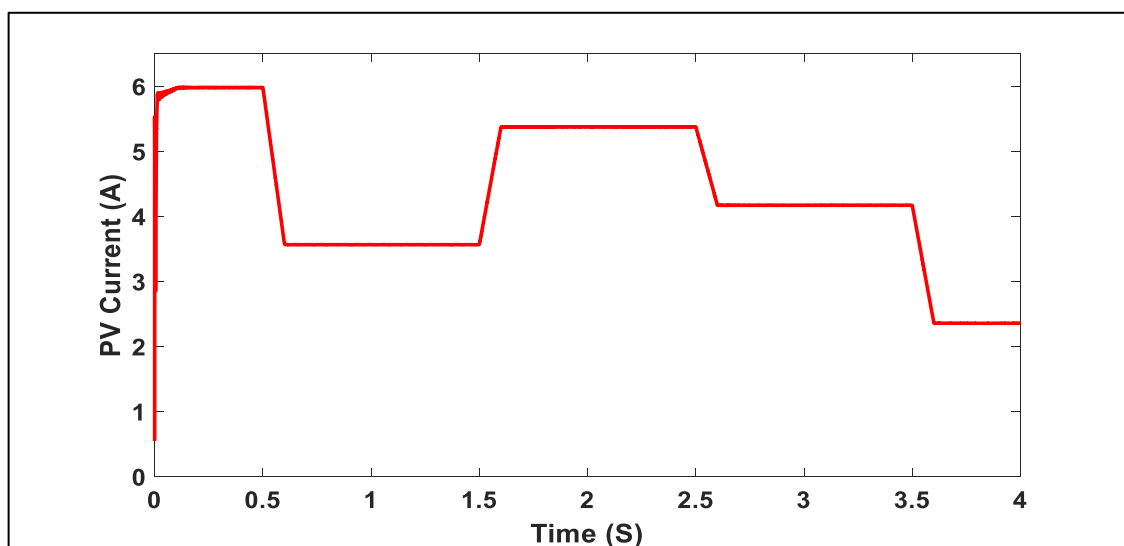
Figure 4.25 PV Current during Pre-Charging Stage under Changing Environment

77

However, since the power supplied to battery during this stage of charging process is small because of minimum charging current. The variation of environmental condition will not affect parameters of battery considerably. This can be shown in Figure 4.26, 4.27 4.28 which represent current, SOC, and voltage of battery respectively.

As can be shown, these Figures have nearly same performance as in STC of environment except in low irradiance condition. At low irradiance condition, the maximum power that can be extracted is reduced considerably. Therefore, the amount of power that is supplied to battery can be affected.

Figure 4.26 Battery Current during Pre-Charging Stage under Changing Environment

Figure 4.27 SOC of Battery during Pre-Charging Stage under Changing Environment

78
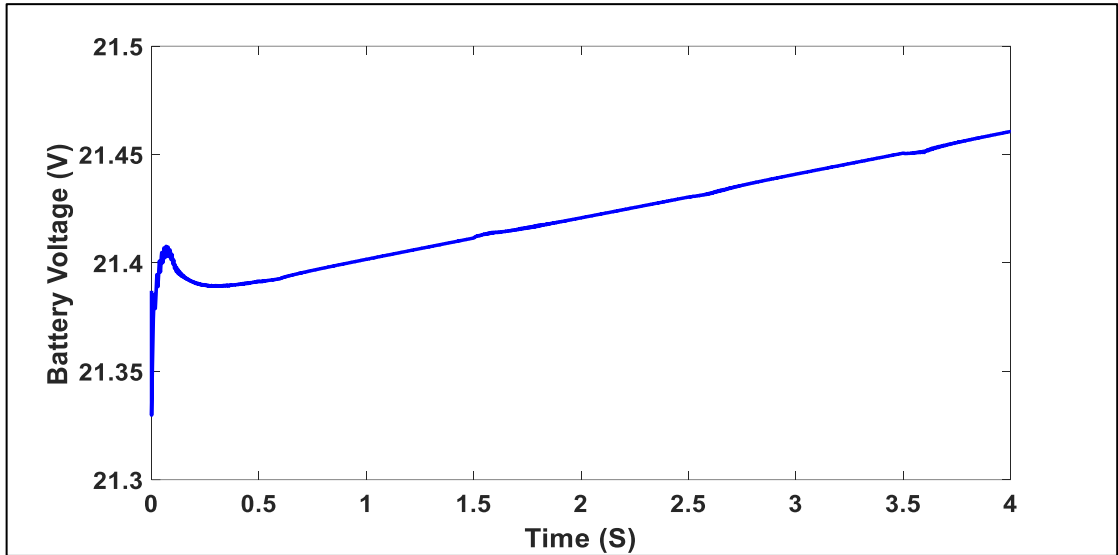
Figure 4.28 Battery Voltage during Pre-Charging Stage under Changing Environment

The power that is supplied is shown in Figure 4.29. As can be shown, the amount of power is not affected by variation of environmental conditions since the level of charging current has not changed considerably.
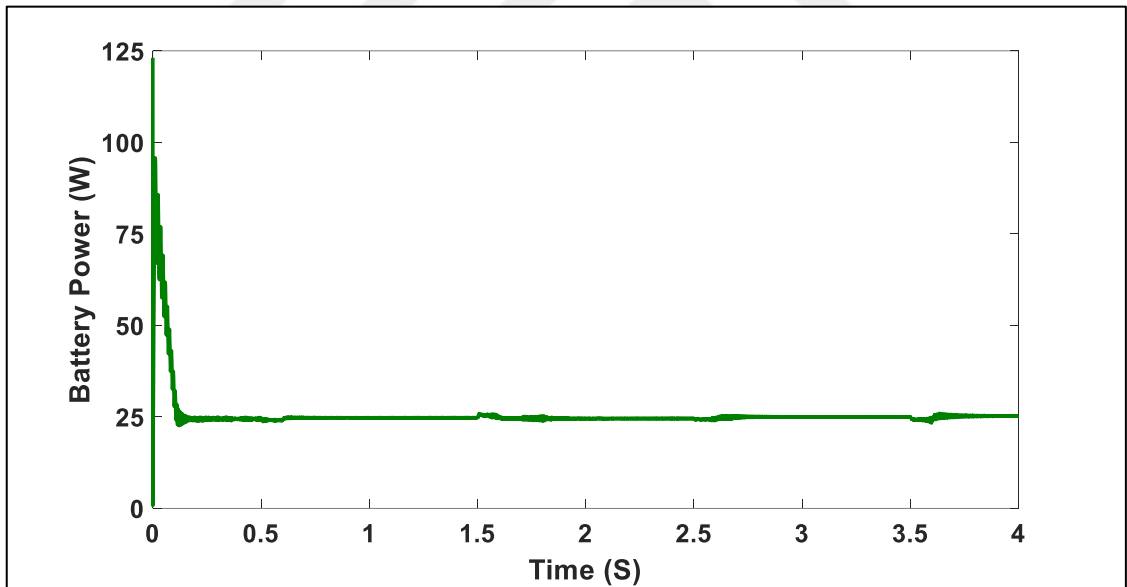
Figure 4.29 Battery Power during Pre-Charging Stage under Changing Environment

In this stage, developed controller depends on the equaling the powers of battery and PV panel. Therefore, the power that is extracted from PV panel is kept constant as can be shown in Figure 4.30.

In order to accomplish this equality of PV power and battery power, the developed system changes the level of PV voltage in accordance with change of PV current as shown in Figure 4.31
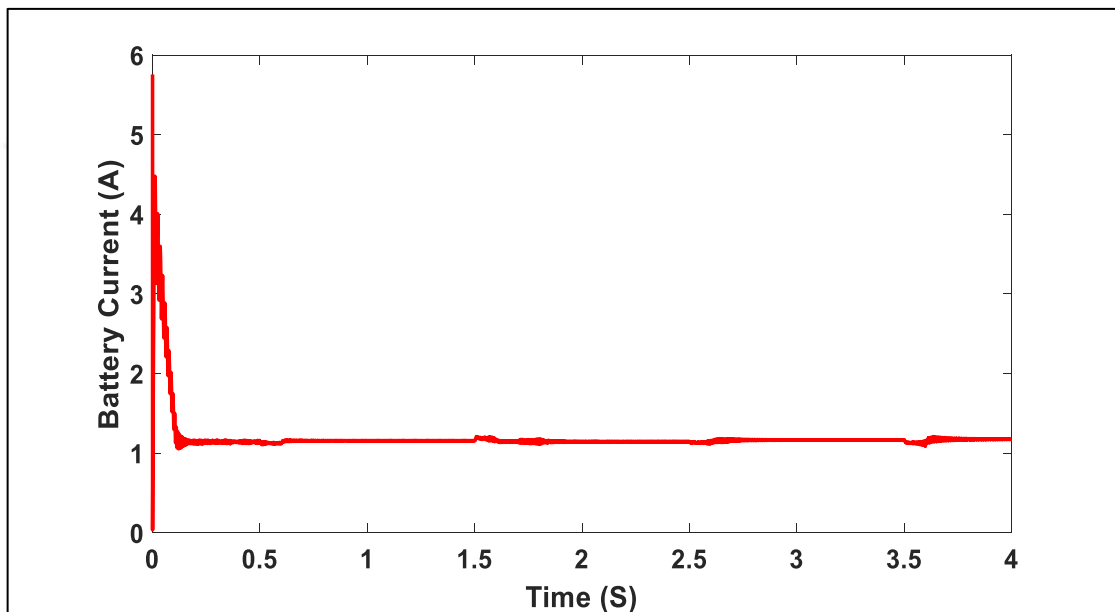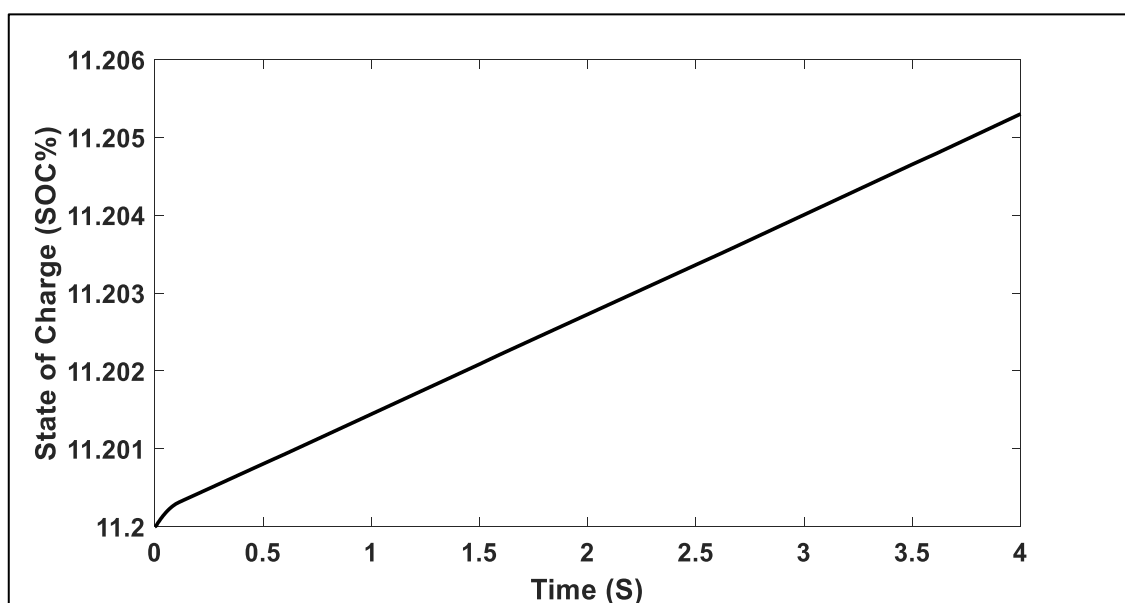
79
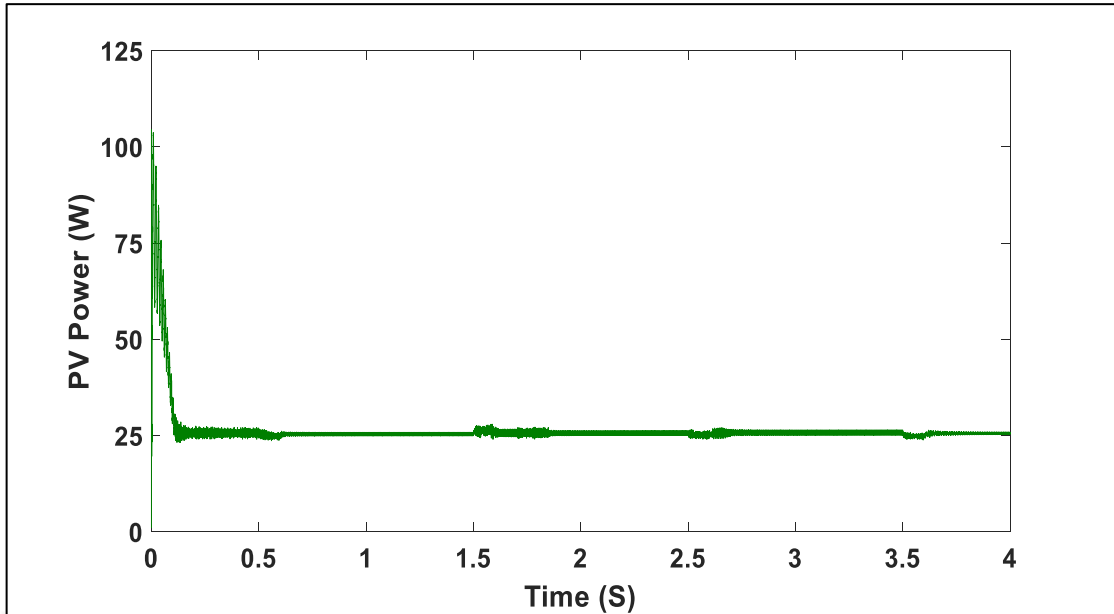
Figure 4.30 PV Power during Pre-Charging Stage under Changing Environment
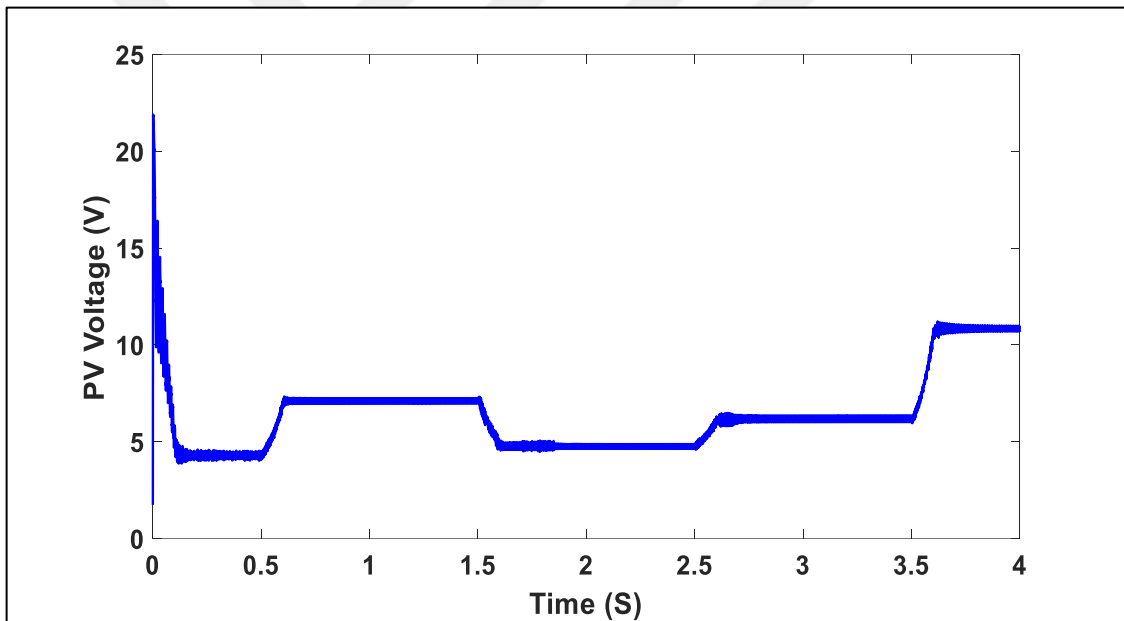
Figure 4.31 PV Voltage during Pre-Charging Stage under Changing Environment

4.2.2.2 Operation of Developed Controller during MPPT-CC charging Stage of Charging Process

In this stage, developed controller works as MPPT controller in order to operate PV panel at maximum power point irrespective of environmental condition. The tracking of PV panel parameters for MPP during changing environmental conditions are shown in Figure 4.32, 4.33, ands 4.34 which represent changes of voltage, current and power of PV panel during changing environment respectively.
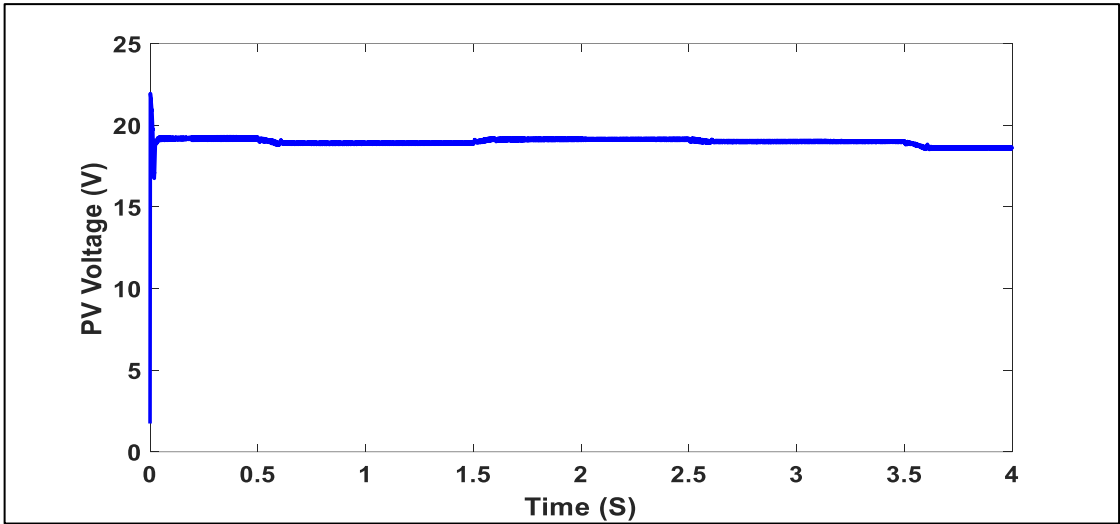
Figure 4.32 PV Voltage during MPPT-CC Stage under Changing Environment

Figure 4.33 PV Current during MPPT-CC Stage under Changing Environment
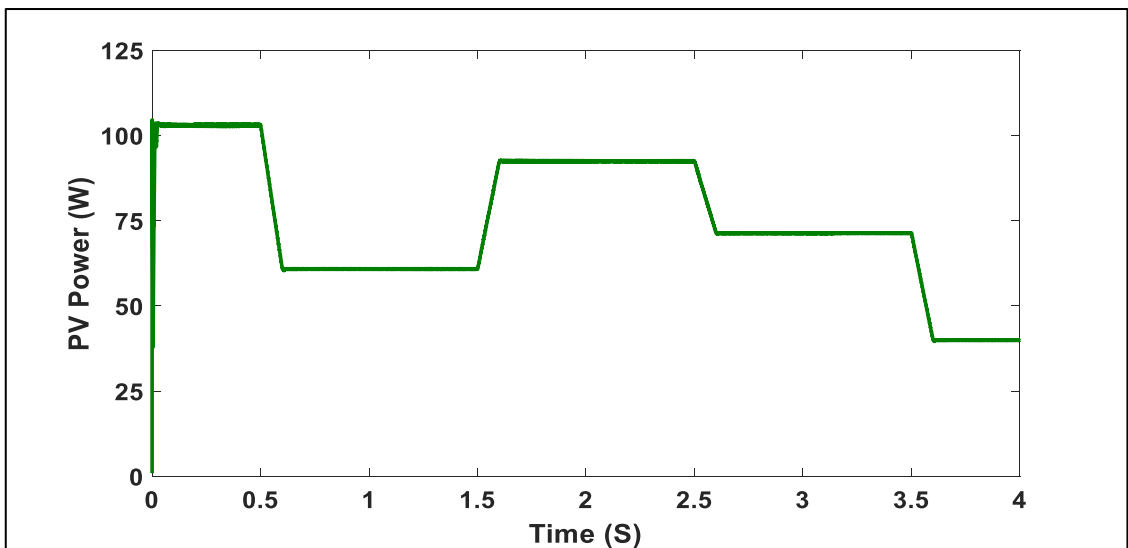
Figure 4.34 PV Power during MPPT-CC Stage under Changing Environment

The behavior of battery parameters though this tracking process can be shown in Figures 4.35, 4.36, 4.37 and 4.38 which represent SOC, voltage, current, and power of battery during changing environment respectively.

As can be shown from Figure 4.36, the decreasing of charging current results in decreasing of battery voltage. The developed system tracks maximum power point continuously to supply maximum available current; so battery voltage is not affected considerably.

Figure 4.35 SOC of Battery during MPPT-CC Stage under Changing Environment
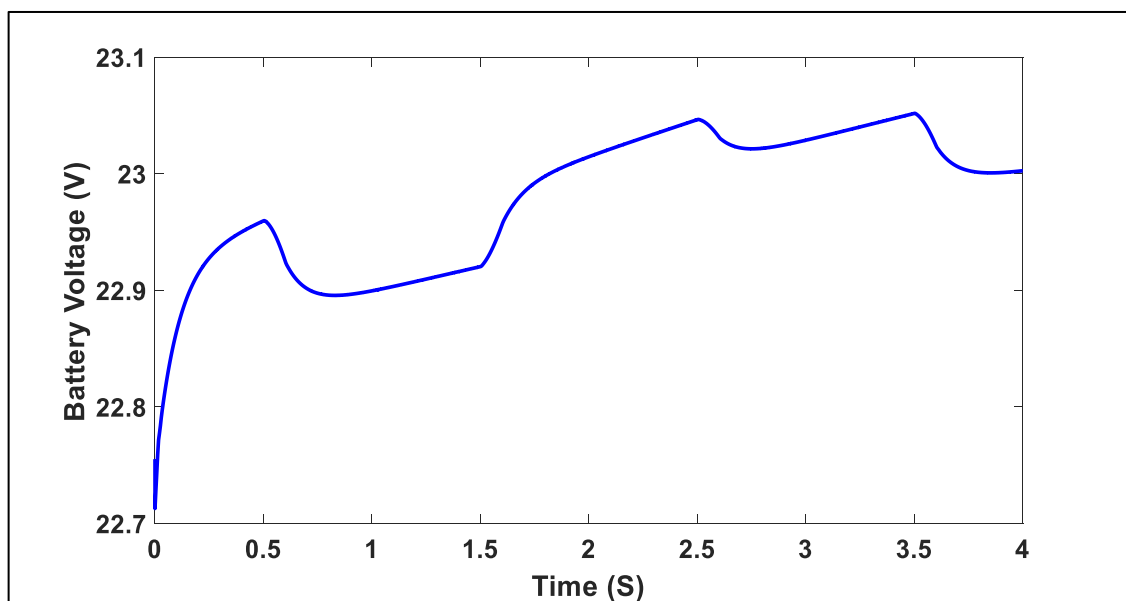
Figure 4.36 Battery Voltage during MPPT-CC Stage under Changing Environment
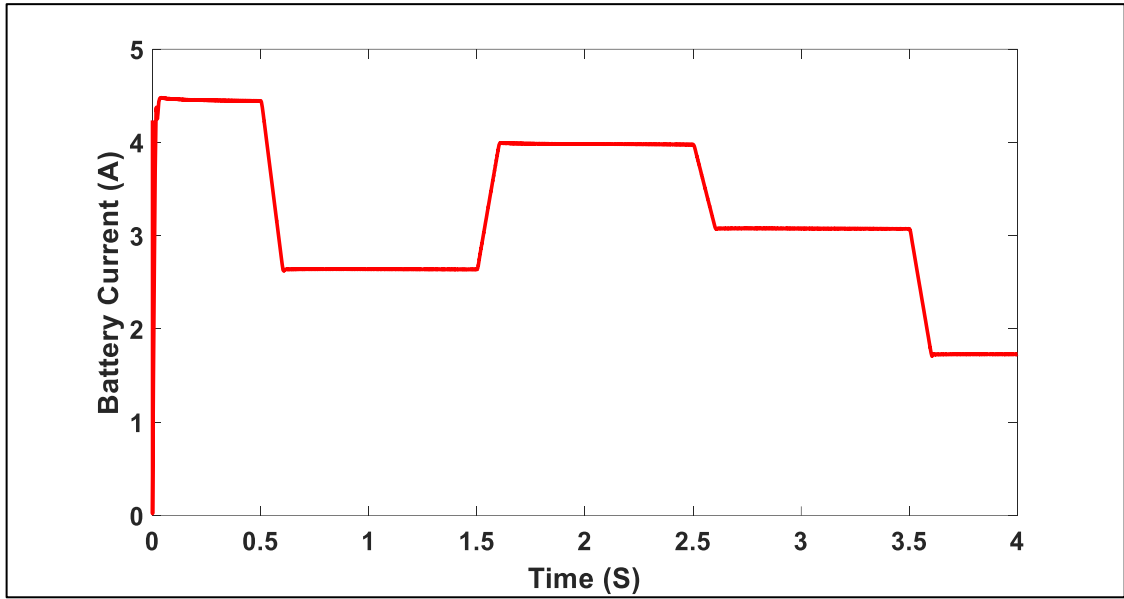
Figure 4.37 Battery Current during MPPT-CC Stage under Changing Environment
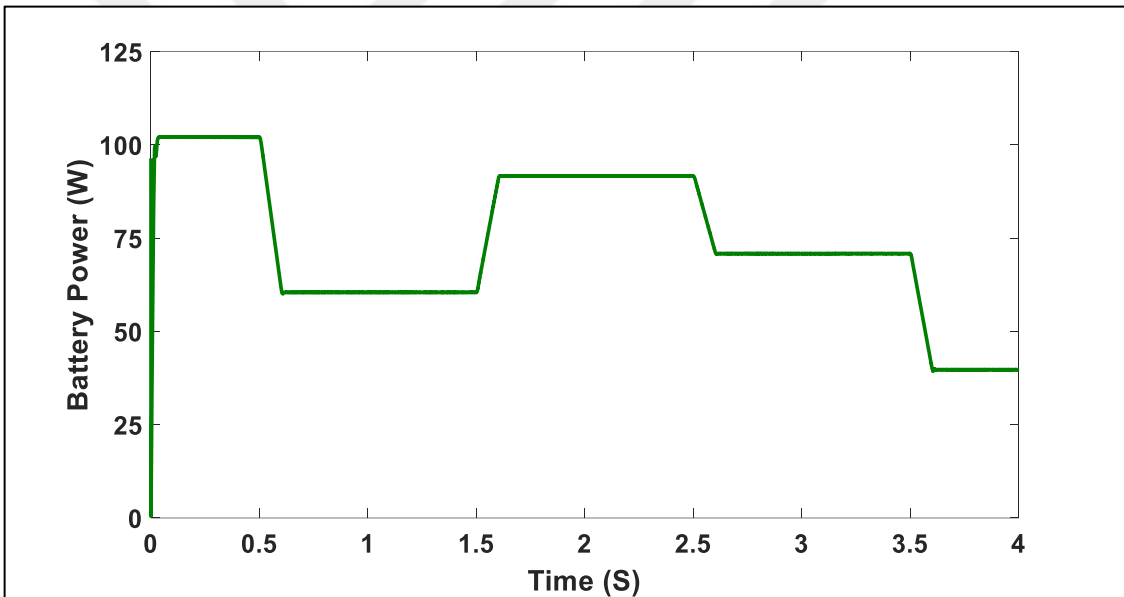
Figure 4.38 Battery Power during MPPT-CC Stage under Changing Environment

4.2.2.3 Operation of Developed Controller during CV Charging Stage of Charging Process

In this stage, PV panel is operated at constant voltage region of I-V curve, which is characterized by mostly constant PV voltage and decreasing PV current. Therefore, under changing environmental conditions, the decreasing of battery current as a result of constant voltage charging happens in a rate faster and high than that of Figure 4.18. Figure 4.39 and 4.40 shows current of PV panel and battery during charging environment conditions respectively.

83
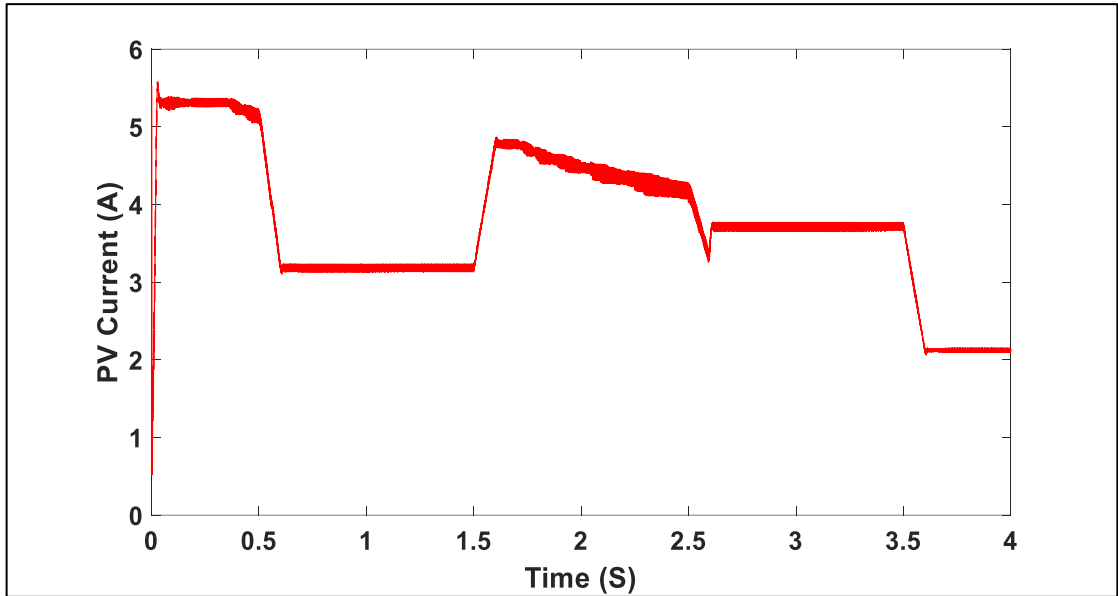
Figure 4.39 PV Current during CV Stage under Changing Environment
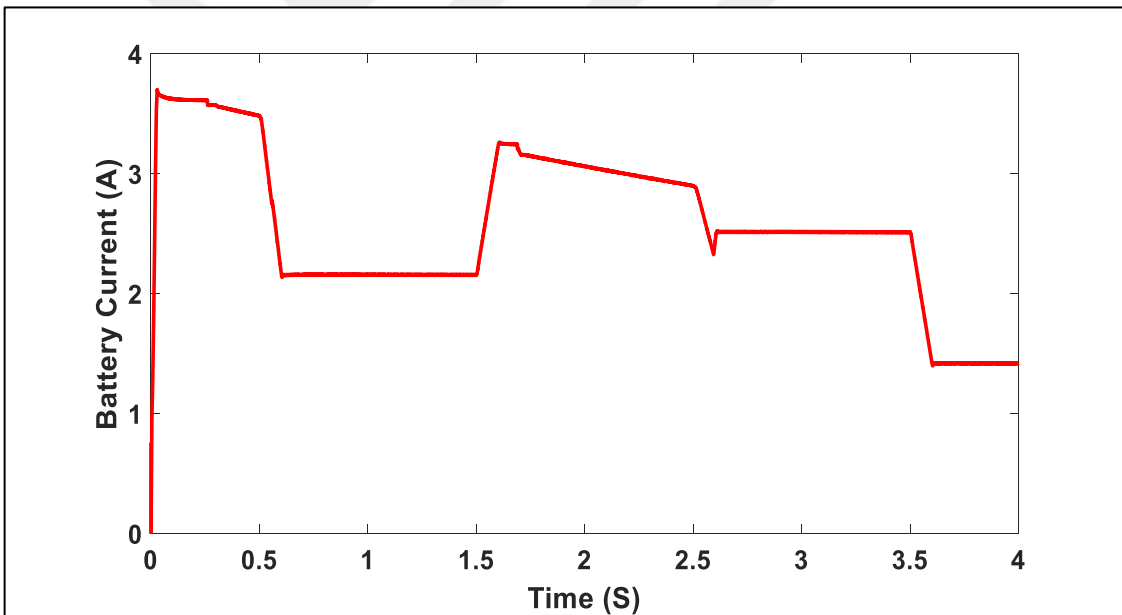
Figure 4.40 Battery Current during CV Stage under Changing Environment

This high rate of decreasing of battery current represents that a change of charging current has been occurred; instead of increasing of SOC of battery. As a consequence, voltage of battery starts to decrease slowly according to the change of charging current as shown in Figure 4.41. The change of battery voltage affects SOC of battery and PV voltage as shown in Figure 4.42 and 4.43. As can be shown, when change in charging current is detected, the developed controller operates as MPPT controller in order to charge battery with maximum power that corresponds to new environmental conditions.
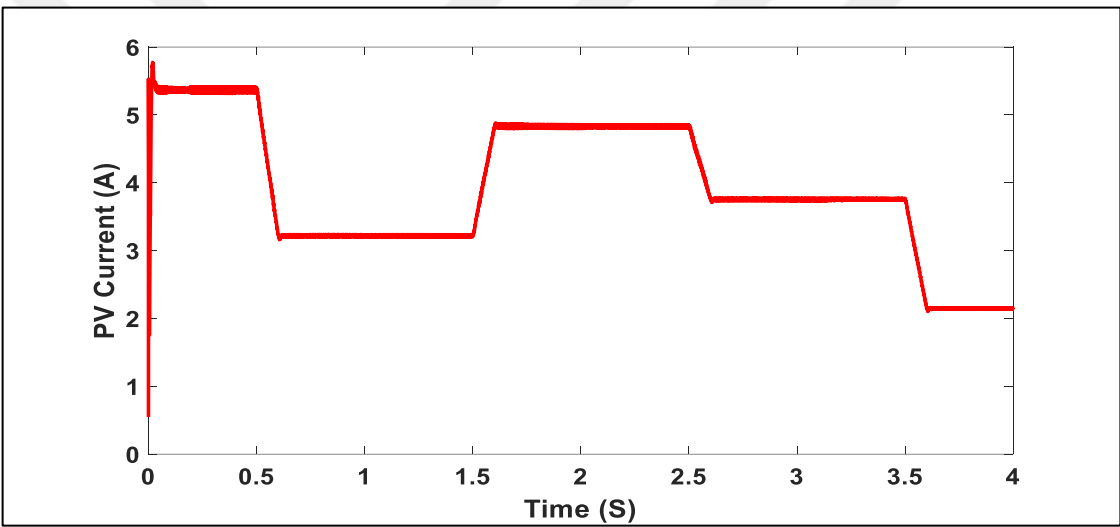
84
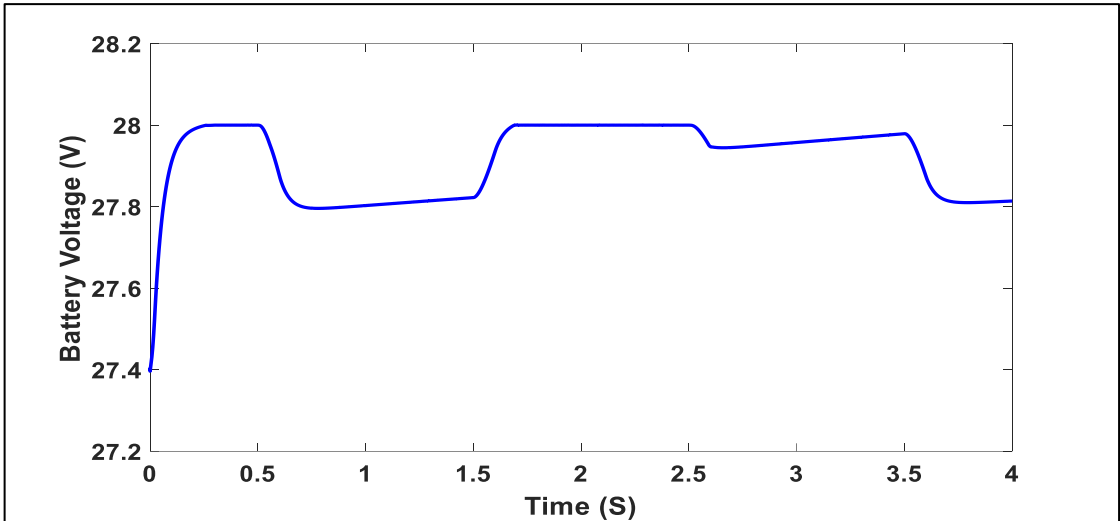
Figure 4.41 Battery Voltage during CV Stage under Changing Environment
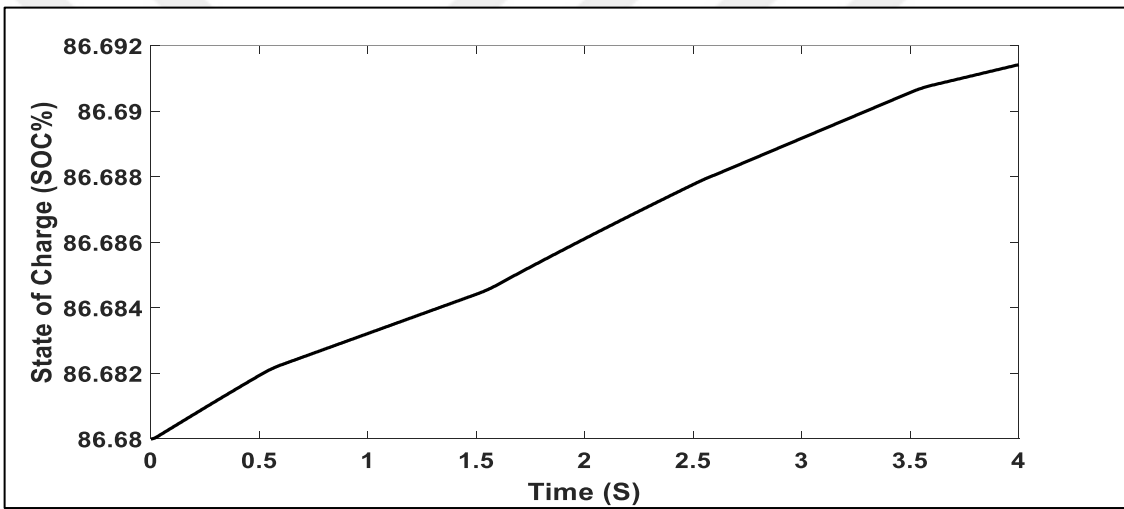
Figure 4.42 SOC of Battery during CV Stage under Changing Environment
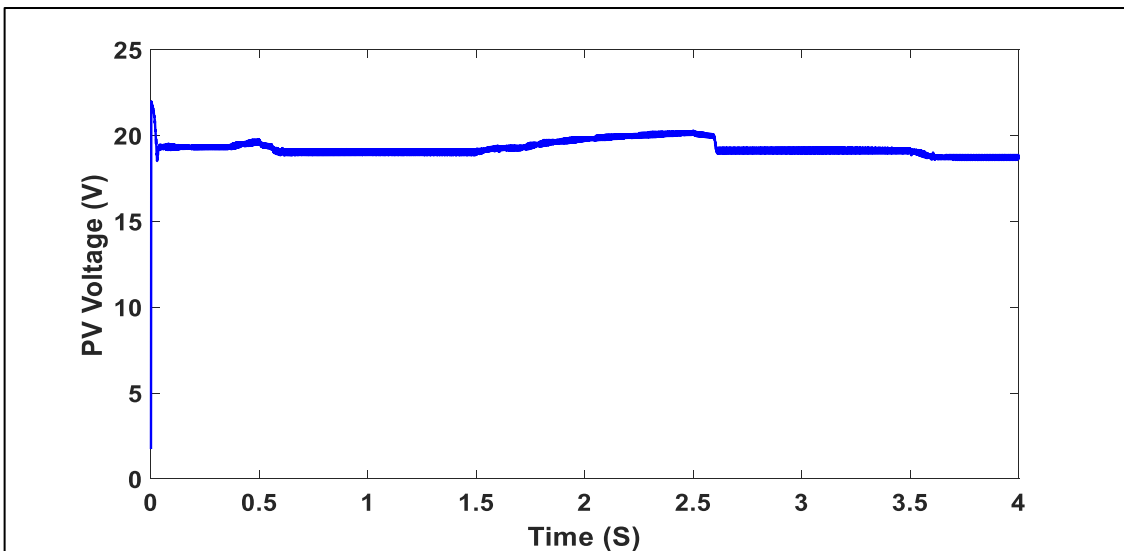
Figure 4.43 PV Voltage during CV Stage under Changing Environment

85

Ac can be shown in Figure 4.41, battery voltage is regulated by Zener diode when measured value of voltage reaches high limit of battery voltage (V_{BATmax}). Figure 4.44 shows the power of Zener diode under changing conditions of environment.
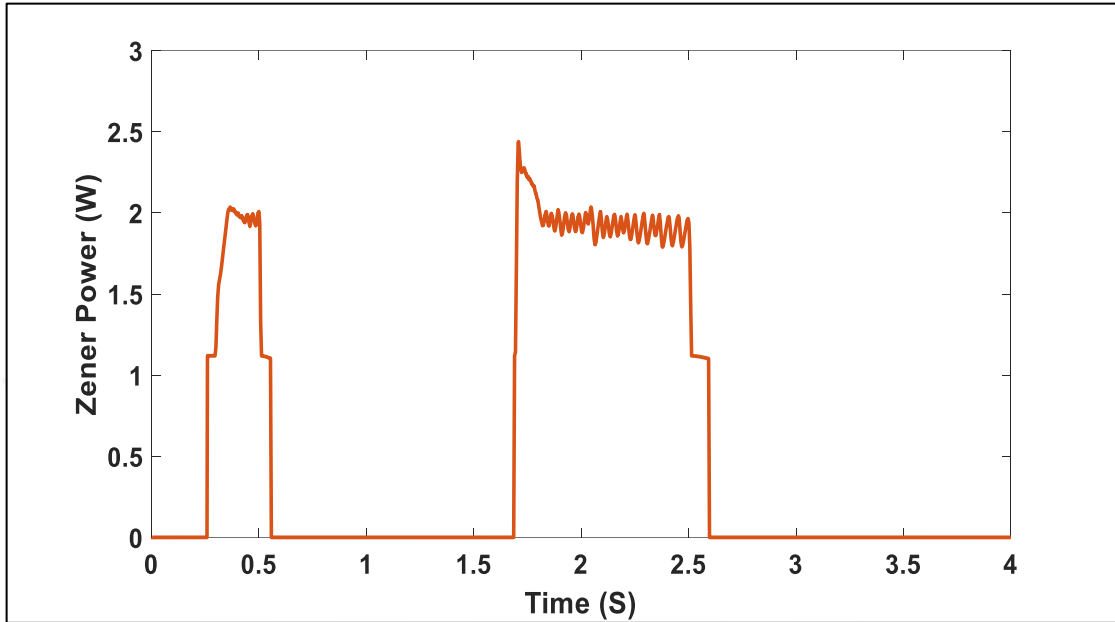
Figure 4.44 Zener Power during CV Stage under Changing Environment

Powers of PV panel and Battery under changing conditions of environment are shown in Figure 4.45 and 4.46 respectively.
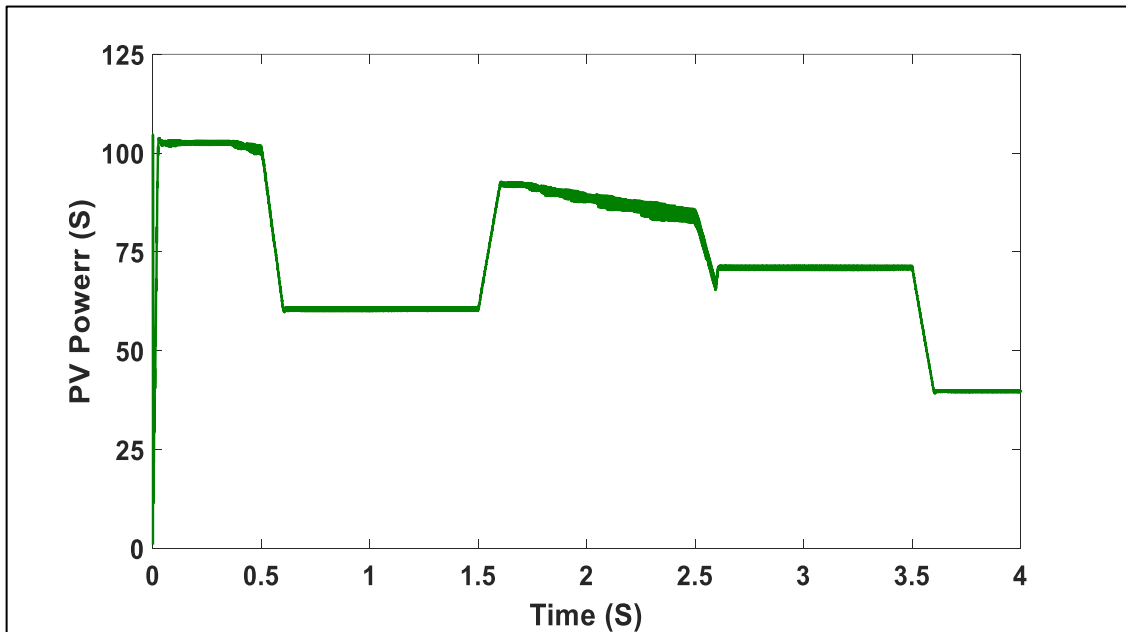
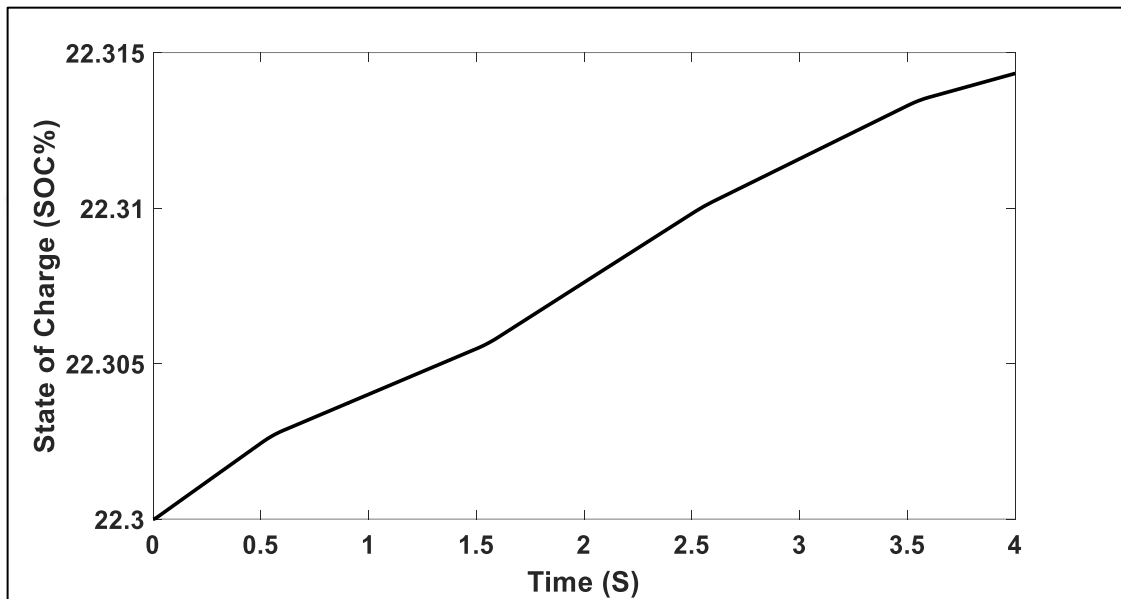Figure 4.45 PV Power during CV Stage under Changing Environment
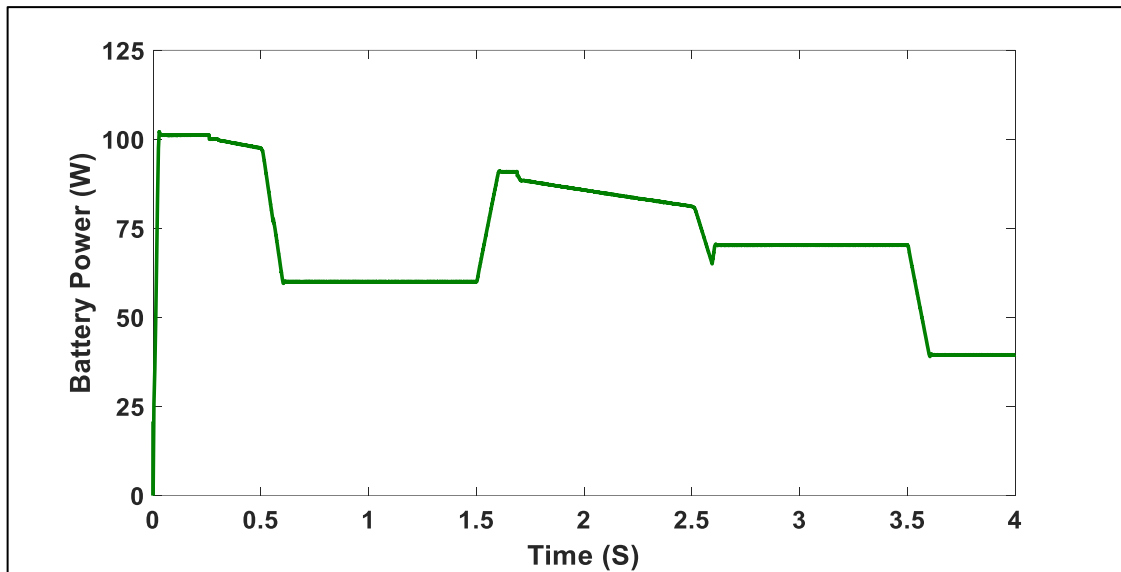
Figure 4.46 Battery Power during CV Stage under Changing Environment

As can be shown from above figures, when battery voltage decreases to 27,95V because of charging conditions of environment, the developed controller operates as MPPT controller in order to ensure the operation the PV panel at maximum power point that corresponds to new environmental condition. As this case, battery is charged with maximum charging current of new environmental condition until battery voltage reaches 28V. When battery voltage reaches 28V again, the developed controller operates PV panel at constant voltage region to charge battery with constant voltage of 28V.

4.3 Performance of developed MPPT controlled DC-DC converter for Solar Charger System

In this research, the efficiency and effectivity of MPPT controlled DC-DC boost converter as battery charge controller is verified by investigating its performance under different conditions of operation. The performance of developed charge controller can be expressed by some parameters that are related to charging process, converter design, and MPPT algorithm.

In the following sections, the performance of developed charge controller will be investigated by analyzing thoroughly input current ripples of developed controller, output voltage ripples of developed controller, tracking efficiency of developed controller, conversion efficiency of developed controller, response speed of developed controller, and end of charge detection.

4.3.1 Input Current Ripples of Developed Controller

As stated in the design process of boost converter that has been described in section 3.2.1.2, the design of inductor and switches of boost converter has been based on value of input current ripples which is determined by the required value of inductor current ripples of boost converter. As can be shown in Table 4.3, the maximum input current ripples that can be tolerated is 1,2A at short circuit current of PV panel that supplies the boost converter.

Throughout charging process of battery, short circuit current of PV panel is supplied during pre-charging stage of charging process. Therefore, the analysis of input current ripples of developed charge controller is considered in this stage of charging.

Figure 4.47 represents magnified figure of PV current during per charge stage of charging process. As can be shown, the PV current ripples is 10 mA which is within the allowed limits of ripples of designed boost converter. This result expresses the effective and proper design of developed charge controller in maintaining the current ripples within allowed limits.
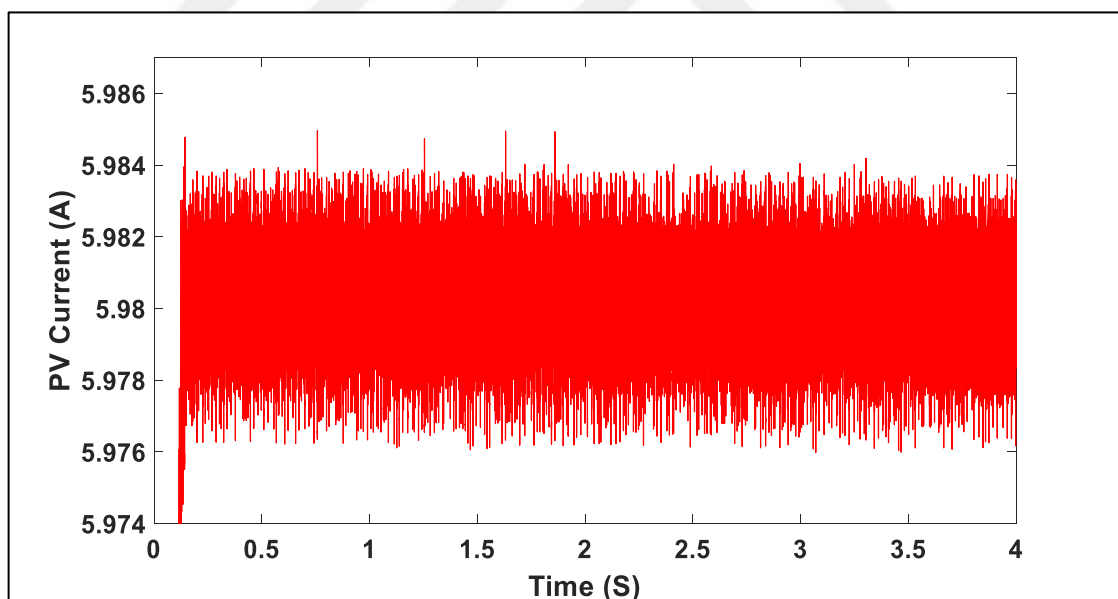
Figure 4.47 Magnified Picture of PV Current during Pre-Charging stage under STC

4.3.2 Output voltage ripples of developed controller

As stated in the design process of boost converter that has been described in section 3.2.1.2, the design of output capacitor of boost converter has been based on value of

output voltage ripples which is determined by the allowed value of battery voltage ripples . As can be shown in Table 4.3, the maximum battery voltage ripples is 1,4V at maximum allowed voltage of battery under consideration.

Throughout charging process of battery, maximum voltage of battery is reached during constant voltage CV stage of charging process. Therefore, the analysis of output voltage ripples of developed charge controller is considered in this stage of charging.

Figure 4.48 represents magnified figure of battery voltage during constant voltage CV stage of charging process. As can be shown, the battery voltage ripples is 100 µV which is so small and within the allowed limits of ripples of battery under consideration. This result expresses the effective and proper design of developed charge controller in maintaining the voltage ripples within allowed limits.
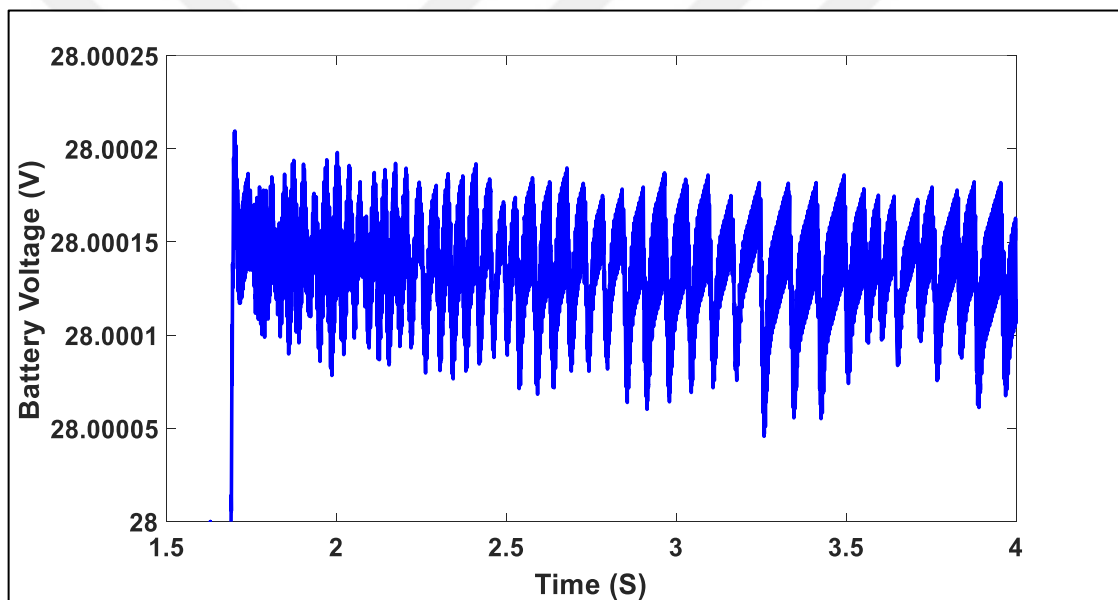
Figure 4.48 Magnified Picture of Battery Voltage during CV Charging Stage under STC

4.3.3 Tracking Efficiency of Developed Controller

In this research, the tracking efficiency of developed controller represents the ability of developed charge controller to track maximum power point (MPP) of PV panel at different environmental conditions. It is expressed by a percent value ranging from 0 to 100.

Higher values of tracking efficiency indicates a good tracking of developed controller for MPP of PV panel; thus higher power of PV panel can be extracted with low losses. In the contrary, lower value of tracking efficiency indicates a bad tracking of developed

controller for MPP of PV panel; thus lower power of PV panel can be extracted with high losses. Consequently, 100% of tracking efficiency indicates the perfect and exact tracking of developed controller for MPP of PV panel; thus maximum power of PV panel is extracted without any losses. Losses, which affect tracking efficiency, can be resulted from applied MPPT algorithm, step size of increment, and accuracy of current and voltage sensors.

Throughout charging process of battery, the developed charge controller is operated as MPPT controller during MPPT-CC stage of develpoed algorithm. Therefore, the analysis of tracking efficiency of developed controller is considered in this stage of charging by investigated Figure 4.34 which represents PV power under changing environmental conditions. This figure is compared with Figure 4.49 that represents P-V curves of PV panel under consideration at different irradiance level. As can be shown, MPP of PV panel is determined at diiferent level of irradiance. Generally, P-V curves of Figure 4.49 are supplied by manufacturer of PV panel. Numerically, the tracking efficiency of developed controller under different level of irradiance can be computed as shown in Table 4.6 which represents tracking efficiency of developed controller under changing environmental conditions.
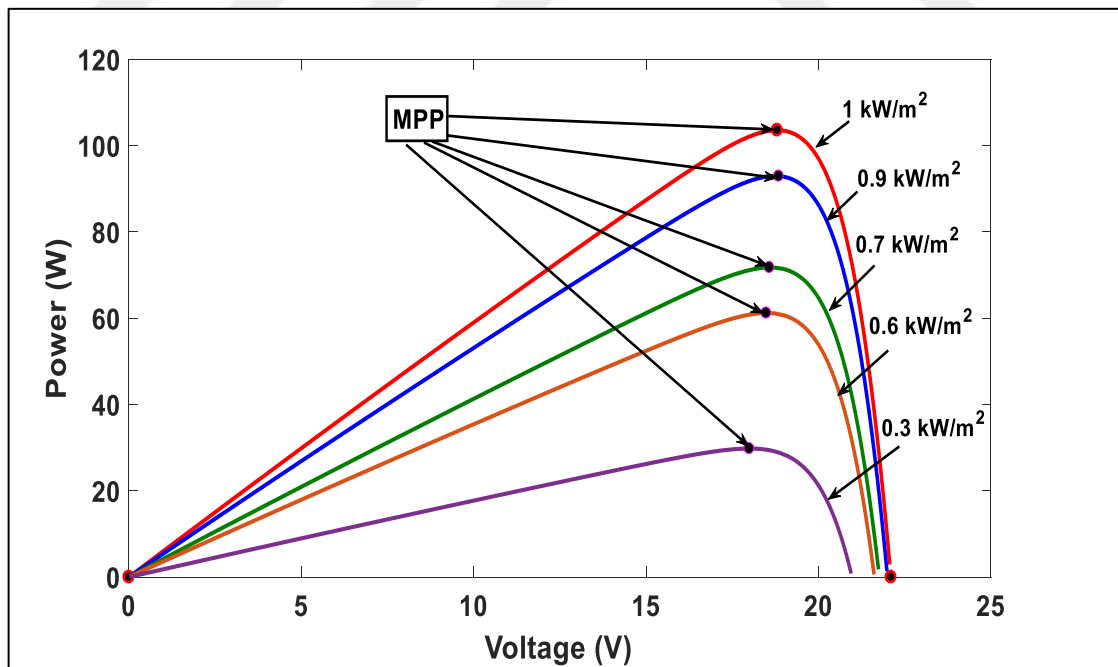
Figure 4.49 P-V Curves of PV Panel at Different Irradiance Levels

In this table, the tracking efficiency (Eff.) of developed controller at certain level of irradiance is calculated as shown in (4.11); where $P_{PV, MAX}$ represents maximum power

of PV panel at the specified level of irradiance, which can be obtained from P-V curves of PV panel shown in Figure 4.49, whereas $P_{PV, EXT}$ represents extracted power of PV panel at the specified level of irradiance, which can be obtained from Figure 4.34.

$$\text{Eff. } (\%) = \frac{P_{PV,EXT}}{P_{PV,max}} * 100 \qquad \text{At certain level of irradiance} \qquad (4.11)$$

Table 4.6 Tracking Efficiency of Designed system under MPPT-CC Stage

Irradiance (W/m²)	$P_{PV, MAX}$ (W)	$P_{PV, EXT}$ (W)	Eff. (%)
1000	103,6	103,06	99,48
900	92,94	92,45	99,47
700	71,77	71,37	99,44
600	61,2	60,85	99,43
400	40,19	39,95	99,40

Depending on Table 4.6, tracking efficiency curve of developed charge controller in term of solar irradiance level is constructed and averaged as shown in Figure 4.50. This curve of tracking efficiency has an average value of 99,444% over the given levels of irradiance. This result expresses the high tracking efficiency of developed controller in tracking maximum power point of PV panel at different environmental condition.
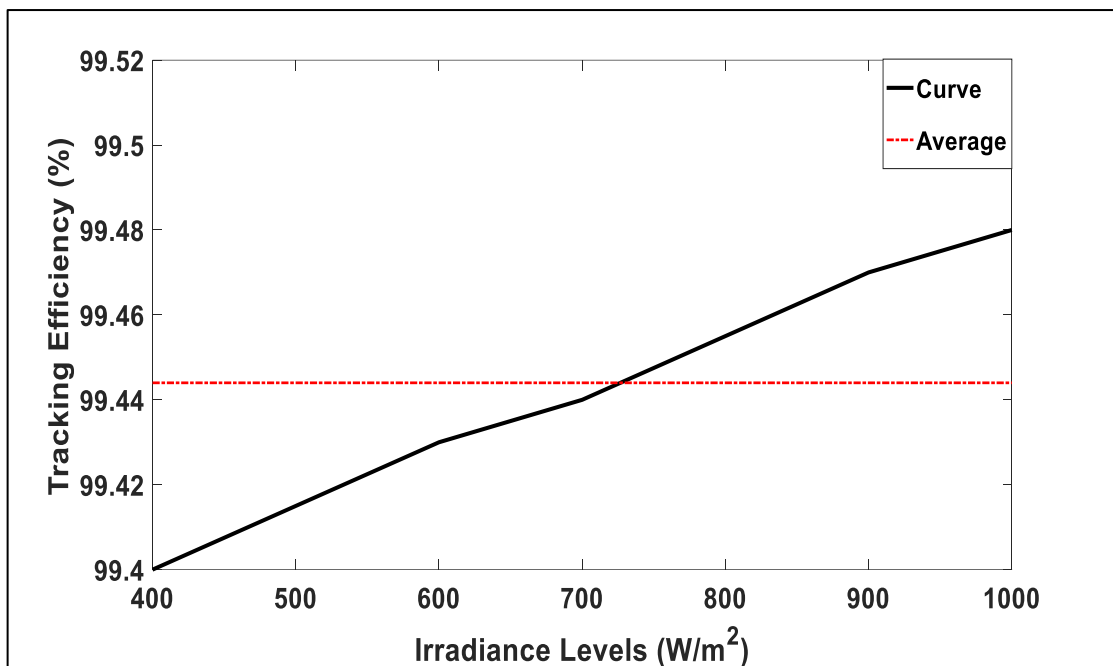
Figure 4.50 Tracking Efficiency Curve of Designed System under Different Irradiance

4.3.4 Conversion Efficiency of Developed Controller

The conversion efficiency of MPPT system represents the amount of maximum power, which is extracted by MPPT system, which is available at the load (or battery) side of PV system. This efficiency is affected by the losses of MPPT system, which can be resulted from losses of boost converter

In this research, the conversion efficiency of developed controller represents the ability of developed charge controller to transmit extracted power of PV panel to the battery bank efficiently at different environmental conditions. It is expressed by a percent value ranging from 0 to 100.

Higher values of conversion efficiency indicates that higher amount of extracted power of PV panel can be transmitted to battery bank with low losses. In the contrary, lower value of conversion efficiency indicates that lower amount of extracted power of PV panel can be transmitted to battery bank with high losses. Consequently, 100% of conversion efficiency indicates that total amount of extracted power of PV panel is transmitted to battery bank without any losses. Losses can be resulted from components of boost converter, Zener diode, and connections of circuits.

Throughout charging process of battery, the amount of extracted power of PV panel required by battery bank is determined by charging process requirements. These amount of power should be transmitted to battery bank efficiently in order to reduce charging time through charging process. Therefore, the analysis of conversion efficiency of developed controller is considered in the three stages of charging by investigated Figure 4.29, 4.38, and 4.46 which represent battery power of Pre-charging, MPPT-CC charging, and CV charging stages under Changing environmental conditions respectively. These figures are compared with Figures 4.30, 4.34, and 4.45 which represent extracted power of PV panel of Pre-charging, MPPT-CC charging, and CV charging stages under Changing environmental conditions respectively. Numerically, the conversion efficiency of developed controller under different level of irradiance can be computed as shown in Table 4.7, 4.8, and 4.9 which represent conversion efficiency of developed controller under changing environmental conditions for pre-charging, MPPT-CC charging, CV charbing stage respectively.

In this table, the conversion efficiency (Eff.) of developed controller at certain level of irradiance is calculated as shown in (4.12); where P_{BAT} represents transmitted power of

PV panel to the battery bank at the specified level of irradiance, which can be obtained from Figures 4.29, 4.38, and 4.46, whereas $P_{PV,EXT.}$ represents extracted power of PV panel at the specified level of irradiance, which can be obtained from Figure 4.30, 4.34, and 4.45.

$$\text{Eff. } (\%) = \frac{P_{BAT}}{P_{PVEXT}} *100 \qquad \text{At certain level of irradiance} \qquad (4.12)$$

Table 4.7 Conversion Efficiency of Designed System under Pre-Charging Stage

Irradiance (W/m²)	$P_{PV, EXT}$ (W)	P_{BAT} (W)	Eff. (%)
1000	25,6	24,42	95,4
900	25,66	24,6	95,87
700	25,73	24.91	96,81
600	25,40	24,73	97,36
400	25,44	24,95	97,87

Table 4.8 Conversion Efficiency of Designed System under MPPT-CC Stage

Irradiance (W/m²)	$P_{PV, EXT}$ (W)	P_{BAT} (W)	Eff. (%)
1000	103,03	102,07	99,1
900	92,46	91,67	99,15
700	71,37	70,87	99,3
600	60,85	60,48	99,4
400	39,95	39,75	99,45

Table 4.9 Conversion Efficiency of Designed System under CV Stage

Irradiance (W/m²)	$P_{PV, EXT}$ (W)	P_{BAT} (W)	Eff. (%)
1000	102,4	99,95	97,61
900	88,2	85.43	96,86
700	71,03	70.23	98,87
600	60,6	59,99	99
400	39,78	39,45	99,17

Depending on Table 4.7, 4.8, and 4.9, conversion efficiency curve of developed charge controller in term of solar irradiance level is constructed and averaged as shown in Figure 4.51, 4.52, and 4.53 for pre-charging, MPPT-CC charging , and CV charging stages respectively. This curves of conversion efficiency have average values of 96,66%, 99,28%, and 98,3% over the given levels of irradiance for the three stages of charging respectively. These result expresses the high conversion efficiency of developed charge controller in transmitting the extracted power of PV panel to the battery bank at different conditions of charging and environment.
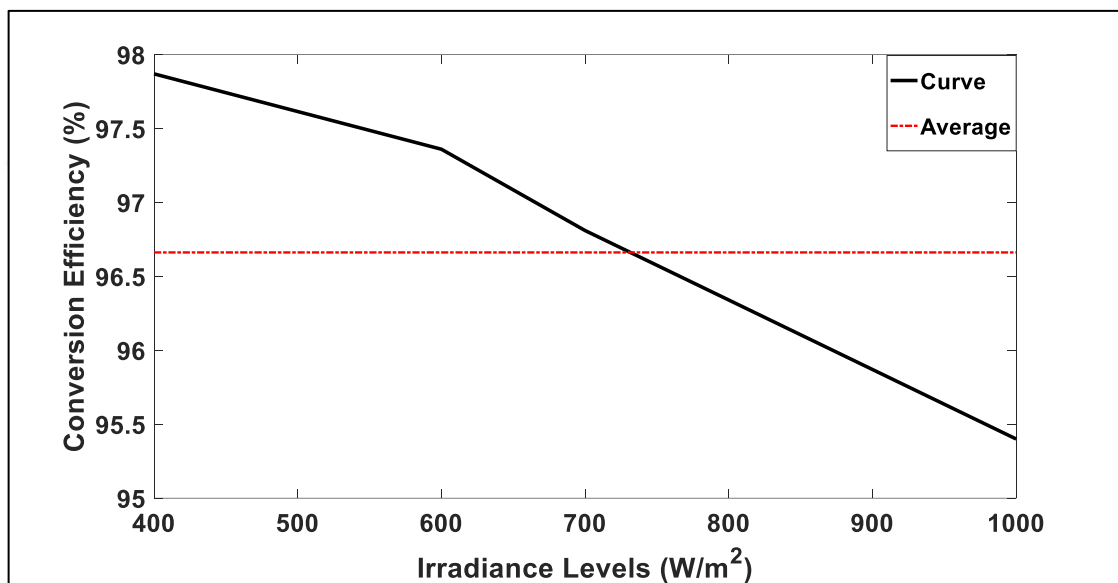
Figure 4.51 Conversion Efficiency Curve of Designed System under Pre-Charging Stage
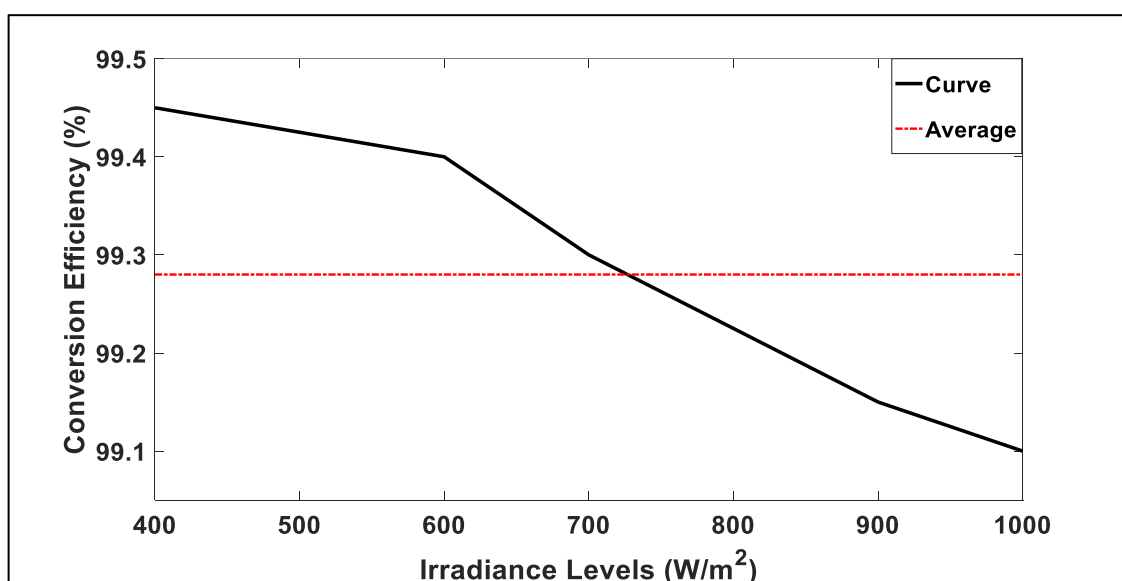
Figure 4.52 Conversion Efficiency Curve of Designed System under CC Charging Stage

94
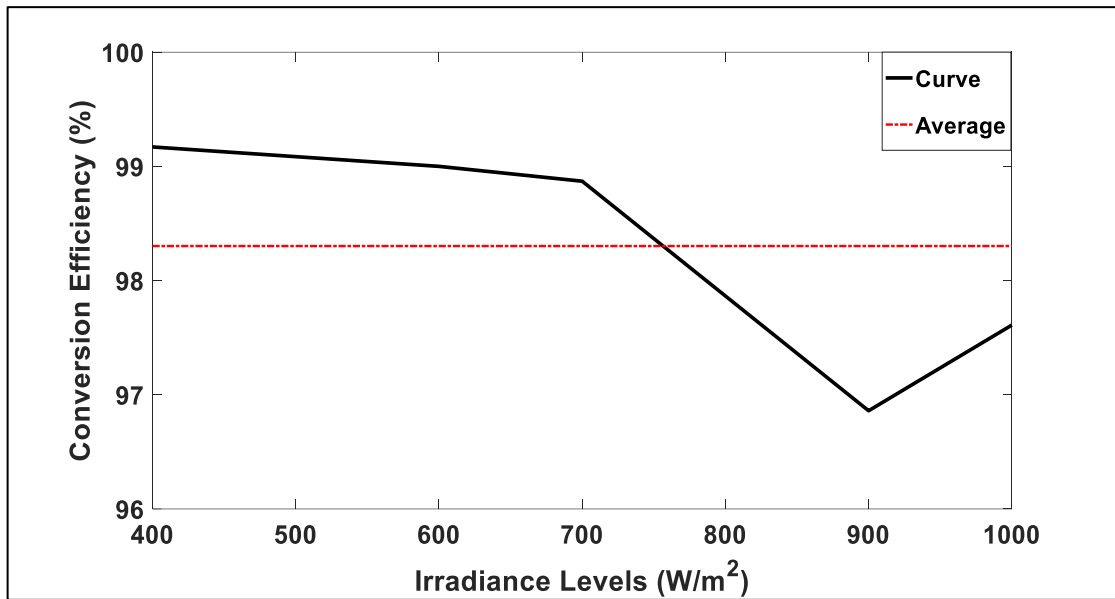
Figure 4.53 Conversion Efficiency Curve of Designed System under CV Charging Stage

4.3.5 Response Speed of Developed Controller

In this research, response time of developed controller represents the ability of developed charge controller to response rapidly to requirements of charging process and variations of environmental conditions. It is expressed by unit of time as a part of simulation time of 4 (s).

Throughout charging process of battery, charging current should be controller carefully in order to ensure the proper charging process. This can be shown through charging battery with charging current of 1,2 A during pre-charging stage, charging current of 4,8A during MPPT-CC charging stage, gradually decreasing current during CC charging stage. Therefore, in order to investigate the response of developed controller to these requirements of charging process, Figure 4.4, 4.10, and 4.54 will be analyzed. Figures 4.4, 4.10 represent battery current in pre-charging and MPPT-CC charging stage of charging process respectively. In these figures, transition periods expresses the rapid response of developed controller to stabilize charging current at 1,2A and 4,8A respectively.

In addition, Figure 4.54 represents oscillation of Zener current as a response of decreasing battery current. In this figure, increasing part of Zener current is resulted from decreasing of battery current. When this current reaches predetermined value, developed controller responses rapidly by changing operating point of PV panel that

95

results in decreasing part of Zener current. This process results in oscillating Zener current around allowed value of current.
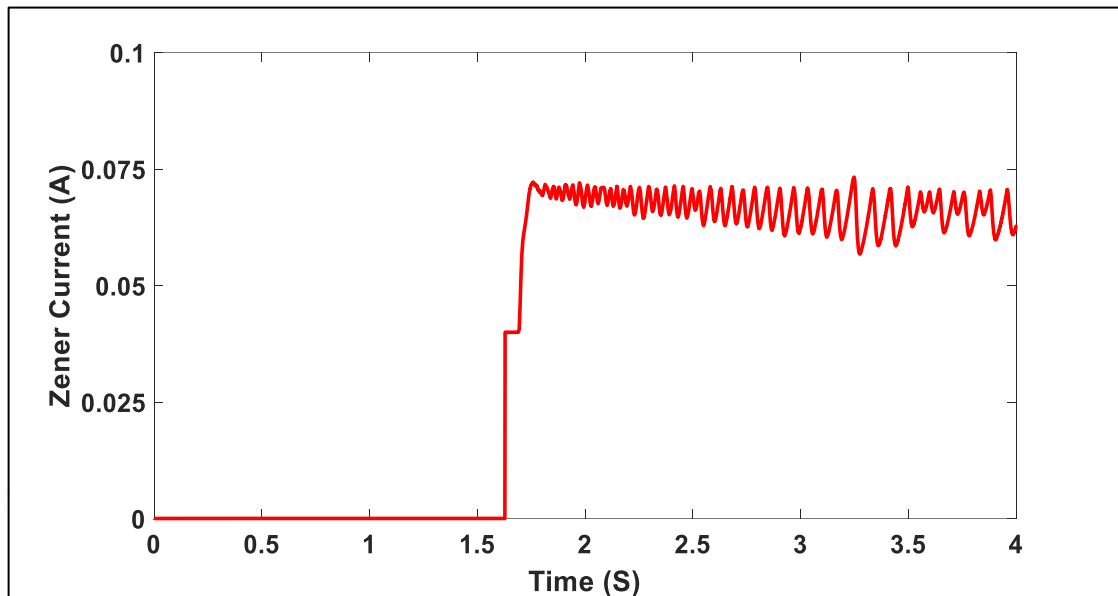
Figure 4.54 Zener Current during CV Charging Stage under STC

As stated previously, variations of environmental conditions is addressed by the operation of developed charge controller as MPPT controller which extracts maximum power of PV panel at different conditions. Therefore, the response of developed charge controller to variation of environmental conditions is investigated in MPPT-CC charging stage of charging process by considering Figure 4.24 and Figure 4.34 that represent the simulated change of environmental conditions and PV power under these conditions respectively. In Figure 4.24, transition period expresses the time through which solar irradiance changes its level; whereas transition period in Figure 4.34 expresses the time required by developed controller to track these variations. The previous observations expresses the fast response of developed charge controller to requirements of charging process and variations of environmental conditions.

4.3.6   End of Charge Detection

In this research, the detection of end of charge of battery is performed by using developed charge controller without any additional sensors. As shown in Figure 3.12, the developed controller detects the end of charge during the CV charging stage of charging process. This detection of end of charge depends on the principle of operation

of developed controller in CV stage of charging, which operates the PV panel at constant voltage region of I-V curve.

As stated previously, the PV power is decreased gradually as response of decreasing of battery current during CV stage of charging. The developed controller detects end of charge by continuously comparing PV power with minimum value that is related to the minimum value of charging current that indicates end of charge according to charging requirements.

Since PV power is used for detecting end of charge of battery, the developed controller has ability of ending of charge under low irradiance Levels when PV power is not enough for charging battery, and continuing charging process under high irradiance levels when PV power is enough for charging battery

RESULTS AND DISCUSSION

This paper has presented the design of MPPT controlled DC-DC boost converter which can be applied for solar charger systems. In this design, the DC-DC boost converter system is controlled by adjusting its duty cycle directly according to Incremental Conductance MPPT algorithm which has been expanded to include CC-CV charging algorithm in a way that meets the requirements of battery charging process and increases the efficiency of PV charger system. By using the developed algorithm, the designed system operates as MPPT tracker system and charger system throughout three stages charging process which are pre-charging, MPPT-CC charging, and CV charging stages. In MPPT-CC charging stage, the designed system operates as MPPT tracker in order to provide battery with maximum available power irrespective of environmental condition. In pre-charging and CV charging stage, the designed system operates as charger system in order to ensure the safe and proper charge of battery. The regulation process of battery voltage during CV charging stage has been performed by Zener diode as voltage controller unit.

The validation of designed MPPT controlled DC-DC boost converter for solar charger system has been performed by SIMULINK-MATLAB program. During this validation process, the operation and performance of the developed system throughout three stages of charging process have been investigated under different conditions of environment. The simulation results have shown that the designed system charged battery with minimum current of 1,2A during pre-charging stage to recover charge of battery safely until battery voltage reached 21,6V. When battery voltage reached 21,6V, the designed system has changed the charging process to MPPT-CC stage by smoothly changing battery current from 1,2A to 4,8A which is maximum charging current to provide battery with most of its energy. The charging of battery at this current has been

continued until battery voltage reached high predetermined limit of 28V. At this point, CV charging stage of charging process has started; at which Zener diode started contacting current to regulate battery voltage at 28V. As has been shown by simulation results, the battery current decreased with constant voltage charging.

Performance of designed system has been approved by simulation results which have demonstrated that the designed system can achieve an average power tracking efficiency of 99,444% over a wide range of irradiance levels (400 W/m2~1000 W/m2) during MPPT-CC charging stage. Furthermore, the designed system has power conversion efficiency of 96,66%, 99,28%, and 98,3% over a wide range of irradiance levels (400 W/m2~1000 W/m2) during pre-charging stage, MPPT-CC charging stage, and CV charging stage of developed algorithm respectively. In addition, simulation results have shown that the designed system has input current ripples of 10mA and output voltage ripples of 100μV during maximum input current and maximum output voltage respectively.

As can be shown from simulation results, the design of MPPT controlled DC-DC converter presented in this research has superiority on other designs that have been proposed in literature. The main contributions of this research can be summarized in the following points.

- Low cost and easily implemented design for MPPT controlled DC-DC converter used in solar charger system has been proposed. The implementation of proposed system is performed fully by DC-DC boost Converter and Zener diode without need for voltage or current regulator. The control of DC-DC converter is performed by simply developed algorithm which requires four voltage and current sensors in its operation.

- The developed MPPT controlled DC-DC converter system has considered the charging of battery under low voltage condition. The charging of battery during this condition requires minimum value of charging current to ensure the safe recovery of charge of battery; thus protect battery from degradation. The control of this stage of charging is performed fully by developed algorithm without need for current regulator.

- The developed algorithm in this research has taken into consideration the variation of environmental conditions during charging process stages to ensure the proper charge of battery under different conditions. During MPPT-CC stage, the environmental

conditions is considered by InC MPPT algorithm which tracks MPP irrespective of environmental conditions. During CV stage, the variation of environment is detected by decrease of battery voltage below than specified value; then accordingly the operation is transferred to MPPT-CC algorithm in order to track the new MPP at which battery will be charged until reach high pre-determined limit. During pre-charging stage, because of minimum power application in this stage, the variation of environmental is detected in low irradiance condition.

- A new method for end of charge detection has been proposed in this research. This proposed method depends on minimum pre-determined value of PV power which is required to be supplied to battery at fully charged condition. The implementation of this method does not require additional sensors since the value of PV voltage and PV current is provided continuously by voltage and current sensors which are used to implement MPPT algorithm. In addition, the proposed method does not only end battery charging in case of fully charged battery but also it ends battery charging in case of low solar irradiance which results in PV power that is below the predetermined value for end of charge; thus the proposed method performs two functions without additional sensors.

Due to the time constraint, the design of MPPT controlled DC-DC boost system has not been verified by practical measurements. In future work, the designed system will be implemented and validated practically in order to address all other practical factors that impact the functionality and performance of the MPPT controlled DC-DC boost converter especially effect of environment temperature. The effect of temperature on operation of PV panel and battery charging parameters will be studied practically. This will help in manufacturing and assembling the developed system in a printed circuit board (PCB) for low and mid- power application.

REFERENCES

[1]   Mekhilef, S., Saidur, R., and Safari, A., (2011). "A Review on Solar Energy Use in Industries", Renewable and Sustainable Energy Reviews, 15: 1777-1790.

[2]   Hossam-Eldin, A., Refaey, M., and Farghly, A., (2015). "A Review on Photovoltaic Solar Energy Technology and its Efficiency", 17th International Middle-East Power System Conference, 15-17 December 2015, Egypt.

[3]   Reddy, B.R.S., Narayana, P.B., Jambholkar, P., and Reddy, K.S., (2011). "MPPT Algorithm Implementation for Solar Photovoltaic Module Using Microcontroller", Annual IEEE India Conference, 16-18 December 2011, Hyderabad, India, 1 - 3.

[4]   Kumari, K.S., Prema, V., Rao, K.U., and Meena, P., (2013). "Efficient MPPT for a Stand-Alone Photovoltaic System", International Conference on Renewable Energy and Sustainable Energy, 5-6 December 2013, Coimbatore, India, 213 - 220.

[5]   Subashini, M. and Ramaswamy, M., (2016). "A Novel Design of Charge Controller for a Standalone Solar Photovoltaic System", 3rd International Conference on Electrical Energy Systems, 17-19 March 2016, Chennai, India, 237 - 243.

[6]   Ali, J., Ijaz, U., Niazi, M.H.K., Amer, M.S., Younis, M.M., and Hassan, W., (2015). "Simulation and Implementation of Solar Power Battery Charger Using Perturb & Observe Algorithm", Power Generation System and Renewable Energy Technologies, 10-11 June 2015, Islamabad, Pakistan, 1 - 5.

[7]   Musa, A., Pratomo, L.H., and Setiono, F.Y., (2014). "Design and Implementation of Solar Power as Battery Charger Using Incremental Conductance Current Control Method Based on Dspic30f4012", The 1st International Conference on Information Technology, Computer, and Electrical Engineering, 8-8 November 2014, Semarang, Indonesia, 324 - 327.

[8]   Padhee, S., Pati, U.C., and Mahapatra, K., (2016). "Design of Photovoltaic MPPT Based Charger for Lead-Acid Batteries", IEEE International Conference on Emerging Technologies and Innovative Business Practices for the Transformation of Societies, 3-6 August 2016, Balaclava, Mauritius, 351 - 356.

[9]   Abu Eldahab, Y.E., Saad, N.H., and Zekry, A., (2016). "Enhancing the Design of Battery Charging Controllers for Photovoltaic Systems", Renewable and Sustainable Energy Reviews, 58: 646-655.

[10]   Dadashzadeh, H., Khosroshahi, A.E., and Hosseini, S.H., (2017). "A Digital Predictive Controller for a SEPIC-Based Battery Charger in Photovoltaic Power

Systems", IV International Electromagnetic Compatibility Conference, 24-27 September 2017, Ankara, Turkey, 1 - 6.

[11]   Lyden, S., Haque, M.E., Gargoom, A., Negnevitsky, M., and Muoka, P.I., (2012). "Modelling and Parameter Estimation of Photovoltaic Cell", 22nd Australasian Universities Power Engineering Conference, 26-29 September 2012, Bali, Indonesia, 1 - 6.

[12]   Layachi, Z., Borni, A., Bouchakour, A., and Terki, N., (2014). "Buck-Boost Converter System Modelling and Incremental Inductance Algorithm for Photovoltaic System via Matlab/Simulink", Revue des Energies Renouvelables, 1: 63 – 70.

[13]   Ishaque, K. and Salam, Z., (2013). "A Review of Maximum Power Point Tracking Techniques of PV System for Uniform Insolation and Partial Shading Condition", Renewable and Sustainable Energy Reviews, 19: 475-488.

[14]   Femia, N., Granozio, D., Petrone, G., Spagnuolo, G., and Vitelli, M., (2006). "Optimized One-Cycle Control in Photovoltaic Grid Connected Applications", IEEE Transactions on Aerospace and Electronic Systems, 42: 954-972.

[15]   Hussein, K.H., Muta, I., Hoshino, T., and Osakada, M., (1995). "Maximum Photovoltaic Power Tracking: an Algorithm for Rapidly Changing Atmospheric Conditions", IEE Proceedings - Generation, Transmission and Distribution, 142: 59-64.

[16]   Kottas, T.L., Boutalis, Y.S., and Karlis, A.D., (2006). "New Maximum Power Point Tracker for PV Arrays Using Fuzzy Controller in Close Cooperation with Fuzzy Cognitive Networks", IEEE Transactions on Energy Conversion, 21: 793-803.

[17]   Liu, C.-L., Chen, J.H., Liu, Y.H., and Yang, Z.Z., (2014). "An Asymmetrical Fuzzy-Logic-Control-Based MPPT Algorithm for Photovoltaic Systems", Energies, 7(4): 2177-2193.

[18]   Ma, S., Chen, M., Wu, J., Huo, W., and Huang, L., (2016). "Augmented Nonlinear Controller for Maximum Power-Point Tracking with Artificial Neural Network in Grid-Connected Photovoltaic Systems", Energies, 9(12): 1005.

[19]   Xiaofeng, S., Weiyang, W., Xin, L., and Qinglin, Z., (2002). "A research on Photovoltaic Energy Controlling System with Maximum Power Point Tracking", Proceedings of the Power Conversion Conference PCC-Osaka, 2-5 April 2002, Osaka, Japan, 822 - 826.

[20]   Faranda, R. and Leva, S., (2008). "Energy Comparison of MPPT Techniques for PV Systems", WSEAS transactions on power systems, 3: 446-455.

[21]   Yuvarajan, S. and Shanguang, X., (2003). "Photo-Voltaic Power Converter with a Simple Maximum-Power-Point-Tracker", Proceedings of the International Symposium on Circuits and Systems, 25-28 May 2003, Bangkok, Thailand, III-399 - III-402.

[22]   Kobayashi, K., Matsuo, H., and Sekine, Y., (2004). "A Novel Optimum Operating Point Tracker of the Solar Cell Power Supply System", IEEE 35th Annual Power Electronics Specialists Conference, 20-25 June 2004, Aachen, Germany, 2147 - 2151.

[23]   Hart, D.W., (2011). Power electronics, Mc Graw-Hill Book Co., New York..

[24]   Zaions, D.F., Balbino, A.J., Baratieri, C.L., and Stankiewicz, A.L., (2017). "Comparative Analysis of Buck and Boost Converters Applied to Different Maximum Power Point Tracking Techniques for Photovoltaic Systems", Brazilian Power Electronics Conference, 19-22 November 2017, Juiz de Fora, Brazil, 1 - 6.

[25]   Enrique, J.M., Durán, E., Sidrach-de-Cardona, M., and Andújar, J.M., (2007). "Theoretical Assessment of the Maximum Power Point Tracking Efficiency of Photovoltaic Facilities With Different Converter Topologies", Solar Energy, 81: 31-38.

[26]   Garraoui, R., Hamed, M.B., and Sbita, L., (2016). "Different Topologies of DC/DC Converter Used in PV Systems with MPPT Controllers Based on Perturb and Observe Algorithm and Sliding Mode Theory", 3rd International Conference on Automation, Control, Engineering and Computer Science, 20-22 March 2016, TUNISIA, 694-700.

[27]   Jossen, A., Garche, J., and Sauer, D., (2004). "Operation Conditions of Batteries in PV Applications", Journal of Solar Energy, 76(6): 759-769.

[28]   Belabbas, B., Allaoui, T., Tadjine, M., and Denai, M., (2017). "Power Quality Enhancement in Hybrid Photovoltaic-Battery System based on three-Level Inverter associated with DC bus Voltage Control", Journal of Power Technologies, 97: 272.

[29]   Treptow, R.S., (2002). "The Lead-Acid Battery: Its Voltage in Theory and in Practice", Journal of Chemical Education, 79: 334.

[30]   Ponnusamy, M., (2013). "An Overview of Batteries for Photovoltaic (PV) Systems", International Journal of Computer Applications, 82(12): 0975 – 8887.

[31]   Solanki, C.S., (2009). Solar Photovoltaics : Fundamentals, Technologies and Applications, Second Edition, PHI Learning Private Limited, New Delhi.

[32]   Ng, K.S., Moo, C.S., Yi-Ping, C., and Hsieh, Y.C., (2008). "State-of-Charge Estimation for Lead-Acid Batteries Based on Dynamic Open-Circuit Voltage", IEEE 2nd International Power and Energy Conference, 1-3 December 2008, Johor Bahru, Malaysia, 972 - 976.

[33]   Weixiang, S., Thanh Tu, V., and Kapoor, A., (2012). "Charging Algorithms of Lithium-Ion Batteries: an Overview", 7th IEEE Conference on Industrial Electronics and Applications, 18-20 July 2012, Singapore, 1567 - 1572.

[34]   Hussein, A.A.H. and Batarseh, I., (2011). "A Review of Charging Algorithms for Nickel and Lithium Battery Chargers", IEEE Transactions on Vehicular Technology, 60: 830-838.

[35]   Armstrong, S., Glavin, M.E., and Hurley, W.G., (2008). "Comparison of Battery Charging Algorithms for Stand Alone Photovoltaic Systems", IEEE Power Electronics Specialists Conference, 15-19 June 2008, Rhodes, Greece, 1469 - 1475.

[36]   Balogh, L., (1997). Implementing Multi-State Charge Algorithm with the Uc3909 Switchmode Lead-Acid Battery Charger Controller, U-155 Application Note, Unitrode Corp, USA.

[37]   Jana, J., Samanta, H., Bhattacharya, K.D., and Saha, H., (2016). "A Four Stage Battery Charge Controller Working on a Novel Maximum Power Point

Tracking Based Algorithm for Solar PV System", 21st Century Energy Needs - Materials, Systems and Applications, 17-19 November 2016, Kharagpur, India, 1 - 4.

[38]   Liu, K. and Makaran, J., (2009). "Design of a solar powered battery charger", IEEE Electrical Power & Energy Conference, 22-23 October 2009, Montreal, QC, Canada, 1-5.

[39]   Sahu, P., Verma, D., and Nema, S., (2016). "Physical Design and Modelling of Boost Converter for Maximum Power Point Tracking in Solar PV Systems", 2016 International Conference on Electrical Power and Energy Systems, 14-16 December 2016, Bhopal, India, 10 - 15.

[40]   Bodur, H., (2017). GÜÇ Elektroniği, BirsenYayinevi, Turkiye.

[41]   Mohamed, H.A., Khattab, H.A., Mobarka, A., and Morsy, G.A., (2016). "Design, Control and Performance Analysis of DC-DC Boost Converter for Stand-Alone PV System", Eighteenth International Middle East Power Systems Conference, 27-29 December 2016, Cairo, Egypt, 101 - 106.

[42]   Boylestad, R.L. and Nashelsky, L., (1999). Electronic devices and circuit theory, Seventh Edition, Prentice Hall, Upper Saddle River, New Jersey .

[43]   Electronics Tutorials, Zener Diode, https://www.electronics-tutorials.ws/diode/diode_7.html, 10 May 2018.

[44]   Lofts, G., (2004). Jacaranda Physics 2, Second Edition, John Wiley & Sons Australia Ltd, Australia.

[45]   Ziegler, S., Woodward, R., Iu, H.H.C., and Borle, L., (2009). "Current Sensing Techniques: A Review", IEEE Sensors Journal, 9(4): 354 - 376.

CURRICULUM VITAE

PERSONAL INFORMATION

Name Surname : Bassam AL-HANAHI

Date of birth and place : 25/12/1987 – Saudi Arabia

Foreign Languages : Arabic – English - Turkish

E-mail : alhanahi.bassam@gmail.com

EDUCATION

Degree	Department	University	Date of Graduation
Master	Electrical Engineering	Yildiz Technical Uni.	2018
Undergraduate	Electrical Engineering E	Sana'a University	2011
High School	Scientific Section	Kuwait High School	2005

WORK EXPERIENCE

Year	Corporation/Institute	Enrollment
2012	Sana'a University	Lecturer
2013	Technical Center for Training & Manufacturing	Trainer

PUBLISHMENTS

Papers

1. Al-Hanahi, B., and Akin, B., (2018). "MPPT Controlled Battery Charger Design and Simulation", Majlesi Journal of Mechatronics systems. 6(3): 1-8.

Conference Papers

1. Al-Hanahi, B., and Akin, B., (2017). "MPPT Controlled Converter Design and Simulation for Solar Charger Application", International Advanced Researches & Engineering Congress, 16-18. November 2017, Osmaniye, Turkey, 979-985.

2. Al-Hanahi, B., and Akin, B., (2018). "MPPT controlled DC-DC converter design and application for three stages battery charger", The 6. European Conference on Renewable Energy System, 25-27 June 2018, Istanbul, Turkey.